UNIVERSIDAD NACIONAL AUTÓNOMA DE MÉXICO
PROGRAMA DE POSGRADO EN CIENCIAS DE LA TIERRA
CENTRO DE CIENCIAS DE LA ATMÓFERA

MITIGACIÓN DE LA ISLA DE CALOR URBANA: UN MODELO GENERAL
URBAN HEAT ISLAND MITIGATION: A GENERAL MODEL

TESIS
QUE PARA OPTAR POR EL GRADO DE
DOCTOR EN CIENCIAS DE LA TIERRA

PRESENTA:
M. EN C. MÓNICA DE JESÚS BALLINAS OSEGUERA

TUTOR PRINCIPAL
DR. VÍCTOR LUIS BARRADAS MIRANDA (INSTITUTO DE ECOLOGÍA)

COMITÉ TUTOR

DRA. MARÍA ENGRACIA HERNÁNDEZ CERDA	INSTITUTO DE GEOGRAFÍA
DR. LUIS GERARDO RUÍZ SUÁREZ	CENTRO DE CIENCIAS DE LA ATMÓSFERA
DR. ARON JAZCILEVICH DIAMANT	CENTRO DE CIENCIAS DE LA ATMÓSFERA

Ciudad Universitaria, CD. MX. Diciembre 2016

Declaro conocer el Código de Ética de la Universidad Nacional Autónoma de México, plasmado en la Legislación Universitaria. Con base en las definiciones de integridad y honestidad ahí especificadas, aseguro mediante mi firma al calce que el presente trabajo es original y enteramente de mi autoría. Todas las citas de, o referencias a, la obra de otros autores aparecen debida y adecuadamente señaladas, así como acreditadas mediante los recursos editoriales convencionales.

Agradecimientos

Al posgrado de Ciencias de la Tierra y al Centro de Ciencias de la Atmósfera de la UNAM, por haber aceptado mi solicitud de ingreso al doctorado y permitirme realizar la presente investigación.

Al Consejo Nacional de Ciencia y Tecnología (CONACYT), por haberme otorgado una beca durante los estudios de maestría (CVU: 348420). Asimismo agradezco al proyecto DGAPA-PAPIIT "Lineamientos climáticos y bioclimáticos para la planeación urbana en México" con clave IT201514 y "Vegetación urbana: una alternativa de mitigación de la contaminación térmica citadina" con clave IN213209-3, y en el inicio al proyecto "Alternativa de mitigación de la isla de calor urbana: un modelo general con clave CONAVI-2009-01-127001, por las facilidades y el apoyo económico otorgado para la realización de este trabajo.

Al Instituto de Ecología de la UNAM, por la infraestructura brindada, el Laboratorio Interacción planta-atmósfera, sobre todo a mis compañeros Dr. Manuel Esperón Rodríguez y M. en C. Martín Bonifacio Bautista.

A mi tutor, el Dr. Víctor Luis Barradas Miranda, mi tutor por años, que me enseño que no hay mejor manera de llegar al sueño deseado con esfuerzo y siempre la motivación de romper barreras, para entregar todos los trabajos con la mejor calidad posible.

Mi Comité Tutoral, Dr. Víctor Luis Barradas Miranda, Dra. María Engrancía Hernández de la Cerda, Dr. Luis Gerardo Ruíz Suárez, Dr. Aron Jazcilevich Diamant, por todas sus aportaciones y guía académica en el transcurso de esta investigación.

A los miembros del sínodo evaluador: Dra. Teresa de Jesús Reyna Trujillo, Dra. María Engracia Hernández Cerda, Dr. Víctor Luis Barradas y Dr. Ricardo Torres Jardón, gracias a todos y cada uno de ustedes por sus muy apreciados comentarios, sugerencias y demás aportaciones que enriquecieron este trabajo y Dr. José Agustín García Reynoso.

También agradezco al Dr. Erik Velasco y a The National Science Foundation and the Metropolitan Environmental Commission of Mexico por suministrar los datos de flujos de calor y del balance de energía de la colonia Escandón, Ciudad de México.

El personal de la RedMet que hace posible la obtención de datos generados para la elaboración de parte de la investigación.

Dedicado a mi ángelito Mijael. Mis grandes amores, mi compañero de vida y mi Tosco.

Titulo: Mitigación de la Isla de Calor Urbana: Un Modelo General

RESUMEN

Sin lugar a duda, la urbanización presenta un drástico y fuerte impacto ambiental. Uno de ellos, es el fenómeno de Isla de Calor Urbana (ICU) que aparece en las ciudades debido al cambio drástico en el uso de suelo. Este fenómeno es principalmente nocturno pero también aparece durante el día en muchas ciudades incluyendo la Ciudad de México. La ICU puede afectar el confort térmico humano que puede influir en la productividad humana y morbilidad en el período primavera/verano. Para contrarrestar este efecto, se utilizan sistemas de aire acondicionado, lo que lleva por un lado a una probable exacerbación de la ICU y por el otro, un aumento en el consumo de energía, principalmente el éctrica. Actualmente, la ICU es muy marcada en la Ciudad de México, ya que el centro cálido se incrementó tanto en el espacio como en su intensidad al compararlo con mediciones de años anteriores, con diferencias de la temperatura del aire hasta de 10 °C entre el área urbana y rural, por lo que es necesario implementar estrategias de mitigación de la ICU.

Se construyó un modelo fenomenológico sencillo basado en el balance de energía para generar un apoyo teórico de la mitigación de la ICU en la Ciudad de México. El modelo consiste principalmente en una aproximación del balance de energía en la que se desprecia tanto el calor antrópico como la advección, además de tomar el almacenamiento del tejido urbano como una constante. Por ello, este modelo se centra en que el incremento del flujo de calor latente por el aumento de la cobertura arbórea puede reducir el flujo de calor sensible y por lo tanto la temperatura del aire ya que ésta es una función del flujo de calor sensible. Este modelo se generó para un barrio típico comercial/residencial de la Ciudad de México utilizando datos de los componentes del balance de energía urbano y su parametrización y datos de medición sencilla y rutinaria (temperatura y humedad del aire, presión, visibilidad, posición geográfica), obtenidos cada media hora, en 15 días del mes de marzo del año 2006.

Para determinar el aumento de la cobertura arbórea fue necesario analizar también las variables que afectan la transpiración de los árboles, tales como la conductancia del

dosel (variable f isiológica) en cu atro es pecies ar bóreas d ominantes (*Eucaliptus camaldulensis, Fraxinus uhdei, Liquidambar styraciflua* y *Ligustrum lucidum*). La transpiración s e es timó u tilizando l a t écnica de l a m edición d e f lujo d e s avia, y l a conductancia es tomática se m idió y s e pa rametrizó ut ilizando e l m étodo de l a f unción envolvente. E l f lujo de s avia t ambién s e pa rametrizó ut ilizando e l m odelo de P enman-Monteith. La conductancia total (conductancia del dosel + conductancia aerodinámica) se estimó a partir de datos promedio de la transpiración y del déficit de presión de vapor. La conductancia del dosel se calculó a través de la conductancia estomática y del índice de área foliar. Las mediciones de flujo de savia se realizaron en cuatro árboles de cada especie y l a conductancia estomática s e m idió en al m enos ci nco h ojas d e c ada ár bol cada 3 0 minutos. Estos experimentos se realizaron en la época seca, dos semanas entre el 11 y el 27 de abril de 2013 para la transpiración, la conductancia estomática y del dosel. Mientras que las mediciones o cálculos de conductancia total se obtuvieron mediante mediciones diarias de transpiración y de déficit de presión de vapor, del 22 al 27 de abril del 2013, al igual que conductancia del dosel para la conductancia estomática y el índice de área foliar.

El pr omedio de l a conductancia e stomática s e l ocalizó e ntre 40 m m s $^{-1}$ (*E. camaldulensis*) y 50 mm s^{-1} (*L. lucidum*). Los resultados muestran que la transpiración fue dominada f uertemente p or e l d éficit d e pr esión de v apor (DPV, v ariable a mbiental) y controlado por l a c onductancia estomática (g_S). D e a cuerdo c on el m odelo de f unción envolvente, las estomas fueron más sensibles al DPV que a la irradiancia y a la temperatura del ai re. Los v alores d e r adiación n eta, en ergía almacenada y flujos de calor s ensible y latente, f ueron alrededor de 449, 224, 153, y 72 W m^{-2}, r espectivamente. E l r ango d e transpiración diario fue de 3.64 a 4.35 Ld^{-1}.

Las tasas de transpiración medidas en este trabajo son capaces de disipar hasta un 20% de la radiación neta en la Ciudad de México (*L. styraciflua* registro la más alta tasa de transpiración 4.35 L d^{-1}). Con estos resultados, es posible construir arreglos de árboles para disipar l a m ayor cantidad pos ible de c alor pr oducido e n l a c iudad. Para r educir l a temperatura de l aire 1 ° C e n l a z ona de e studio, s on ne cesarios 63 árboles gr andes de *Eucaliptus camaldulensis* por hectárea, mientras que para reducir la temperatura del aire 2° C se necesitarían sólo 24 árboles grandes de *Liquidambar styraciflua*.

Este estudio sugiere que no solo con el aumento de la cobertura del dosel de árboles en la ciudad se puede mitigar la ICU adecuadamente, sino que requiere de la elección de las especies de árboles más adecuados para resolver este problema. También es imperativo incluir este tipo de estudios en la selección de árboles y la planificación del desarrollo urbano para mitigar adecuadamente la ICU. En este trabajo, en un punto de vista particular, también se presentan las estrategias a seguir para resolver este problema en un país en desarrollo, con un crecimiento urbano caótico y complejidad climática.

Toda esta investigación da la pauta para generar estrategias y lineamientos de urbanización acorde con un medio ambiente saludable.

ABSTRACT

There is no doubt, the urbanization creates a drastic and strong environmental impact. One of them is the Urban Heat Island (UHI) phenomenon that appears in cities due to the drastic change in land use. Although, it is generally a nocturnal phenomenon also occurs during the day in many cities including Mexico City. The UHI can affect the human thermal comfort that can influence in the human productivity and morbidity mainly in the spring/summer period. To counter this effect, air conditioning systems are used, which carry an increase in the energy consumption, electric principally. Currently, the UHI is marked in Mexico City, being that the warm center increased, as in space as in intensity, compared to measurements from previous years, with air temperatures differences up to 10 °C between urban and rural area. Therefore, it is necessary to implement strategies in UHI mitigation.

A phenomenological model based in energy balance was built to generate a theoretical support in the UHI mitigation in Mexico City. This model is focused on the concept of latent heat flux increasing by enlarging tree cover, to reduce sensible heat flux and therefore air temperature. This model was generated in a typical commercial/residential neighborhood using urban energy balance components data and parameterizations by data of easy and routine measurements (air temperature, humidity, pressure and visibility), obtained every 30 minutes, in fifteen days in March, 2006.

To determinate tree cover increase, it was necessary analyze the variables that affect transpiration, such as, canopy conductance (physiological variable), in four arboreal dominant species (*Eucaliptus camaldulensis, Fraxinus uhdei, Liquidambar styraciflua* and *Ligustrum lucidum*). The sap flow technique was used to estimate tree transpiration rates and stomatal conductance was measured and parameterized using the envelope function method. Sap flow was also parameterized by the Penman-Monteith transpiration model. Total conductance (canopy conductance + aerodynamic conductance) was estimated from time averaged transpiration and mean vapor pressure deficit. Canopy conductance was computed from stomatal conductance and leaf area index. Sap flow measurements were made in four trees of each species and stomatal conductance was measured in at least five leaves of each tree every 30 minutes. These experiments were carried out in the dry season, in two weeks between April 11 to 27, 2013 related to transpiration, and stomatal and canopy conductance. While measurements or calculations of total conductance were obtained through daily measurements of transpiration and vapor pressure deficit, from April 22 to 27, 2013; and also canopy and stomatal conductance and leaf area index.

Stomatal conductance average value was located between 40 mm s^{-1} (*E. camaldulensis*) and 50 mm s^{-1} (*L. lucidum*). The results show, that transpiration was strongly dominated by the pressure vapor deficit (DPV, environmental variable) and controlled by the stomatal conductance (g_s). According to the envelope function method, the stomata were more sensitive to DPV than irradiance and/or air temperature. Net radiation values, storage energy and sensible and latent heat flux, were around 449, 224, 153, and 72 W m^{-2}, respectively. Transpiration daily range was from 3.64 to 4.35 L d^{-1}.

Finally, transpiration rates presented here were capable to dissipate up to 20% of net radiation in Mexico City. *L. styraciflua* registered the highest transpiration rate 4.35 L d^{-1}. With these results, it is possible to built tree arrangements to dissipate the maximum amount of heat produced in the city. To reduce the air temperature 1°C in the study area, it is necessary 63 big trees of *Eucaliptus camaldulensis* by hectare, while to reduce 2 °C air temperature is just necessary 24 big trees of *Liquidambar styraciflua*.

This study suggests that not only with the increasing of the tree canopy cover in the city is possible to mitigate the UHI adequately; but it is also required to select tree species

more adequately to resolve this problem. It is also imperative include these type of studies in the selection of trees and the planning of urban development to mitigate the UHI effectively. This work, in a particularly point of view, also presents strategies to continue solving this problem in a developing country, with a chaotic urban growth and climatic complexity.

All this investigation provides guidelines to generate strategies and guidelines to the urbanization a consistent with a healthy environmental.

TABLE OF CONTENTS

Ballinas M, Barradas VL. 2016. The urban Tree as a Tool to Mitigate the Urban Heat Island in Mexico City: A Simple Phenomenological Model. Journal of Environmental Quality 45: 157-166. DOI:10.2134/jeq2015.01.0056. **Impact Factor: 2.238.**

Ballinas M, Barradas VL. 2016. Transpiration and stomatal conductance as potential mechanisms to mitigate the load in Mexico City. Urban Forestry & Urban Greening 20:152-159 DOI: 10.1016/j.ufug.2016.08.004. **Impact Factor: 2.006.**

I. Figure list

II. Table list

CHAPTER 1. INTRODUCTION AND BACKGROUND

Charles Darwin in 1859 stated that it is not the strongest species that survive, nor the most intelligent, but one that responds better to change (Comín del Rio, 2009).

While most living organisms have adapted to the environment, mankind has turned the environment to his own benefit. With the agriculture invention, mankind becomes sedentary, and it is precisely at this moment that man begins to adapt the environment to settle and large-scale urbanization begins or starts. The urbanization, like a phenomenon beginning with agriculture invention, as was mentioned, has it origin in the prehistory and actually is an economical sector indispensable and fundamental to feeding human population in entire world (Bottino Benardi, 2009). Agriculture development would have from 8,000 to 10,000 years, and along with hunting, fishing and cattle-raising led to human settlements, and therefore the beginning of urban development, which led to the impulse of cities, and in turn to a great population growth (Cadena, 2011). These civilizations were distributed near large rivers such as the Tigris and Euphrates (Mesopotamia) and Nile (Egypt) or around/on lakes (Mexico), which they provided enough water and nutrients to have a great food production (Bottino Benardi, 2009). Later, industrial revolution took a prominent role in urban growth, since the economic development is concentrated in cities; there was a large labor demand to improve lifestyle (Montenegro, 1998).

Bottino-Bernardi (2009) affirmed that cities are agglomerations covering considerable areas and occasionally overstep their bounds, in which historically were demarcated by a past political decision. Now-a-day, a great city expands beyond its original administrative area, reaching out to other cities and spaces forming a large metropolitan area, bringing a political-administrative entity, where human population is engaged in commercial, administrative or industrial activities, and where the utilities (water, electricity, telephone, etc.) and facilities (schools, parks, hospitals, etc.) are. Their legal status distinguishes it from rural and/or country. Borja (2003) defined the city as *a historical,*

geographical, cultural, even political, human concentration and diverse (urbs), provided with identity and self-government (*Civitas, polis*) reality.

Rapid urban growth and the spread of cities is one of the most important events taking place from the second half of the XX century until now, provoking in confined spaces a highly concentrated population due to migration from the countryside over the site natural increase. In the year 2000, there were 402 cities where the population was between 1 and 5 million inhabitants and 22 cities holding between 5 and 10 million. For example, in 1950, New York was the only city with more than 10 million, and in 2015, it is estimated that there are 30 cities with similar inhabitants number or more of which 23 of them, belong to developing or emerging countries (Alberto, 2005; Saltenyte, 2016). It is noteworthy that both, rich regions as well as the poor, the accelerated and disorderly urban growth generates a strong spatial and environmental impact as the loss of biodiversity, the urban heat island, and air, water and soil pollution. Furthermore, with the increasing of urbanization occurs, in both domestic or private and public and commercial, a higher consumption of energy (Alberto, 2005).

As an example of the effect of urbanization, when an urban area expands, it creates its own and distinctive microclimate, a clear example of this effect is the phenomenon called Urban Heat Island (UHI), where the air temperature is greater in the urban area than its surroundings. Wilhelm Schmidt was the one of the precursors on the study of this phenomenon conducted in Vienna in the early fifteenth century (Gartland, 2008). However, the UHI investigation formally began in 1820 with Luke Howard when studied London climate. Another researcher who conducted these types of studies was Emilien Renou (1862) in Paris, who set several thermometers in the entire urban area and found that air temperature increased from 1 to 2 °C with their surroundings (Landsberg, 1981). The phenomenon of heat island is present in all cities, no matter their size or location, regardless of its latitude (Capelli de Steffens, et al., 2005), and it is a weather-climate phenomenon (Gartland, 2008). Types of surfaces such as paved roads, parking lots and buildings have a great influence on the increase in urban temperature (Oke, 1982).

At the present and probably with the climatic change effect, the UHI has become more notable in the Metropolitan Area of Mexico City (MAMC) (Jáuregui, 1997). Which

has been generated mainly by the urban expansion, which implies a drastic change in land use (Cruz, 2000), with a difference on urban minimum temperature and rural area (T_{U-R}) near to 6 °C (Jáuregui and Luyando, 1998) and the minimum T_{U-R} 1.8 °C between Chapingo and San Agustín. At that time the warm center was located at the Circuito Interior area (≈ 112.7 km^2). However, to date UHI is also established during the daytime, with maximum temperature differences up to 10 °C (T_{U-R}) (Ballinas, 2011).

It is important to note that UHI also has been observed in other Mexican cities such as Tampico (22°15'19"N, 97°52'07"W, 30 m asl), where the difference was up to 6 °C (Fuentes-Pérez, 2014), while in Veracruz-Boca del Rio (19°11'25"N, 96°09'12"W, 10 m asl), this difference may be up to 5 °C (Baca-Cruz, 2014). In Villahermosa (17°59'13"N, 92°55'10"W, 9 m asl) and Xalapa (19°32'24"N, 96°55'39"W, 1417 m asl), UHI was less intense (2.5 °C). Even in the desert cities as the case for Mexicali (32°39'48"N, 115°28'04"W, 6 m asl) the temperature difference was 3.2 to 4 °C (García-Cueto, et al., 2007). This phenomenon becomes so conspicuous and threatening occupying spaces in the news as follows: *By 2050, the warmth in Mexico City will be so intense which will lead to an increased use of air conditioning. The cities of Cuernavaca, Tijuana, Acapulco and Monterrey, among others, will suffer from increased temperature. But, especially in cities where the called heat island occurs* (Reforma Journal, 2014).

As a consequence, the increasing of air temperature (T_A) in the urban area exacerbates the human thermal comfort, and people would experience more stress by heat and human health could be seriously affected (Laschewski and Jendritzky, 2002). Furthermore, heat waves or heat strokes could increase or be enhanced by the UHI effect (Luber and McGeehin, 2008; Basara, et al., 2010). This can affect human productivity mainly in spring-summer period in temperate and subtropical regions.

Furthermore, these T_{U-R} differences can increase with the global climatic change (Brazel and Quattrocchi, 2005). Indeed, from the thermal comfort and human health point of view, the heating produced by urbanization can be considered as some sort of thermal contamination, which it could be defined as thermal pollution, since heat contamination is more related to the heat released by nuclear power, thermoelectric plants and/or other

significant heat sources; meanwhile, thermal pollution is more related to the low heat production as it is the urban case.

Air conditioning systems (ACS) have been installed in workplaces with the objective of improving the thermal comfort to get a better human productivity, but with a considerable increase in energy consumption and a considerable increase in the energetic costs (Wong and Chen, 2009). In Mexico City, for example, in 1996 the electricity sold to the domestic sector by *Comisión Federal de Electricidad* was 28,400 GW h^{-1}, 23.4% of the total consumption (121,579 GW h^{-1}), from this energy consumption by the domestic sector, 20% was required to condition the environment inside buildings (air conditioning, evaporative cooling and fans) (Ramos, 1998), and 30% in commercial and buildings services in metropolitan area and the 50% was domestic consumption. These ACS which have a very low efficient and "take" the heat inside of the buildings and they "put" it outdoors, generate an increasing in the thermal pollution exacerbating the UHI effect, having feedback and therefore the human heat loads incrementing energy consumption too.

As UHI affects directly to human energy balance, mitigation can understanding in the limit when people starts to experiment heat stress. In an urban environment, it is well known that vegetation when transpiring, redistribute the energy balance with a result of cooling the air in and out of the vegetated area, forming the so called "cold island", not only in the site where they find but two or three times more than the size of the green area (Barradas, 1991; 2000). Unfortunately, it is a fact that in the cities there is a drastic reduction of open spaces suitable for the construction of parks due to other urban priorities. Mexico City just annually loses 1.5% of green areas to optimize vehicular traffic (Ezcurra, 1991). Therefore, it is imperative to investigate the energy redistribution in the city and how this affect to T_A, taking the energy balance as a framework and to implement linear models linking, air temperature (T_A) with latent heat flux (Q_H) and indirectly with thermal comfort (bioclimatic comfort index). At the present, UHI mitigation is an important issue due to problems noted before (Rosenfeld, et al., 1998; Solecki, et al., 2005; Takebayashi and Moriyama, 2007; Rizwan, et al., 2008; Shahmohamadi, et al., 2011).

There are several alternatives to mitigate the UHI by manipulating the urban energy balance, and changing some terms and/or factors: 1) Changing the albedo to reduce net

radiation, 2) improving ventilation affecting human heat load, and 3) increase evaporative potential areas. However, the first two alternatives are permanent and can potentially lead to negative effects during the autumn/winter period when albedo increases due to solar inclination reducing net radiation, and cool winds could increase thermal sensation (wind chill). Nonetheless, the third alternative may not lead to negative effects in winter especially when it comes from vegetation, particularly trees. Accordingly with the proper implementation of urban vegetation, it is possible to mitigate the UHI due to the cooling potential given by transpiration (Barradas, 1991; 2000; Susca, et al., 2011; Kornaska, et al., 2015).

The release of water vapor to the atmosphere by transpiring plants causes an increasing in air humidity and a decrease in air temperature. Transpiration is mainly controlled by stomatal resistance and dominated by environmental conditions (e.g. Jones, 1992; Meinzer, et al., 1993); whereas, stomatal resistance depends on the physiological behavior of the plant and is controlled by environmental conditions, too (e.g. Whitehead, et al., 1981; Jones, 1992; Barradas, et al., 2004). Because of that, transpiration rates are different among plant species, and also individuals of the same species may present transpiration rates variations depending on the prevailing environmental conditions.

However, in proposing the release of water vapor as a mechanism to mitigate UHI, it is necessary to understand the exchange between water vapor, surface and the atmosphere which is one of the most important components of the energy exchange process in the air-land interface (Kumagai, et al., 2004), and any correlation between radiation, stomata behavior and transpiration decrease or increase, can be determinate in detail for each specie and the environment.

Therefore, to develop an appropriate urban vegetation structure to mitigate UHI, it is required at first instance, to establish the transpiration behavior of each involved plant species and their structural characteristics; and secondly to build up a theoretical model to articulate mitigation scenarios choosing different plant species and modifying environmental conditions. The well-known Penman-Monteith equation (Jones, 1992) is an appropriate model to establish transpiration behavior of each concerned species, which involves physiological and environmental conditions, and it is also well-known that air

temperature (T_A) depends on sensible heat flux (Q_H), giving the support to a theoretical model based on the urban energy balance ($T_A = f(Q_H)$).

The structure of this thesis is organized in such a way that begins with the urban heat island analysis in Mexico city, such as in dry season (November to May), as in wet (June to October), over the years 2009 and 2010. Where, UHI is emphasizes and is also established in daytime and, have differences in temperatures up to 10 °C. Subsequently, an ecophysiological and environmental transpiration analysis is realized in four dominants species (*Fraxinus uhdei, Liquidambar styraciflua, Eucaliptus camaldulensis* and *Ligustrum lucidum*) in the city, overhanging that transpiration is strongly dominate by VPD and controlled by stomatal conductance and *Liquidambar styraciflua* presents higher transpiration, while *Fraxinus uhdei* the lower. Next step, a phenomenological model is presented to mitigate UHI, based in the first thermodynamic law and parameterize in such way that is possible realized, diagnostics or predictions with routines and easy measurement variables as geographical position, temperature, relative humidity, visibility, etc., with which is possible determinate the number of tress quantity to reduce air temperature until 1 to 3 °C or the necessary. Overhanding, it is required, 63 *Eucaliptus camaldulensis* big tress by hectare to reduce temperature 1 °C, while to decrease 2 °C, only 24 *Liquidambar styraciflua* big trees are needed. Finally, to reflect and tackle about this problematic of mitigate the heat island in Mexico, since every city presents its own characteristic, giving differences in comfort index in conurban areas of Mexico cities as Veracruz-Boca del Río. And, with this, to implement a strategy to take the first steps to mitigate heat island in cities with over 500,000 inhabitants, based on the climate type in each city.

CHAPTER 2. AIMS AND HYPOTHESIS

2.1 Aims and objectives

The main objective of this work was to build a simple phenomenological model based on the energy balance to explore the effect of dominant urban trees on the mitigation of the UHI in a typical neighborhood of Mexico City in the dry season. The more specific aims were:

1) to establish the extent and intensity of the urban heat island in Mexico City

2) to analyze the energy balance components in urban areas and in totally different vegetation arrangements

3) to characterize the potential cooling of the air through tree transpiration of different tree species

4) to calculate/estimate the net radiation from easily and routine data such as air temperature, air humidity and visibility

5) to parameterize the sensible heat flux versus air temperature

6) to suggest changes in the urban structure to mitigate the urban heat island

7) to suggest urban heat island mitigation strategies in main cities of Mexico in function of climate and population

2.2 Hypothesis

The mitigation of the urban heat island can be performed through the manipulation of the energy balance components, by increasing the latent heat flux by tree transpiration which leads to a decrease of the sensible heat flux and therefore the air temperature.

CHAPTER 3. METHODOLOGY

3.1 Study site

3.1.1 Location

Measurements were made in the Metropolitan Area of Mexico City (MAMC), with 16 delegations from Ciudad de México and 18 municipalities from the Estado de México. The metropolitan area is found in an originally closed hydrological basin that was open in an artificial way at principles of XVII century (INECC, 2013). This basin includes the MAMC and some areas such as portions of Hidalgo, Tlaxcala and Puebla states (Ezcurra and Mazari, 1996).

Mexico City is one of the biggest cities in the world (Barradas, et al., 1999), it extends over an area of 7,500 km ^{2} and located within the transversal neovolcanic axis (INEGI, 2011a), surrounded by groups of mountains at east, west and south, and in the north limited by a discontinued series of short mountains. Highest picks are Popocatépetl and Iztacíhuatl, with an altitude 5,465 and 5,230 m asl, respectively (Ezcurra and Mazari, 1996) (Fig. 3.1).

Mexico City has had a rapid and steady growth, in both population and urban area, for example, between 1980 and 2010, human population increased from 14,052,263 (Cruz, 2000) to 20,137,152 (INEGI, 2011b) and urban area was from 1,115.6 km^2 (Sánchez, 1996) to 1,627.0 km ^{2} (INEGI, 2011 b). Seven of the sixteen delegations has urban ground: Azcapotzalco, Benito Juárez, Coyoacán, Cuauhtémoc, Iztacalco, Miguel Hidalgo and Venustiano Carranza and the nine remaining has conservation soil: Álvaro Obregón, Cuajimalpa, Gustavo A. Madero, Iztapalapa, Magdalena Contreras, Milpa Alta, Tlalpan, Tláhuac and Xochimilco. This conservation soil serves to water catchment and infiltration, climate regulation and improve air quality and biodiversity.

The location of the metropolitan area is within the area comprised in the extreme north and south between 19.665 N and -99.083 W, corresponding to Villa de las Flores and

19.255 N and -98.999 W for Tláhuac and the east and west ends 19.474 N and -98.896 W to Chapingo and 19.373 N and -99.282 W to Cuajimalpa, respectively, and an average altitude of 2,240 m asl (INEGI, 2011a).

3.2 Vegetation

The 5% from this city extension of 7, 500 km^2 is occupied by public accessible vegetation. 20.4 % from urban soil is public and private green areas, which 56% are woods, and the remaining 44% is grass and shrub (INEGI, 2011a). Benito Juárez, Tlalpan, Coyoacán and Cuauhtémoc have above 74% of woods surfaces; however, Tláhuac only have 4.4% and Venustiano Carranza and Iztapalapa are below 28% woods.

Figure 3.1, shows that the metropolitan area occupies more than half of the whole region, however, this region contain an area of temporal agriculture. Whereas in the south, it is found a predominant part of pine forest, and a small area of grassland and a fir forest.

3.3 Climate

Metropolitan Area of Mexico City has a highland subtropical climate, modified by altitude where annual temperature range is relatively narrow due to its geographical location. In the dry season (cold and warm season; November to May) the Bermuda anticyclone moves southward allowing polar air masses to invade most of the country inducing that the study area has low rainfall and weather types as clear skies and calm conditions (Alemán and García, 1974).

In the wet season (warm season) when the Bermuda high moves northward, it allows to trade winds prevails in the study area causing atmospheric instability and moist conditions (Alemán and García, 1974). Mean annual rainfall (mean of 40 years) is 748 mm and nearly 94% occurs during the rainy season (June-November). Winds are light and predominantly from the Northeast (SARH, 1982).

Extreme temperatures occur in April (26 ºC) and January (5.3 ºC) (SARH, 1982), with a marked heat island effect in the urban areas (Jáuregui, 1971), not only at night but also during daytime, with differences of up to 10 °C (T_{U-R}) compared to surrounding areas (Ballinas, 2011).

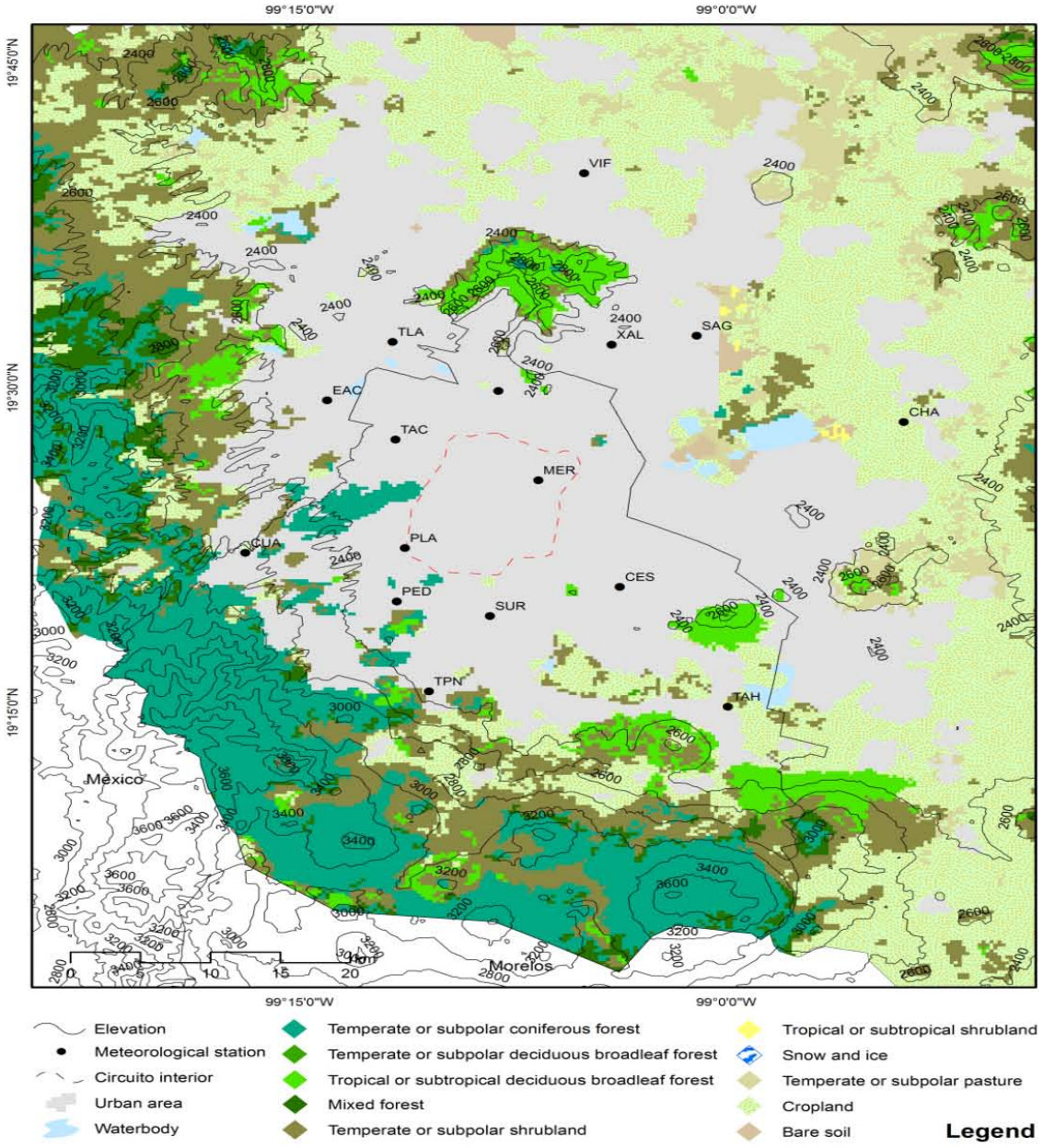

Figure 3.1. Mexico City Metropolitan Area configuration, vegetation distribution, elevation and spatial distribution of stations of the meteorological network (modified from INEGI, 2011b).

Energy balance measurements were performed in a district (Escandon district) near to the center of the Metropolitan Area of Mexico City. Delimited by streets with intensive vehicular traffic, and the land use in the study area is mainly commercial and residential with 57% occupied by buildings of three to four stories, 37% for roads and paved areas, and the remaining 6% is covered by vegetation (Fig. 3.2). The mean height (Z_h) of the surrounding buildings is 12 m, and it was estimated that the aerodynamic surface roughness (Z_0) was 1 m. The zero displacement plane *d* was calculated to be 8.4 m height according to the rule-of-thumb estimate (d=0.7Z_h) (Grimmond and Oke, 1999a). During the measurements period the footprint calculation averaged 1150 m (Velasco, et al., 2009).

Figure 3.2. Aerial view around the study site (marked with a white disk). The white circle indicates the 1000-m distance around the measuring tower.

3.4 Theoretical framework

3.4.1 The urban energy balance

As it was mentioned in chapter 1, UHI is a climate-meteorological phenomenon that it is mainly generated by the change of land use from rural to urban, where the energy is redistributed. A simple model of the energy balance ($W m^{-2}$) in a city is given by the following expression (Oke, 1988):

$$Q_N + Q_A = Q_E + Q_H + Q_S + Q_{AD} \quad [1]$$

where Q_N is the net radiation (available energy), Q_A is the energy given to the system by human activity (industry, internal combustion machines, heating, air conditioning, etc.), Q_E is the latent heat flux (evaporation/transpiration), Q_H is the sensible heat flux (air warming), Q_S is the energy storage in the urban fabric and Q_{AD} is the horizontal transport of energy (advection).

In many cases Q_A term can be neglected since the energy consumption is frequently very low compared with solar radiation. This term becomes significant in cold climate urban centers as New York (USA) where human activities and energy use are high; ranging between 20 and 160 $W m^{-2}$ as compared to energy provided through solar radiation, ranging between 700 to 1000 $W m^{-2}$ (Taha, 1997). Considering the low energy consumption in Mexico City, this term can be neglected. Also Q_{AD} term is commonly neglected in the urban area because the urban fabric is uniform and there is no significant energy sources or sinks in the representative area of measurements. Accordingly to these assumptions ($Q_A = Q_{AD} = 0$) the urban energy balance is reduced to: $Q_N = Q_E + Q_H + Q_S$. Where Q_N is given by:

$$Q_N = [(1 - \alpha)R_{SI} + (I\downarrow - I\uparrow)] \quad [2]$$

where α is the albedo, R_{SI} the impinging solar radiation and $(I\downarrow - I\uparrow)$ the fraction of long wave radiation from the surface and from the air.

3.4.2 The UHI mitigation phenomenological model

The phenomenological model is based on the reduced urban energy balance, first at all by estimating Q_N and Q_S. Net radiation can be calculated by this form of Q_N :

$$Q_N = \left[(1-\alpha)R_{SI} + \varepsilon_A \sigma T_A^4 - \varepsilon_C \sigma T_C^4\right] \qquad [3]$$

where R_{SI} is the incident solar radiation (W m^{-2}), α is the surface albedo (urban canopy), ε_A and ε_C are the atmospheric and surface emissivity, respectively; T_A and T_C are air and surface temperature (°K), respectively and σ is the Stefan-Boltzmann constant (4.903 10^{-9} MJ K^{-4} m^{-2} d^{-1}). R_{SI} can be estimated as follow (Schmetz and Raschke, 1978):

$$R_{SI} = (\bar{R}/r)^2 (S_0 \cos\Theta)(a.b^m) \qquad [4]$$

where S_0 is the solar constant (1360 Wm^{-2} ≈ 2750 μmol m^{-2} s^{-1}), Θ is the zenith distance of the sun and cosΘ calculation is given as:

$$\cos\Theta = [(\text{sen}\varphi \cdot \cos\eta)(-\cos\alpha_z \cdot \text{sen}\chi) - \text{sen}\eta \cdot (\text{sen}\alpha_z \cdot \text{sen}\chi)$$

$$+ (\cos\varphi \cdot \cos\eta) \cdot \cos\chi] \cdot \cos\delta + [\cos\varphi\lambda \cdot (\cos\alpha_z \cdot \text{sen}\chi)$$

$$+ (\text{sen}\varphi \cdot \cos\chi] \cdot \text{sen}\delta$$

where φ, η, δ, α_z y χ are the latitude, angular time of the day, day of year (solar declination), azimuthal orientation, and the slope of the surface, respectively, and δ is given by: δ = -23.4 cos[360(t_d + 10)/365], and t_d is day of year or the Julian day (Jones, 1992), and a and b are the effective transmission factor, *m* is the optical air mass, r and $\bar{R}$ are, respectively, the actual and the mean distance of the Earth from the Sun, in astronomical units (ua) and $\bar{R}$ = 149,600,000 km = 1 ua, and r = 1+0.033cos[($t_d 2\pi$/365)] where t_d is day of the year or the Julian day, and

$$m = [\cos\Theta + 0.15(93.885 - \Theta)^{-1.253}]^{-1} [P_M/P_{NM}] \qquad [5]$$

being P_M the average atmospheric pressure on the site and P_{NM} is the atmospheric pressure at sea level; and a and b depend on the visibility (km) which is a function of the urban aerosols given by: a = 0.0096 ln(visibility) + 0.7947 and b = 0.144 ln(visibility) + 0.2397. The atmosphere emissivity $\varepsilon_{A,}$ estimation is given by:

$$\varepsilon_A = 0.179 e^{1/7} \exp(350 / T_A)$$

where e is the actual vapor pressure (kPa) = e_SRH and e_S = 0.6108 exp[(17.27T_A)/(T_A + 237.3)] where T_A is in °C and RH is the relative humidity (0-1).

Energy storage (Qs) is one of the factors that can make the UHI more intense (Grimmond, et al., 1991):

$$Q_S = a_1 Q_N + a_2 \left(\frac{\Delta Q_N}{\Delta t}\right) + a_3 \qquad [6]$$

where t is the time (30 or 60 min), and a_1, a_2 and a_3 are constants depending on the distribution and the characteristics of the urban fabric. These parameters are 0.671, 0.450 s and −52 W m^{-2}, respectively (Velasco, et al., 2011). Energy storage in this paper is taken constant in each time step, then the residual of Q_N is distributed only in Q_H and Q_E in every time step ($Q_N = Q_H + Q_E$). As it is well-known, sensible heat flux is the responsible for the air warming, thus it is possible to parameterize Q_H as a function of T_A ($Q_H = f(T_A)$). Therefore $T_A = f(Q_H)$ and $Q_H = Q_N - Q_E$, finally $T_A = f(Q_N - Q_E)$, and Q_H and Q_E could be parameterized using the simplified Penman-Monteith approach as follows (Holtslag and Van Ulden, 1983):

$$Q_H = \frac{(1-\alpha_{PM}) + (\frac{\gamma}{S})}{1+\frac{\gamma}{S}} (Q_N - Q_S) - \beta \qquad [7]$$

$$Q_E = \frac{\alpha_{PM}}{1+\frac{\gamma}{S}} (Q_N - Q_S) + \beta \qquad [8]$$

where S is the slope of the saturation vapor pressure versus temperature, γ is the psychrometric constant α_{PM} and β are empirical parameters. These parameters are 0.029 and 7.33, respectively, for the study site (Velasco, et al, 2011). Nevertheless, Q_E in this case is the measured flux and the added flux due to tree transpiration is Q_{ETRP}. Finally, the air temperature mitigation would be: $T_A = f(Q_N - [Q_E + Q_{ETRP}])$. Also Bowen ratio was estimated from the relation Q_H/Q_E.

Latent heat flux produced by trees (Q_{ETRP}) was calculated using the Penman-Monteith model (Bosveld and Bouten, 2001):

$$Q_{ETRP} = \lambda_E = \frac{S Q_N + \rho C_P \left[\frac{VPD}{r_A}\right]}{S + \gamma\left[1 + \frac{r_C}{r_A}\right]} \qquad [9]$$

where $Q_{ETRP} = \lambda_E$ is the latent heat flux (W m^{-2}) due to tree transpiration, S is the slope of the saturation vapor pressure (kPa $°C^{-1}$), ρ is the density of air at constant pressure (kg m^{-3}), C_P is the specific heat of air at constant pressure (J kg^{-1} K^{-1}), *VPD* is the vapor pressure deficit (kPa), γ is the psychrometric constant (kPa K^{-1}), r_C is the resistance of the canopy (s m^{-1}) and r_A is the aerodynamic resistance of the canopy (s m^{-1}). Vapor pressure deficit was calculated with the equation: VPD = e_S(1-RH), where e_S is the saturation vapor pressure. Aerodynamic resistance (r_A) (s m^{-1}) was estimated with the following relation:

$$r_A = \left[\frac{1}{(K^2)(u)}\right] \ln\left[\frac{z_W - d}{z_O}\right] \ln\left[\frac{z_O - d}{(0.2)(z_O)}\right] \qquad [10]$$

where Z_W is the height at which the wind was measured (m), d (m) is the level of displacement of zero, K is the constant of von Karmann , u is the wind speed (m s^{-1}), and Z_0 is a measure of the aerodynamic surface heterogeneity, in our case, vegetation (m). Resistance of the canopy (r_C) (m s^{-1}) was calculated as follows:

$$r_C = \frac{r_S}{LAI} = \frac{1}{g_C} \qquad [11]$$

where LAI is the leaf area index (m^2 m^{-2}), r_S is the stomatal resistance which is the inverse of stomatal conductance (g_S), and g_C is the canopy conductance.

The model used for analyzing and predicting stomatal conductance ($g_S = 1/r_S$) from the driving variables has been previously described by Jarvis (1976) and modified by Dolman (1993) and Wright, et al., (1996). The model is based on the hypothesis that steady-state stomatal conductance depends on environmental variables (Stewart, 1988; Roberts, et al., 1990; Barradas, et al., 2004). This method consists in selecting the data of the likely upper limit of the function (envelope function) represented by a cloud of points in each of the diagrams produced by plotting stomatal conductance versus any environmental variable. The envelope function method has three assumptions: 1) the envelope function represents the optimal stomatal response to a selected climate variable (*e.g.* irradiance); 2) the points below the selected function are the result of a change in any of the other variables (*e.g.* vapor pressure deficit, air temperature), and 3) there are no synergistic interactions (Jarvis, 1976; Fanjul and Barradas, 1985; Barradas, et al. 2004). The model takes the form:

$$g_S = g_{SMAX}\left[g(Q_N)g(VPD)g(T_A)\right] \qquad [12]$$

where g_{SMAX} is the maximum value of the measured stomatal conductance, and $g(Q_N)$, $g(T_A)$, g(VPD), are the normalized boundary-line functions (0–1 values) that incorporate the effects of irradiance I, air temperature T_A, air vapor pressure deficit (VPD) and are as follow: $g(Q_N) = (aQ_N)/(b + Q_N)$, $g(VPD) = c + dVPD$ and $g(T_A) = e + f\,T_A + g\,T_A^2$ where a, b, c, d, e, f and g are parameters of the model.

3.4.3 Transpiration, total conductance and decoupling coefficient

Total conductance (g_T, m s^{-1}) was estimated from time averaged transpiration (TRP, kg m^{-2} s^{-1}) and mean vapor pressure deficit (VPD, Pa) as:

$$g_T = \frac{\lambda\gamma}{\rho\varepsilon C_p}\frac{TRP}{VPD} \qquad [13]$$

where γ (Pa °C^{-1}) is the psychrometric constant, λ (J kg^{-1}) is the latent heat of evaporation of water, ρ (kg m^{-3}) is the air density, ε is the mole fraction of water in air (0.622 kg water per kg air) and Cp is the specific heat of dry air at constant pressure (J kg^{-1} °C^{-1}). Vapor pressure difference or deficit was calculated as the vapor leaf–air gradient $VPD_G = e_{SL} - e$, where e_{SL} is the saturated vapor pressure of the leaf and e is the actual air vapor pressure; but $e = RHe_S$ where RH is the relative humidity (0–1) and $e_{SA}$is the saturated air vapor pressure, therefore $VPD_G = e_{SL} - RHe_S$ and $e_S = 0.6108\exp[(17.27T)/(T + 237.3)]$ where T is the leaf temperature (T_L) in the case of e_{SL} and /or the air temperature (T_A) in the case of e. However, when $T_L = T_A$; $VPD = e_S(1 - RH)$ which is the air vapor pressure deficit. When T_L was measured, the 95% of the cases was equal to T_A, therefore all calculations were referred to air vapor pressure deficit (VPD) and calculated every 30 min.

Total conductance is the sum of canopy (g_C) and aerodynamic (g_A) conductance ($g_T = g_C + g_A$). Canopy conductance (m s^{-1}) was estimated as the product of mean stomatal conductance (m s^{-1}) and leaf area index (LAI, m^2 m^{-2}; $g_C = g_S LAI$). Aerodynamic conductance (m s^{-1}), calculated as the inverse of aerodynamic resistance ($g_A = 1/r_A$), was estimated from the difference of total resistance ($r_T = 1/g_T$) and canopy resistance ($r_C = 1/g_C$) as:

$$\frac{1}{g_A} = r_A = \frac{1}{g_T} - \frac{1}{g_C} \qquad [14]$$

and g_S was calculated using the parameterization of equation 13.

A dimensionless decoupling coefficient (Ω_C) was calculated to analyze the dependence of canopy transpiration on physical or physiological factors. A formula to express the relative sensitivity of canopy transpiration to a marginal change in stomatal conductance was introduced by Jarvis and McNaughton (1986):

$$\Omega_C = \frac{1}{(1+\left[\frac{\gamma}{s+\gamma}\right])(g_A/g_C)} \qquad [15]$$

where S (Pa °C^{-1}) is the rate of change of saturation water vapor pressure with temperature (°C).

3.5 Measurements, materials and data

3.5.1 Urban heat island data

The meteorological data generated by the metropolitan meteorological network (REDMET) of Mexico City were used for the analysis. It consists of 15 stations in strategic locations as shown in figure 3.1 and table 3.1. Meteorological data for the years 2009 and 2010 were chosen, because with such years will have a very updated determination of the distribution and intensity of the UHI, but also in those years El Niño and La Niña occurred, respectively. Data were corrected by altitude mainly at Cuajimalpa and Chapingo where the elevation is 200 and 60 m higher than the rest of the meteorological stations, respectively. Like temperature change with altitude, was necessary used potential temperature (dry adiabatic), as a correcting form to have a better understanding of differences temperatures between stations areas.

The UHI distribution was determined with monthly average hourly temperature and plotted in charts corresponding to each month of the analyzed years using spline interpolation with a geographic information system (ArcGIS version 9.2; ESRI, CA, USA). Its intensity was determined by calculating the temperature difference between each of the urban weather stations and a rural station (T_{U-R}) that was located in Chapingo.

3.5.2 Transpiration and total conductance

Measurements of transpiration and stomatal conductance were made on four individuals of four dominant species to Mexico City: *Fraxinus uhdei* (Wenz.) Lingelsh. (Oleaceae), *Ligustrum lucidum* W.T. Aiton (Oleaceae), *Eucaliptus camaldulensis* Dehnh. (Myrtaceae) and *Liquidambar styraciflua* L. (Hamamelidaceae). *F. uhdei* and *L. styraciflua* are deciduous trees and native to Mexico, whereas *L. lucidum* and *E. camaldulensis* are evergreen and introduced species. Trees were located in public areas, in a street lateral platform formed a single row of planted trees completely surrounded (around a radius of 300 m) by paved areas of asphalt and cement, in a area with no buildings around, and a water collection area (bare soil) around the trunks of the trees of 0.25 m^2 (square of 0.5 m).

Table 3.1. Name, location and predominant land use as the building-paved ratio (B/P) and green area (GA) of each station of the meteorological network.

				Land use (%)	
Station	Name	Latitude °N	Longitude °W	B/P	GA
TAC	Tacuba	19.460	-99.194	82.7	15.0
EAC	ENEP Acatlán	19.490	-99234	84.2	14.0
SAG	San Agustín	19.540	-99.017	67.3	1.0
TLA	Tlalnepantla	19.535	-99.195	90.5	9.9
XAL	Xalostoc	19.533	-99.067	94.9	5.1
MER	La Merced	19.429	-99.110	85.4	14.0
PED	Pedregal	19.336	-99.193	73.4	25.0
CES	Cerro de la Estrella	19.347	-99.062	90.8	9.1
PLA	Plateros	19.337	-99.188	88.4	11.5
VIF	Villa de las Flores	19.665	-99.083	95.3	4.6
CUA	Cuajimalpa	19.373	-99.282	79.0	21.0
TPN	Tlalpan	19.267	-99.174	80.5	19.0
SUR	Santa Ursula	19.324	-99.138	78.5	21.5
TAH	Tláhuac	19.255	-98.999	45.8	54.0
CHA	Chapingo	19.474	-98.896	9.00	91.0

Trees were planted in north-south rows spaced 6 m apart with no assembly of their crowns. Tree species structural parameters are shown in Table 3.2. Urban vegetation in public areas is administered by the municipality.

Table 3.2. Leaf area indices (LAI, m^2 m^{-2}), diameter at breast height (DBH, cm), crown diameter (CD, m) and leaf size (LS, long (*l* , cm), wide (*w*, cm)) for the studied species. LAI was estimated with a canopy analyzer (LAI-2000, LI-COR Ltd., Lincoln, Nebraska, USA) (n=4 for LAI, DBH and CD) and (n=40 for LS).

Species	LAI	DBH	H	CD	Leaf Size (*l*,*w*)
F. uhdei	4.5	21.0	15.0	11.0	8.02 (1.57), 3.50 (1.16)
L. lucidum	4.0	14.8	13.0	8.10	6.13 (1.14), 3.02 (0.86)
E. camaldulensis	4.1	15.1	14.0	7.2	11.63 (2.42), 3.15 (0.81)
L. styraciflua	4.5	26.5	14.0	14.5	6.25 (1.17), 5.95 (1.38)

Transpiration of these species was estimated from sap flow measurements made in the trunk using steady-state xylem water mass-flow metering systems similar to those described by Čermák, et al. (1984) and Schulze, et al. (1985) with one instrumental set per tree. Xylem water mass-flowmeters were connected to a data logger (21XL, Campbell Scientific, Logan, Utah, USA); voltage and gauge signals were scanned every 20 s and averages were logged every 30 minutes. Total conductance was obtained from daily measurements of transpiration and vapor pressure deficit between 101 and 116 doy in 2013.

3.5.3 Sap flow

Sap flow was calculated from $F = (P_S - P_l)k/(C_W \Delta T)$, where Ps is input power to the heater, C_W is the heat capacity of water, k is the dimensionless relation of measured segment length to total tree circumference, ΔT is the temperature difference across the heater which is maintained constant and P_1 reflects heat loss due to conduction and convection which is determined during nights when sap flow is absent. During steady-state conditions the applied power does not normally exceed 2 W (with a potential maximum of 20 W). During the measuring period, 5 electrodes per system of the size 60 x 15 x 1 mm were inserted up to 50 mm into the trunk while depth of insertion of thermocouples was 25 mm according to the measured sapwood depth (3-4.5 cm) obtained by taking samples with a Pressler drill.

The measuring point was insulated with a polyurethane and aluminized mylar jacket from outside by protecting against weathering and to minimize external effects on ΔT. Xylem water mass-flowmeters were connected to a data logger (21XL, Campbell Scientific, Logan, Utah, USA); voltage and gauge signals were scanned every 20 s and averages were logged every 30 min. Heat storage in the stem segment during each 30 min interval was estimated by measuring the changes in stem temperature during the first and the last minutes of each interval.

3.5.4 Stomatal and canopy conductance

Stomatal conductance was measured in the same individuals of each species at four sites on at least five fully sunlit and shaded expanded leaves per plant, with a steady-state diffusion porometer (LI-1600, LI-COR, Lincoln, Nebraska, USA); air and leaf temperature (T_A, T_L), relative humidity (RH) and photosynthetically active radiation (PAR) were also measured with the mounted sensors in the porometer (Fanjul and Barradas, 1985). Concomitantly, irradiance, air temperature and humidity, wind speed and direction were measured with a pyranometer (Eppley PSP, Campbell-Scientific, USA), a temperature-humidity probe (HMP35C, Campbell-Scientific, USA), and an anemometer and vane set (03001, R M Young, USA), respectively. Irradiance, wind sensors and temperature-humidity probe were installed 3 m above the highest tree canopy in a telescopic tube, that is to say these sensors were installed 18 m above the floor surface. The outputs from all sensors were connected to a data logger (21X, Campbell Scientific, USA) and scanned every 30 s and 30 minutes averages logged. Sensors above the canopy were calibrated before the study and cleaned every week during the study period. Sap flow measurements were made during eight days in March (doy 82-89) and 16 days in April (doy 101-116) in 2013 (hottest month) in Mexico City from 07:00 to 20:00 LT, and extensive measurements of stomatal conductance and related measurements were made during six days (84, 87, 104, 106, 110 and 114) in 2013. It did not rain either before, during or after measurements.

3.5.5 Energy balance measurements

Net radiation, sensible and latent heat fluxes were measured continuously for 13 days from 17 to 30 March, 2006. March is one of the warmest months of the year in Mexico City with mean minimum and maximum temperatures of 7.7 °C and 24 °C, respectively, and average monthly precipitation rate of 9.3 mm.

Instruments for measuring heat fluxes were installed on a 25 m tower mounted on a 17 m tall building giving a total height of 42 m, almost three times the average height of the surrounding buildings. Net radiation was measured with a Kipp and Zonen net radiometer CNR1. Wind speed, virtual temperature, and humidity fluctuations were sampled at 10 Hz with a 3 D sonic anemometer (Applied Technologies, Inc., model SATI-3K) and an open-path infrared gas analyzer (OP-2 IRGA, ADC BioScientific). Fluxes were calculated every 30-min using the eddy covariance method and corrected for the effects of air density using the Webb corrections. A detailed description of the instrumentation and methodology used in the eddy covariance system is provided by Velasco, et al. (2009).

3.5.6 The human thermal comfort index

As the UHI directly affects the human energy balance, mitigation must be understood in the limit when people begin to experience heat stress which is possible to do it by applying different thermal comfort indexes, and so far the most recommended is the physiological equivalent temperature (PET). This index is defined as the temperature at any location (inside or outside of buildings) and equivalent to T_A, in a typical interior arrangement (no solar radiation and wind), the heat load of the human body remains and body and skin temperatures are equal to external conditions where is evaluated (Höppe, 1999). This index has the advantage of being universal and is independent of clothing and metabolic activity, is given in degrees Celsius and thus can easily relate to the common experience, it is not based on subjective measures and is used in both temperate and warm climates. Furthermore, this index can be easily calculated if the program RayMan is used (Matzarakis, et al., 2007) with at least hourly data of temperature and relative humidity

(RH) of the site. Table 3.3 shows the different categories of thermal perception and physiological stress of PET index.

Table 3.3. Physiological equivalent temperature (PET) intervals and different categories of temperature perception and physiological stress in humans, with typical heat production (80 W) and the resistance to heat transfer by clothing (0.9 clo) (Matzarakis and Mayer, 1996).

PET	Thermal perception	Grade of physiological stress
< 4 °C	Very cold	Extreme cold stress
4 °C	Cold	Strong cold stress
8 °C	Cool	Moderate cold stress
13 °C	Slightly cool	Slight cold stress
18 °C	Comfortable	No thermal stress
23 °C	Slightly warm	Slight heat stress
29 °C	Warm	Moderate heat stress
35 °C	Hot	Strong heat stress
41 °C	Very hot	Extreme heat stress
> 41 °C		

With this index type, apart from determining the degree of thermal human comfort/discomfort, can also be used as a suitable tool to establish in which areas and in what time it can be considered the existence of thermal pollution, understanding the latter as a heat excess generating a heat stress, which in PET case could be above 23 °C and it may be equivalent to an air temperature as low as 14 °C with relative humidities from 60 to 90%. However, the limit of 23 °C PET could rise to 29 °C (boundary between light- warm and warm) which corresponds to a T_A and RH of 19 °C and 40%, respectively.

Finally, figure 3.3 shows in a flow chart the sequence of practical steps to mitigate the UHI as a general model where it is necessary first, to locate and analyze the existing UHI in each city and the determination of a human comfort index, in this case the

physiological equivalent temperature (PET) and it is taken equal or greater than 23 °C corresponds a human perception of slightly warm with a physiological stress of slight heat stress (Matzarakis, et al., 2007) (Table 3.3).

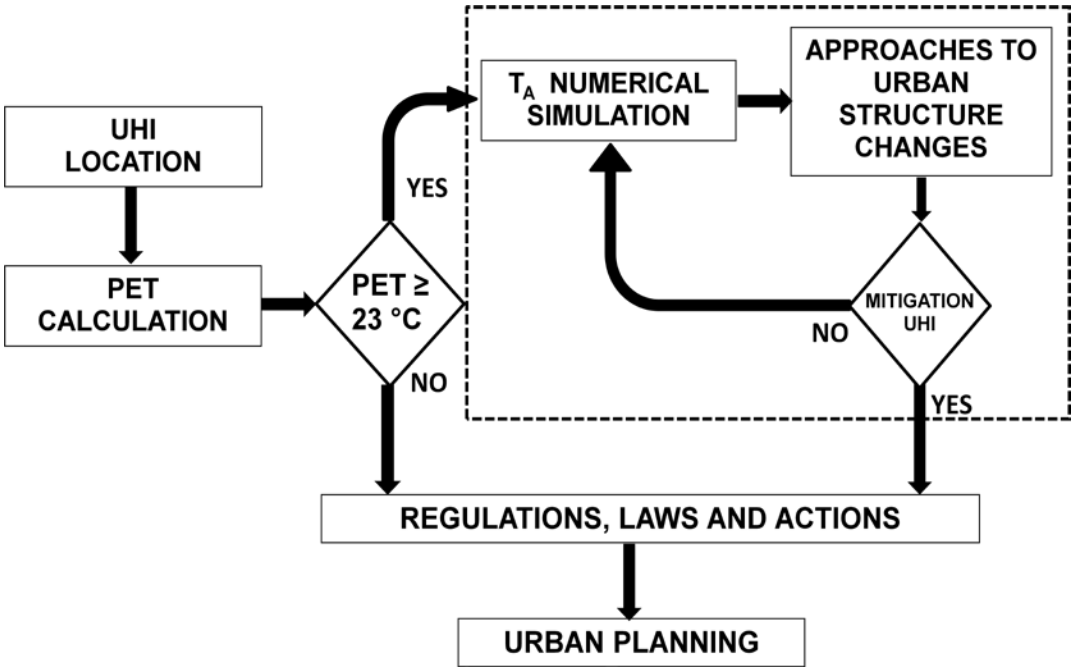

Figure 3.3. Flowchart of a general model to mitigate UHI. The discontinuous line represents the UHI mitigation phenomenological model based on the energy balance.

CHAPTER 4. RESULTS AND DISCUSSION

4.1 The urban heat island in Mexico City

Figure 4.1 shows the spatial distribution of the average temperature at 06:00 and 14:00 local time (LT) in January and May 2010 in Mexico City. At 06:00 LT, a warm center is developed and located in the area surrounding by Cerro de la Estrella (CES), San Agustín (SAG), Villa de las Flores (VIF), ENEP-Acatlán (EAC) and Pedregal (PED) stations, oriented to the center-north of the city, with temperature differences (T_{U-R}) near of 3.5 °C and the highest T_A of 8.5 °C (Fig. 4.1A). Whereas at 14:00 LT (Fig. 4.1B), the warm area has shifted to the west of the city, and is smaller than that observed at 06:00 LT with a T_{U-R} of approximately 2.5 °C and the highest T_A around 21 °C. However, a large area was established in much of the city where temperatures were lower than their surroundings forming a new island, probably this effect is due to the ventilation of the city as wind speed increases from 13:00 to 15:00 LT up to 4.4 m s^{-1} in combination with the topography of the area (Jazcilevich, et al., 2005).

On May 2010 the distribution and the location of the warm center was similar to that presented in January but with higher temperatures. In the morning (06:00 LT) the T_{U-R} was 0.5 °C higher than that observed in January (Fig. 4.1C); however, T_{U-R} was higher about 2 °C in May than in January at 14:00 LT (Fig. 4.1D), with the highest temperature around 26 °C. These results are very similar for that observed in 2009.

The temperature difference in the area of La Merced (MER) may be up to 7.1 °C as occurred at 04:00 LT on January 21. However, there are periods of low T_{U-R} which are between 0.09 and 1 °C, around 01:00 and 14:00 LT, respectively (Fig. 4.2).

In June the UHI thermal intensity is similar in the selected meteorological stations (MER, EAC) than that observed in January (Fig. 4.3). However, there is an intensity inversion at VIF and TPN, since TPN shows a similar behavior to VIF in January and viceversa in June. Thermal intensity at MER area was up to 8.9 °C as occurred at 17:00 LT on June 8. However, at the same time at EAC area T_{U-R} was 12.1 °C and 6.32 and 9.3 at VIF.

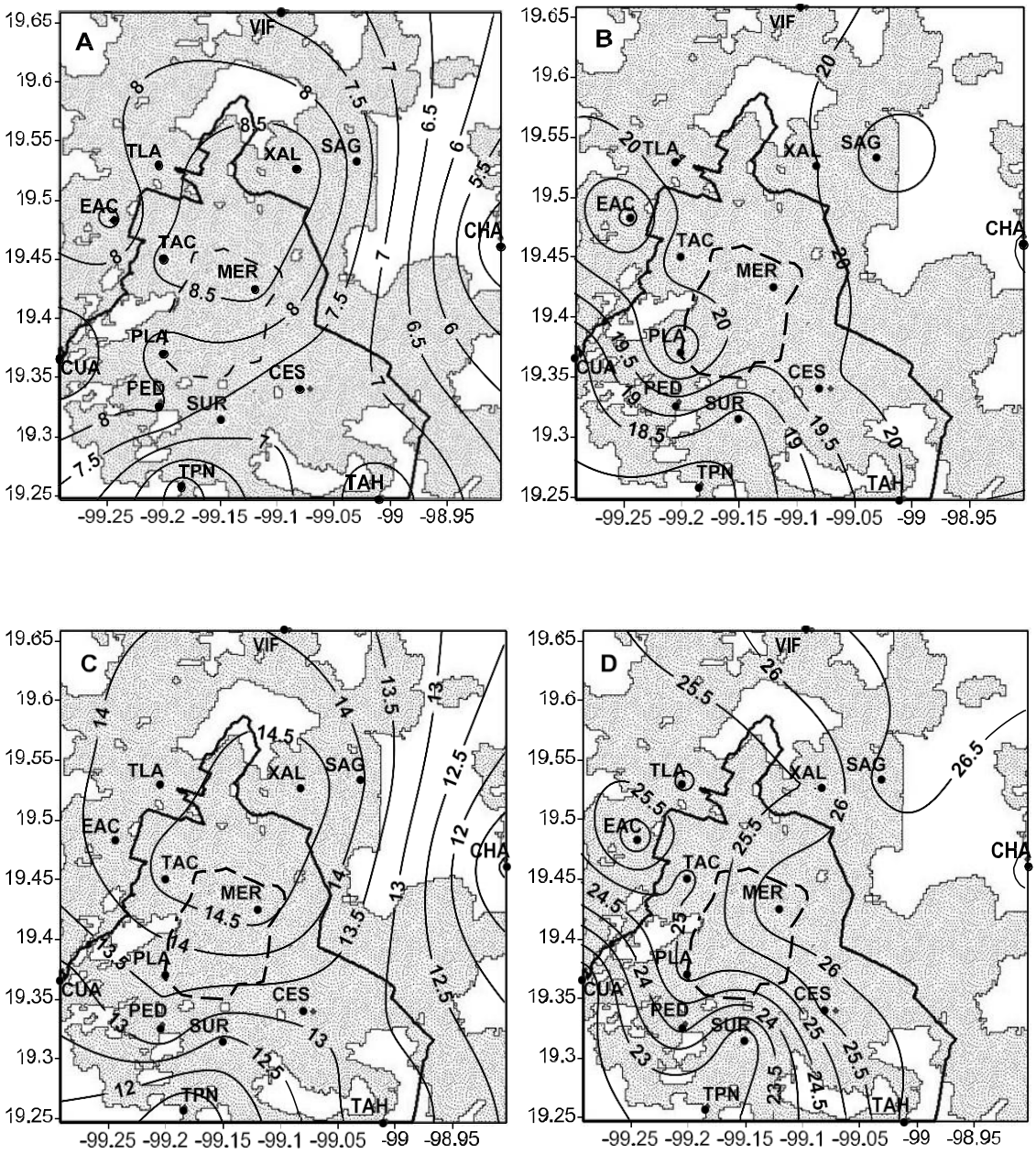

Figure 4.1. Average air temperature (°C) distribution in January (A, B) and May 2010 (C, D) at 06:00 (A, C) and 14:00 LT (B, D) in Mexico City.

and TPN, respectively. In average, $T_{U-R} > 0$ was 2.5, 2.0, 2.7 and 0.8 °C, whereas $T_{U-R} < 0$ was -1.1, -0.73, -0.8 and -1.47 °C at MER, VIF, EAC and TPN, respectively (Fig. 4.2). This behavior shows a shifting of the UHI to the south maybe due to the fact that the rainy season is establishing.

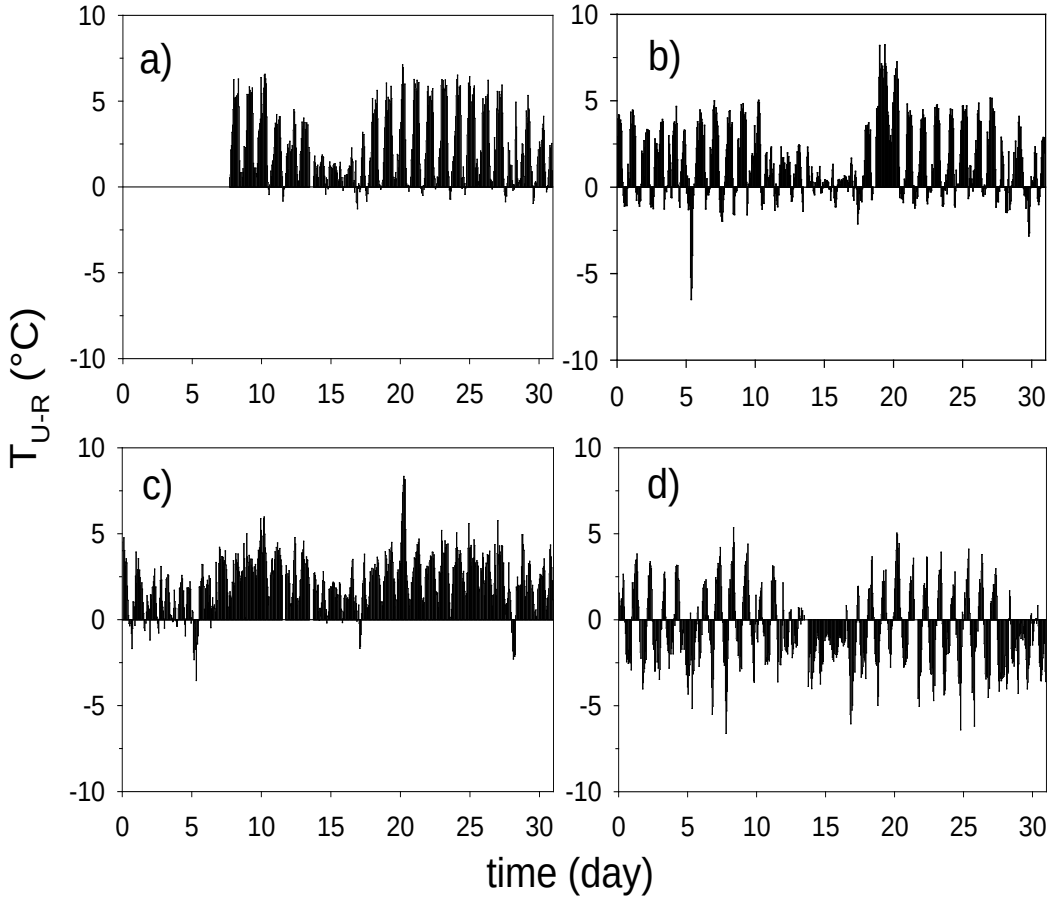

Figure 4.2. Temperature difference T_{U-R} (°C) in January 2009 at a) La Merced-Chapingo, b) Villa de la Flores-Chapingo, c) ENEP Acatlán-Chapingo and d) Tlalpan-Chapingo.

Urban heat island distribution and intensity in 2009 were very similar to that observed in 2010 (Fig. 4.2 and 4.3); with temperature differences up to 10 and 9° C in January and June, respectively at MER. With these results it is possible deduce the effect of El Niño and La Niña on both the distribution and the intensity of the heat island is not significant. Clearly, in cases when $T_{U-R} >> 3$ °C is possibly due to the effect of some synoptic factors governing the season, or weather types as cloudy, rainy or windy, mainly due to the cooling of the surroundings of the rural meteorological station as occurs after raining than heating the urban area. Currently, the actual UHI compared with that reported by Jáuregui and Luyando (1998) increased from 112.7 km^2 (Circuito Interior) to the area between the meteorological stations of Cerro de la Estrella (CES), San Agustín (SAG),

Villa de las Flores (VIF), ENEP-Acatlán (EAC) y Pedregal (PED) (≈754.29 km^2), and its intensity increased 2 °C . However, unlike the typical, UHI is also established during the daytime, with intensities of up to 10 °C (T_{U-R}).

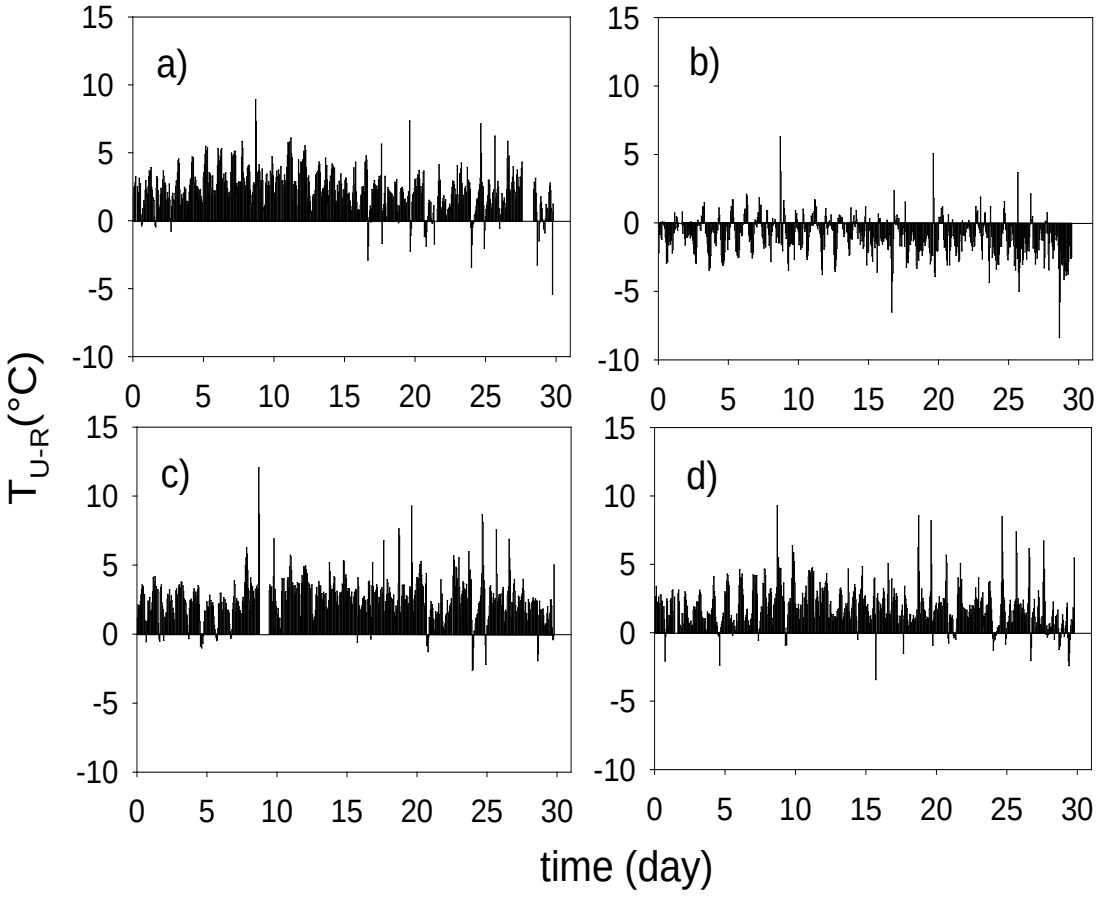

Figure 4.3. Temperature difference T_{U-R} (°C) in June 2010 at a) La Merced-Chapingo, b) Villa de la Flores-Chapingo, c) ENEP Acatlán-Chapingo and d) Tlalpan-Chapingo.

This temperature increase involves a direct effect in the thermal comfort index, where undoubtedly people will experience more heat stress and thus it is very likely that energy consumption could increase to cool the living spaces and human health will be severely affected (Laschewski and Jendritzky, 2002). Furthermore, this actual temperature differences could be enhanced with the global climate change (Brazel and Quattrochi, 2005). Also, heat shocks will increased or be enhanced by the UHI effect (Luber and

McGeehin, 2008; Basara *et al*., 2010). From these points of view, UHI could be considered as a form of thermal pollution. Therefore, it is urgent and necessary to implement UHI mitigation strategies since those differences can significantly affect human health and increase energy consumption. Further studies are being conducted to explore alternatives for the UHI mitigation in Mexico City.

4.2 Transpiration and canopy conductance

The environmental conditions during the experimental period are shown in figure 4.4 VPD average was 1.28 kPa fluctuating between 3.27 (maximum) and 0.087 kPa (minimum). Of 0.0871 (night time) (Fig. 4.4A). Irradiance increased rapidly from early in the morning to around midday, reaching the maxima values between 850 and 1050 W m^{-2} with an average value for all the measurement period of 445.7 W m^{-2} (Fig. 4.4B). Changes in the total amount of transpiration per day (TRP) were observed during the experiment for the four species (Fig. 4.4C). TRP was non similar for every species during the experiment. In general *Liquidambar styraciflua* reached the highest values as high of 5.43 L on day 116 whereas *Eucaliptus camaldulensis* registered as low as 2.69 L on day 102. Over the measuring period (days 101-116), average TRP values for species were 4.35, 4.09, 3.90 and 3.64 L d^{-1} for *Liquidambar styraciflua, Fraxinus uhdei, Eucaliptus camaldulensis* and *Ligustrum lucidum*, respectively. These transpiration rates represent a gross energy consumption of 10.64, 9.99, 9.52 and 8.9 MJ d^{-1} per species, equivalent to 37, 35, 33 and 31% of the average incoming short-wave radiation, respectively.

Figure 4.5 shows transpiration rates of the four species on day 114. Transpiration throughout the day showed generally a uni-modal pattern with some slight changes and increasing as irradiance to reached its maximum value around midday. Sequences of TRP patterns show that transpiration before 8:00 and after 17:00 LT was negligible. The highest daily transpiration was registered by *L. styraciflua* (936 g m^{-2} d^{-1} = 0.936 mm d^{-1}) and the lowest by *L. lucidum* (755 g m^{-2} d^{-1} = 0.755 mm d^{-1}) with maxima rates of 0.043 and 0.034 g m^{-2} s^{-1}, respectively, registered between 12 and 14: 00 LT. Maximum diurnal

transpiration rates represent an energy consumption of 77.3, 80.2, 104.7 and 91.8 W m^{-2} for *E. camaldulensis*, *F. uhdei*, *L. styraciflua* and *L. lucidum*, respectively.

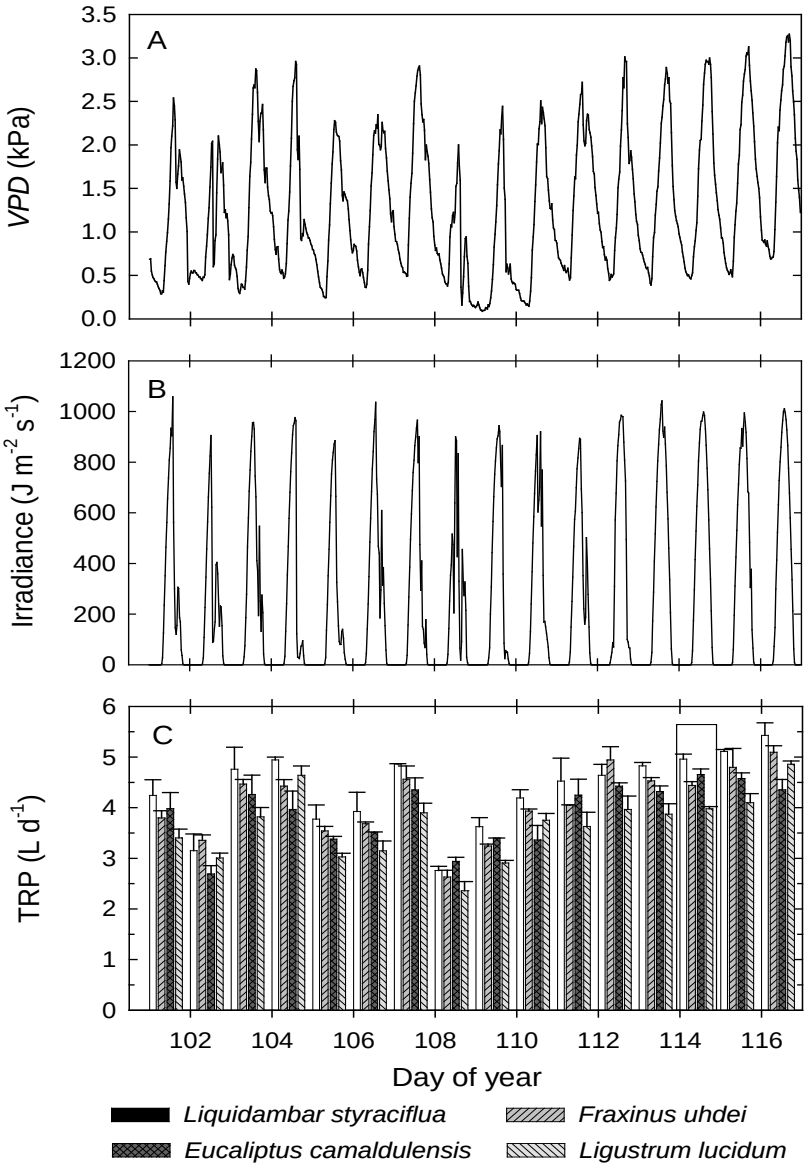

Figure 4.4. Vapor pressure deficit (VPD) (A), irradiance (B) and daily transpiration (C) during the experiment in four tree species in Mexico City. Each histogram is the mean of four trees. Vertical bars on histograms are S.E. of the mean. Box represent one of the day when intensive measurements were done and presented in figures. 4.5, 4.6 and 4.7.

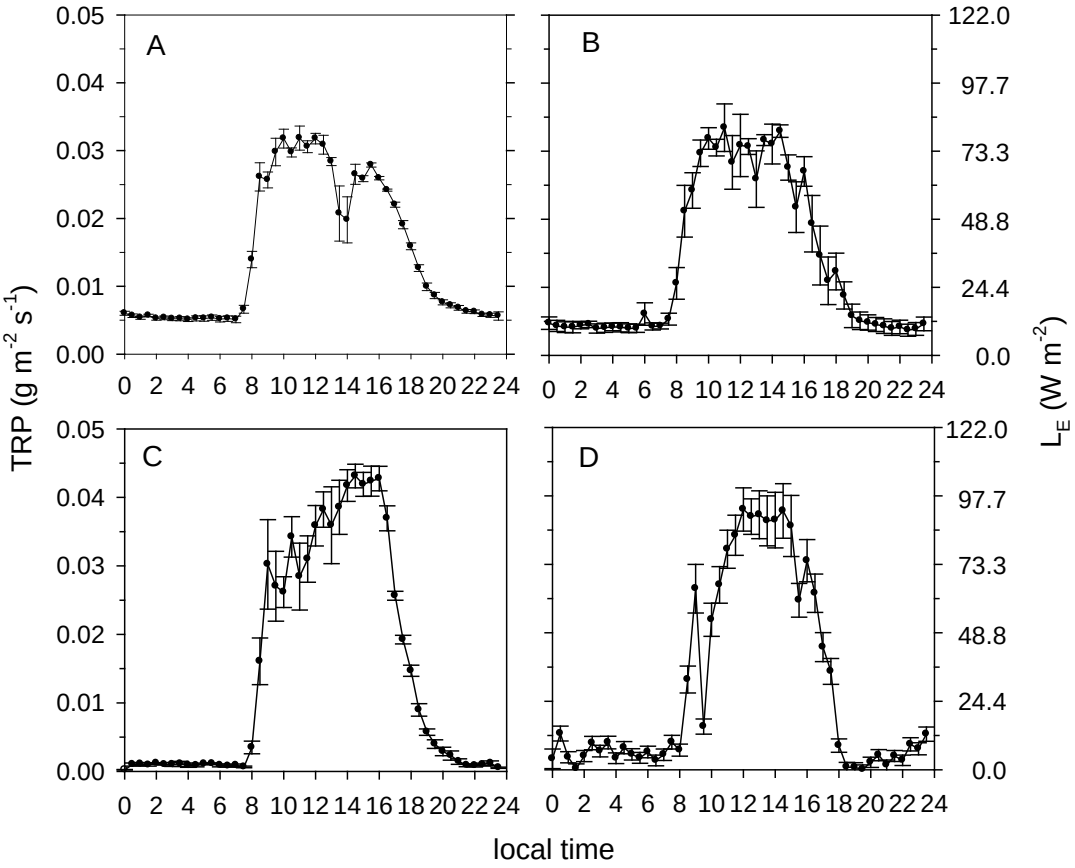

Figure 4.5. Diurnal patterns of transpiration rate (TRP) and latent heat flux (L_E) for *Eucaliptus camaldulensis* (A), *Fraxinus uhdei* (B), *Liquidambar styraciflua* (C) and *Ligustrum lucidum* (D) during day of year 114. Data points represent the mean of four measurements on different trees. Bars represent the standard error.

The diurnal course of total conductance (g_T) was similar in the four species showing a maximum value between 12 and 16:00 LT. However, g_T was lower than those values corresponding to g_C after midday for *L. styraciflua* and *L. lucidum*, and around 16:00 LT for *E. camaldulensis* and *F. uhdei* (Fig. 4.6). Aerodynamic conductance (g_A) patterns were similar in the four species with two peaks, one from midnight to early morning (24:00-06:00 LT) and the other from late in the morning until the evening (10:00-20:00 lh) with values as high as 111.41 mm s^{-1} at noon (*L. lucidum*). During daylight time, g_C in average registered values between 39.8 (*E. camaldulensis*) and 49.74 mm s^{-1} (*L. lucidum*) and 21.8

(15:00 LT) and 33.7 (13:30 LT) mm s^{-1}, respectively. Aerodynamic conductance was from three to five times higher than canopy conductance (Fig. 4.6).

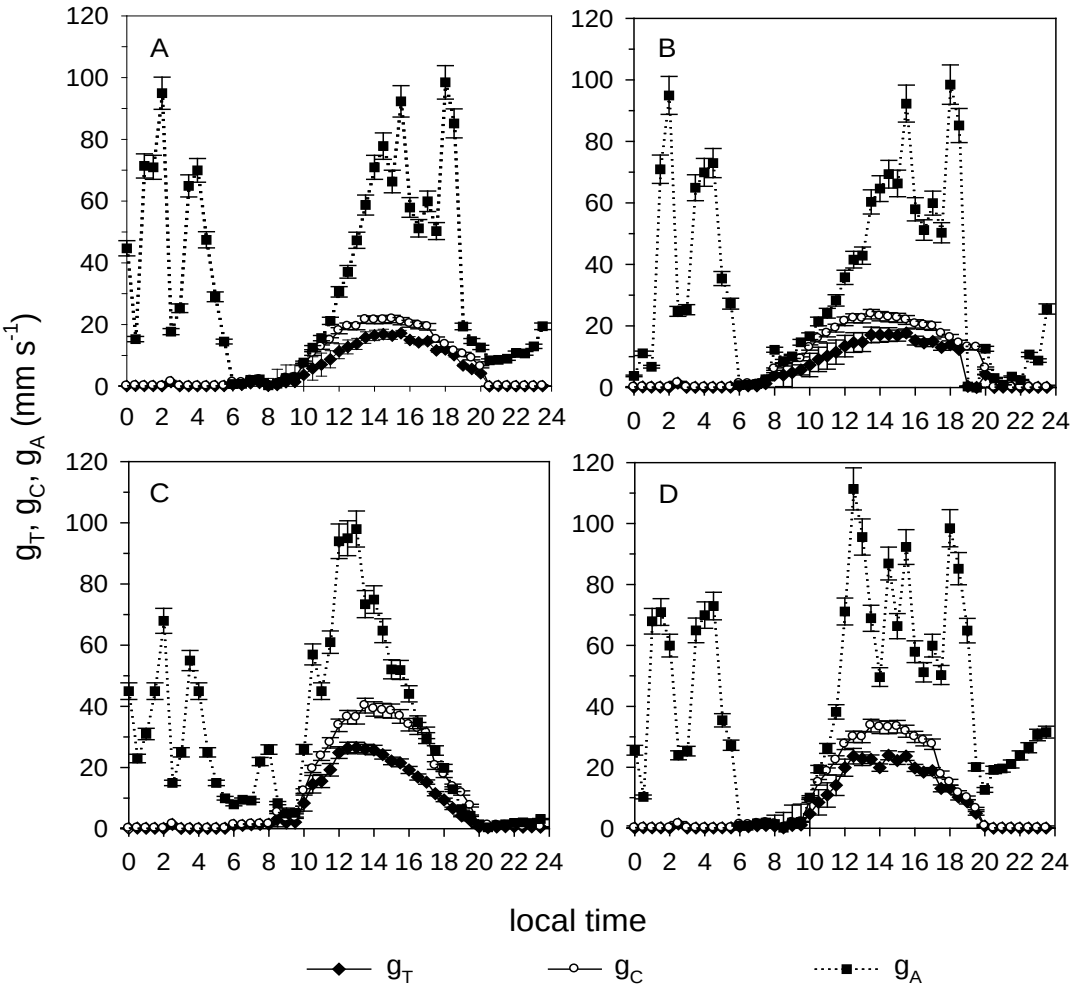

Figure 4.6. Diurnal patterns of total conductance (g_T, black diamonds), canopy conductance (g_C, white circles) and aerodynamic conductance (g_A, black squares) for 114 day of year, when intensive measurements were made. Values are the averaged and bars represent the standard error (n = 4), for canopy conductance N=20.

Tree transpiration is a reliable mechanism to mitigate high heat loads in Mexico City, and therefore to mitigate the urban heat island effect, even with the relatively low transpiration rate registered by *E. camaldulensis* on day 102. However, it looks like that *L. styraciflua* and *L. lucidum* have the greatest cooling potential to mitigate UHI, because they registered the highest transpiration rate values, as much as 105 W m^{-2} early in the afternoon

(14:00-16:00 LT). It also appears, in the scope of this study, that *L. styraciflua* and *L. lucidum* are better options to reduce the heat load, mainly in the early afternoon, when the maximum temperature is recorded. Although it is difficult to compare transpiration rates in different places in the world because of the particular micrometeorological and soil conditions, transpiration rates of the studied species were in reasonable agreement with other results in the world. Transpiration rates here appear to be low compared with other TRP values found in other species and in other sites. TRP for the studied species were much lower than those observed in non-stressed Douglas fir in Vancouver (Tan *et al.*, 1978) or beech forest in Maruia, New Zealand (Kelliher, et al. 1992) or red maple in South Carolina, but higher than stressed red maple (Bauerle, et al. 2002). It is necessary to point out that in Mexico City, trees are not commonly irrigated and probably the observed transpiration rates are low. Nevertheless, actual transpiration rates presented in this investigation can dissipate up to 20% of maximum net radiation registered in Mexico City and reported by Barradas, et al. (1999) at noon when it is around 560-600 W m^{-2}.

In general, Ω_C values were low, averaging from 0.086 (*L. lucidum*) to 0.125 (*F. udhei*) with maximum values between 0.67 (*F. uhdei*) and 0.56 (*L. lucidum*) and minimum from 0.0003 (*L. lucidum*) and 0.0007 (*L. styraciflua*). The highest Ω_C values were recorded around sunrise and/or sunset and the lowest from 12:00 to 18:00 LT, showing a similar pattern for *L. styraciflua*, *L. lucidum* and *F. uhdei*; and the contrary to *E. camaldulensis* (Fig. 4.7). High values are consistent with low g_A values in the four species.

According to Leuning, et al. (1991) and Roberts and Rosier (1993), the response of stomatal conductance to vapor pressure deficit is an important factor in deciding the amount of water used by trees. Several authors have indicated the role of leaf conductance in the control of water use and its relationship with the coupling between canopy and atmosphere (Dye, 1987; Hinckley and Braatne, 1994). In this sense, Jarvis and McNaughton (1986) introduced a dimensionless decoupling coefficient (Ω_C), which approaches unity as stomatal control decreases. One implication of $\Omega_C \rightarrow 0$ is that the stomatal control of transpiration is high, while a fractional change in stomatal conductance (proportional to canopy conductance) would lead to an equal change in transpiration. Stomata exert less control on canopy transpiration as $\Omega_C \rightarrow 1$ and, as a result, transpiration

becomes increasingly dependent on the net radiation received and less dependent on vapor pressure deficit (Gu, et al., 2005; Nicolas, et al., 2008).

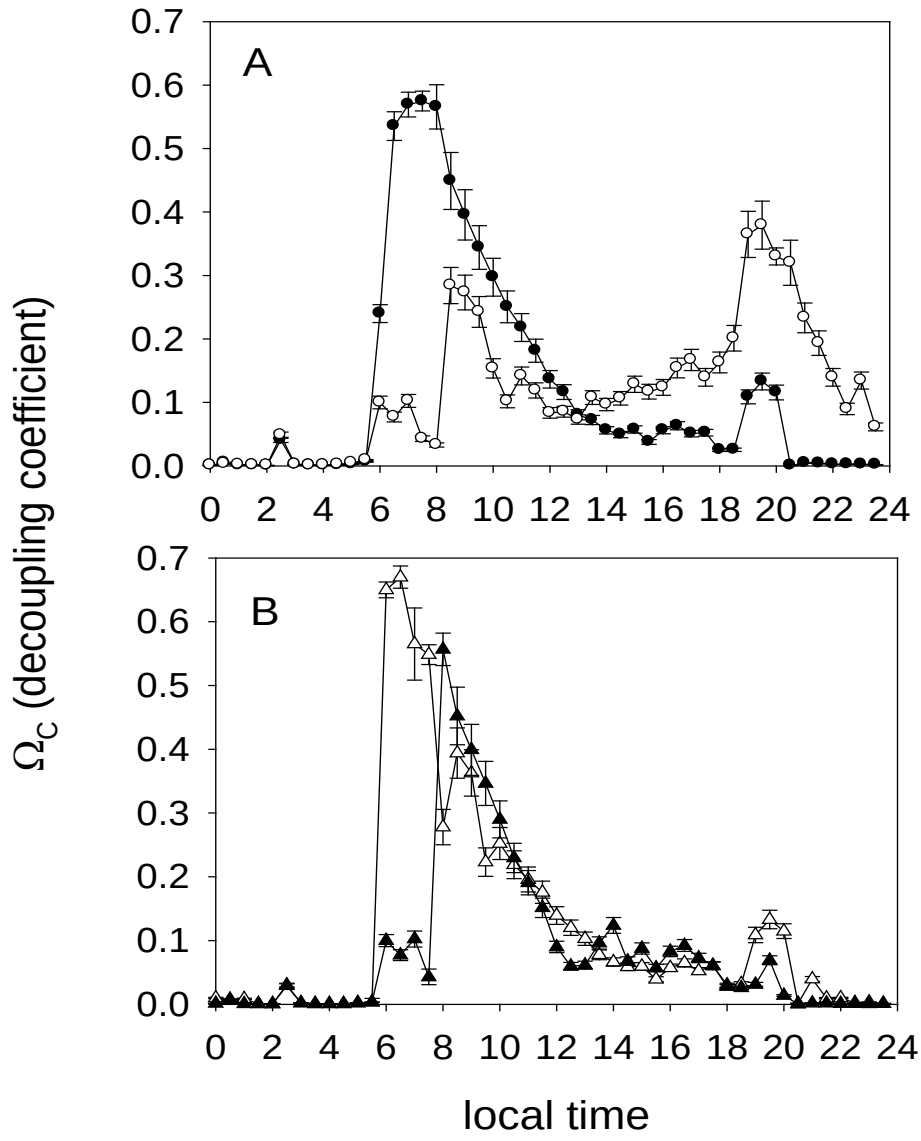

Figure 4.7. Diurnal patterns of decoupling coefficient (Ω_C) for 114 day of year, when intensive measurements were made for *Eucaliptus camaldulensis* (open circles) and *Liquidambar styraciflua* (closed circles) (A), and *Fraxinus uhdei* (open triangles) and *Ligustrum lucidum* (closed triangles) (B). Values are the averaged and bars represent the standard error (n= 4).

The low values of the decoupling coefficient (Ω_C) found in this study suggest that all the studied species were well coupled to the atmosphere mainly from 10:00 to 18:00 LT. It is interesting to note that *E. camaldulensis* presents a different behavior through the day to the pattern showed for the other species. This could be due to the size of its crown (1.3 to 1.5 fold) and the length of its leaves (2 fold) which are larger than the ones of the others species. *L. lucidum* was slightly more coupled to the atmosphere than the other species, which had relatively higher Ω_C values. Nevertheless, the other three species also showed low Ω_C values. These results demonstrate that water vapor exchange was strongly dominated by VPD and controlled by stomatal conductance, mainly in between sunrise and sunset.

4.3 The stomatal conductance model

The plotted data of individual measurements of normalized stomatal conductance (g_S) plotted against Irradiance (*I)* (Fig. 4.8) during the experiment, showed a significant scatter, but the probable envelope function of the data was described by a hyperbolic relationship of the form: $g(I) = AI/(B+I)$ with coefficients of determination between 0.90 and 0.98. The relationships and parameter values for the four species are given in figure 4.8. The values of *B* for *L. Lucidum* and *F. udhei* were consistently lower than those for *L. styraciflua* and *E. camaldulensis* reflecting a lower sensitivity to irradiance for these species.

The effect of T_A on g_S was described by a second degree polynomial of the form: $g_S = a + bT_A + cT_A^2$ where *a*, *b* and *c* are constants. These constants and relationships are shown in figure 4.8 with coefficients of determination (r^2) between 0.91 and 0.98. The optimal (T_O) and cardinal temperatures (T_{min} and T_{MAX}) of stomatal function were calculated from this polynomial relationship by computing the roots and the first derivative for each species and season. Maximum stomatal conductance occurred around 28.3 ± 2.0 °C for the four studied species, whereas cardinal temperatures of g_S were similar for *E. camaldulensis*, *F. uhde*i and *L. lucidum* with higher values than *L. styraciflua*.

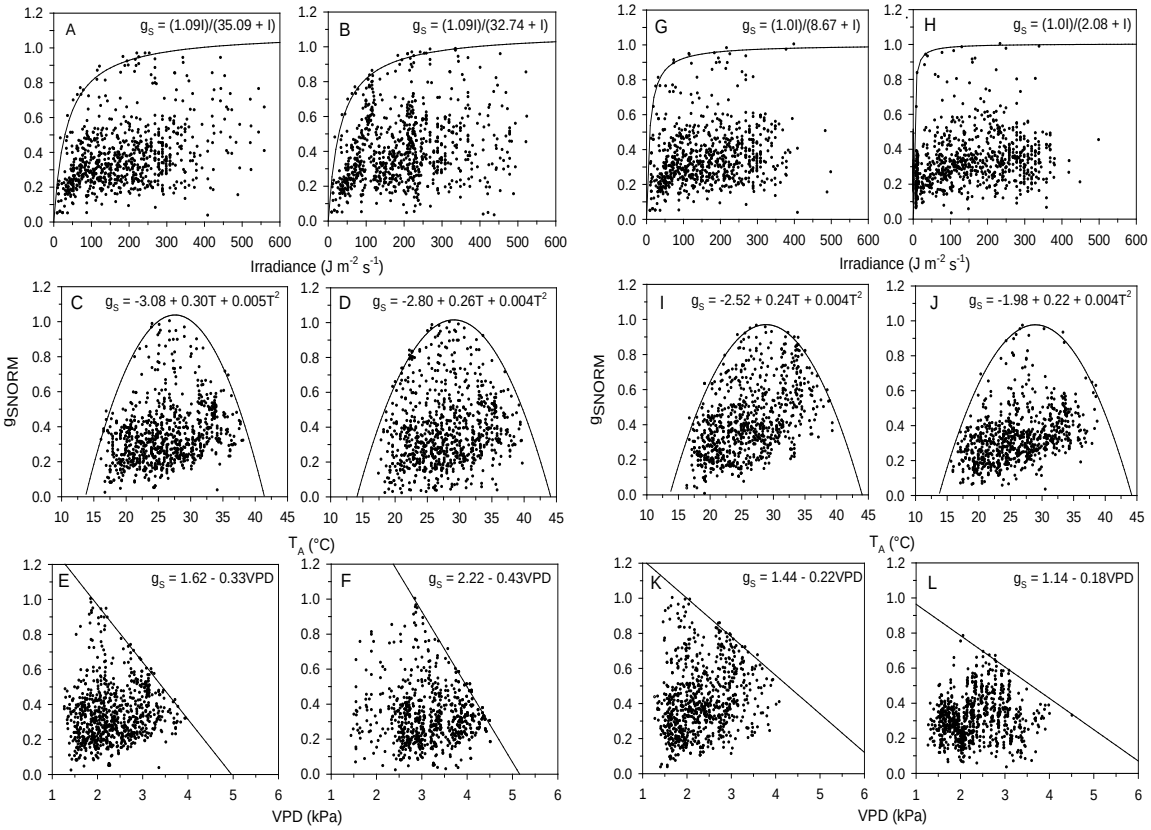

Figure 4.8. Scatter diagram and probable boundary line of normalized stomatal conductance (g_S) plotted against irradiance (I), air temperature (T_A) and vapor pressure deficit (VPD) for *Liquidambar styraciflua* (A, C, E), *Eucaliptus camaldulensis* (B, D, F), *Fraxinus uhdei* (G, I, K) and *Ligustrum lucidum* (H, J, L) when intensive measurements were made during the experiment.

Stomatal conductance in the four species tended to decrease linearly as VPD increased. Stomatal sensitivity to VPD was different for the four species. *E. camaldulensis* and *L. styraciflua* registered the higher sensitivities to VPD than *L. lucidum* and *F. uhdei*. *E. camaldulensis* was approximately 25, 49, and 59% more sensitive to VPD, than *L. styraciflua*, *F. uhdei* and *L. lucidum*, respectively (Fig. 4.8).

Liquidambar styraciflua registered the maximum stomatal conductance (10.05 mm s^{-1}), whereas *Ligustrum lucidum* was intermediate (8.42 mm s^{-1}), to *F. uhdei*, and *E. camaldulensis* with the lowest values (6.00 and 5.41 mm s^{-1}, respectively).

However, stomatal conductance also depends on the VPD. The higher the VPD, the smaller the g_S. The fit of g_S versus VPD (r^2 = 0.91- 0.97) showed a higher sensitivity of g_S to this driving variable in the four studied species. *E. camaldulensis* was the species which responded more sensitively to changes in VPD than the others (Fig. 4.8).

On the other hand, the decreasing/increasing in stomatal conductance has been attributed to an increasing/decreasing in VPD and T_A (Schulze and Hall 1981; Schulze 1986; Maroco, et al., 1997; Meinzer, et al., 1997), or to a combination of these factors. The curve lines of g_S versus T_A show that the responses of g_S to T_A are very similar between species, but *L. styraciflua* showed a slightly lower range (Tmin - T_{MAX}) than the others species.

Furthermore, previous studies also have been demonstrated the effect of *I* on g_S (Pitman, 1996; Meinzer, et al., 1997; Gao, et al., 2002; Zweifel, et al., 2009). Although the four studied species reach the maximum conductance at an irradiance of 300 W m^{-2}, *L. lucidum* reached 80% of the change of g_S at 9 W m^{-2} (the more sensitive species to *I*) and *L. styraciflua* at 100 W m^{-2} (the less sensitive species to *I*).

Because of the different transpiration rates of the studied species, it is possible to select the most suitable species according to the microenvironment where the species are to be planted; however, the most suitable species would be those that showed the highest transpiration rates, as *Liquidambar styraciflua* and *Ligustrum lucidum*, while it would be better to build tree arrangements using the four species making a more biodiverse system since dissipation of net radiation is not large enough to make a difference. In this regard, it should be stressed that two of the studied species are not native, and therefore they may be objectionable because of the current preference of native species. However, the city as a completely artificial system could benefit from introduced species with the highest transpiration rates. Most likely, the studied species may have a higher transpiration rate if they were irrigated, and then further reduce of the urban heat load. Therefore, a recommendation could be a controlled irrigation to the studied species in the dry season in order to increase transpiration, and thereby reduce the heat load. Furthermore, irrigation could be extended to the whole urban vegetation system. However, this issue must be

correctly addressed since water supplies are scarce in the dry season and trees would be competing with human consumption.

Results of this study show clearly that reduction of heat loads is possible even in the dry season with no irrigation through evaporative cooling from tree soil water uptake and transpiration that would probably reduce surface and near-surface air temperatures. Additionally, this reduction in temperatures could be enhanced from the tree shading effect (Oliveira, et al., 2011).

It is important to notice, in addition to reduce heat load and energy demand using trees to mitigate Mexico City's heat loads, they also could improve air quality by removing particles from air (Al-Alawi, et al. 2007; Guzmán-Morales, et al. 2011) and public health, as well as reduce the city's contribution to greenhouse gas emissions. It is relevant to mention that some tree species could generate volatile organic compounds (VOC) which can increase air pollution (Guenther, et al. 2000; Karl, et al. 2003; Yang, et al. 2009). On the other hand, Song, et al. (2016) found that VOC´s in some way it could improve human health.

4.4 Energy balance

Figure 4.9 shows the performance of the components of energy balance for a typical day (day of year, doy 78) in the period of measurements. Net radiation increased rapidly from dawn (-106.6 W m^{-2}) to around midday, reaching a maximum of 693. 5 W m^{-2}. In the afternoon Q_N tended toward zero to reach its minimum in the sunset. In average Q_N was 449.0 W m^{-2} for $Q_N > 0$.

Sensible and latent heat fluxes increased with the rise in Q_N in the morning to reach their maxima around midday. However, during the day Q_E, Q_H and Q_S were not as regular as Q_N. Most of the available energy (53%) was dissipated by Q_S with values up to 428.0 W m^{-2} early in the afternoon (average daytime value was 224.0 W m^{-2}), followed by Q_H with a maximum value of 210.0 W m^{-2} late in the morning, and an average of 153.0 W m^{-2}. Q_E registered the lowest values with 204.0 W m^{-2} around midday, and an average of 72 W m^{-2},

just 16% of Q_N (Fig. 4.9). Bowen ratio in average was 2.92. During the whole experiment averaged values were 373.3, 190.0, 121.43 and 41.52 W m^{-2} for Q_N, Q_S, Q_H and Q_E, respectively.

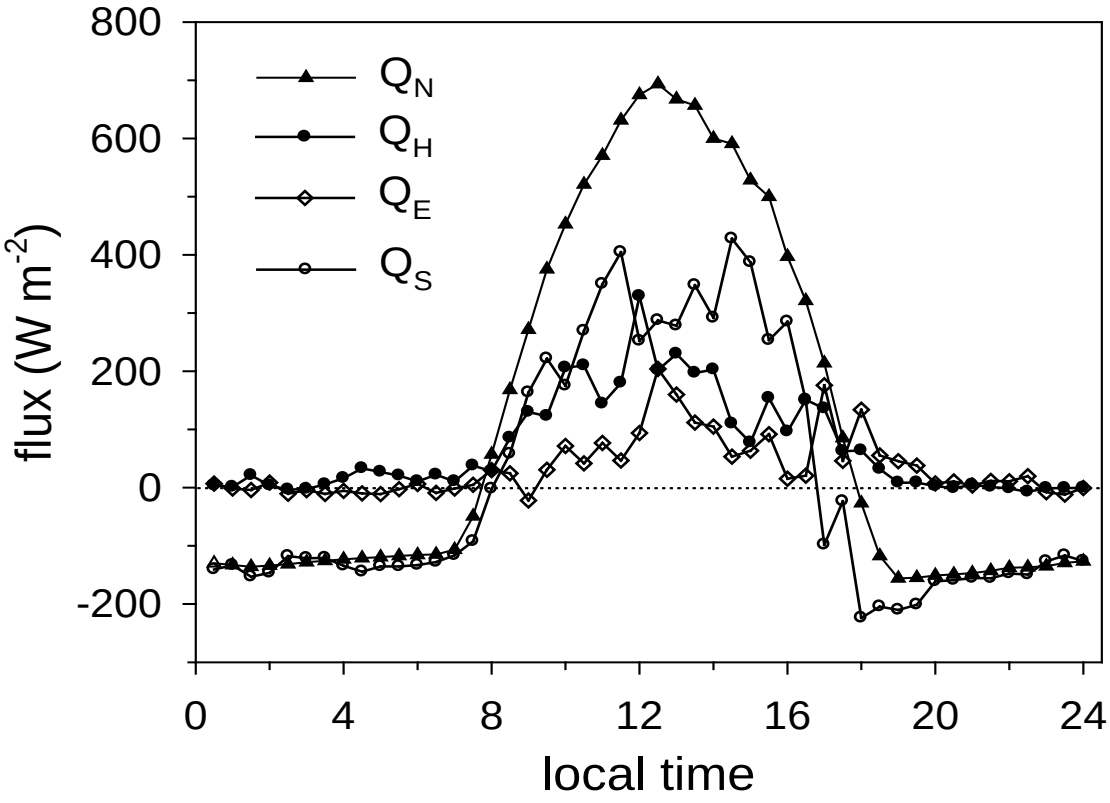

Figure 4.9. Energy balance components (W m^{-2}) in the Escandon district in Mexico City in a typical day of the dry season on doy 78.

4.5 Relationship between T_A and Q_H

Energy balance and micrometeorological data measured in the Escandon district were used to relate air temperature versus the sensible heat flux, taking into account the delay between the emission of sensible heat and T_A for $Q_N>0$. T_A that is not directly proportional to Q_H in time, while having a measured flux, the heating of the air and therefore its temperature, is showed after certain time. Table 4.1 shows the relationship between T_A and Q_H at different

time steps. It is noteworthy that among the changes from one to two hours, the regression coefficient increases its value, not so for the third time lag (after three hours) when this value decreases. This means that air temperature at a given time is given around two hours after the actual sensible heat flux. As a result, it is possible to consider that there is a time delay of two hours that produces it, i.e. air temperature has a delay time of two hours versus Q_H. Therefore, the relationship of air temperature depending on the sensible heat flux is given as $T_A = 0.03892Q_H + 15.3136$, and finally the diagnosis equation is:

$$T_A = 0.03892[Q_N - (Q_E + Q_{ETRP})] + 15.3 \quad [16]$$

where it can be seen that there is a basal temperature around 15 °C during the day when $Q_N > 0$. Q_E is the latent heat flux measured in the study site as a result of the remains of the 6% of vegetation, and it can be calculated with Eq. 8, and Q_{ETRP} is the necessary latent heat flux provided by vegetation to reduce T_A and can be identified as Eq. 9. Consequently, this relationship is key in the estimation of air temperature after increasing the latent heat flux by augmenting vegetation.

Table 4.1. Simple regression parameters of T_A versus Q_H ($T_A = aQ_H + b$) for all data $Q_N>0$ measured at Escandon district, for actual and delayed for 1, 2 and 3 hours (τ). Parameters values and (standard errors) are shown, $p<0.05$. Numbers in bold indicate the best fit of T_A versus Q_H.

a (°C m^2 W^{-1})	b (°C)	r^2	τ (hour)	n
0.02863 (0.00161)	15.8831 (0.177)	0.2503	0	1152
0.03544 (0.00147)	15.4896 (0.162)	0.3807	1	1056
0.03892 (0.00137)	**15.3136 (0.152)**	**0.4582**	**2**	**960**
0.03865 (0.00139)	15.3698 (0.153)	0.4505	3	864

4.6 Transpiration and canopy conductance

The environmental conditions during the experimental period are shown in figure 4.10, Net radiation increased rapidly from early in the morning to around midday, reaching the maxima values between 640 and 790 W m^{-2} with an average value for all the measurement period of 356.4 W m^{-2} when Q_N>0. VPD average was 9.0 hPa fluctuating between 23.58 (maximum, registered around midday) and 1.23 hPa (minimum, registered at night). Transpiration differed among species during the experiment, in general *L. styraciflua* showed the highest values and *L. ligustrum* the lowest. Changes in the total amount of transpiration per day (TRP) were observed during the experiment for the four species, ranging between 3.64 - 4.35 L d^{-1}. Averaged TRP values were 4.22, 3.82, 3.64, 3.59 L d^{-1} for *L. styraciflua*, *F. uhdei*, *L. lucidum* and *E. camaldulensis*, respectively. This transpiration rates represent a gross energy consumption of 10.30, 9.33, 8.89 and 8.77 MJ d^{-1}, respectively per each species.

Figure 4.11 shows transpiration rates of the four species on doy 84. Transpiration throughout the day showed generally a uni-modal pattern with some slight changes and increasing as irradiance reaches its maximum value around midday. The highest daily transpiration was registered for *L. styraciflua* (1098 g m^{-2} d^{-1}) and the lowest for *E. camaldulensis* (993 g m^{-2} d^{-1}) with maxima rates of 0.043 and 0.032 g m^{-2} s^{-1}, respectively, registered between 13:00 and 15:00 LT. Maximum diurnal transpiration rates represent an energy consumption of 98.9, 105.25, 101.83 and 78.14 W m^{-2} for *F. uhdei*, *L. styraciflua, L. lucidum*, and *E. camaldulensis*, respectively.

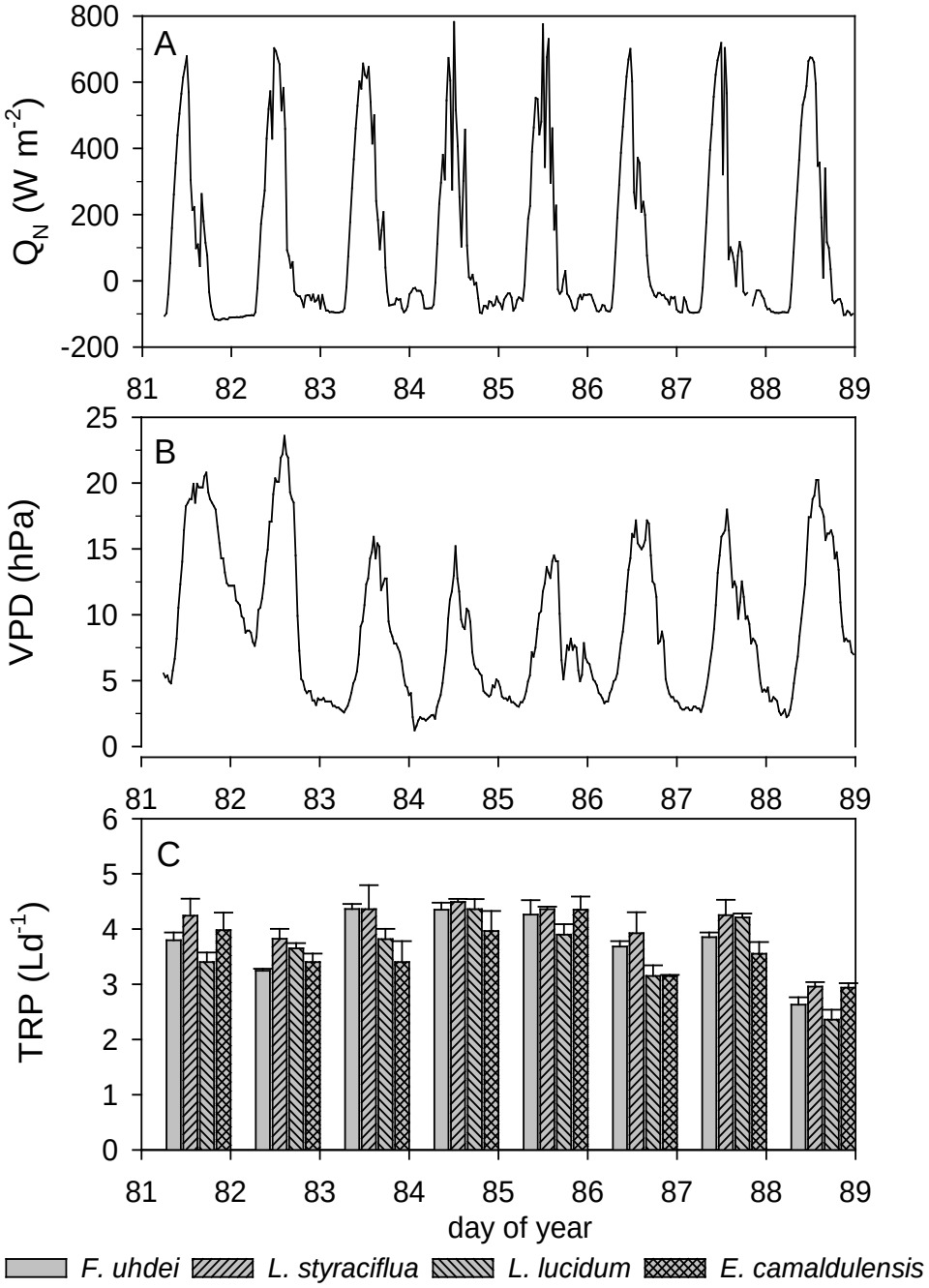

Figure 4.10. Net radiation (A,), vapor pressure deficit (VPD) (B) and daily transpiration (C) during the experiment in four tree species in Mexico City. Each histogram is the mean of four trees. Vertical bars on histograms are standard error (S.E.) of the mean.

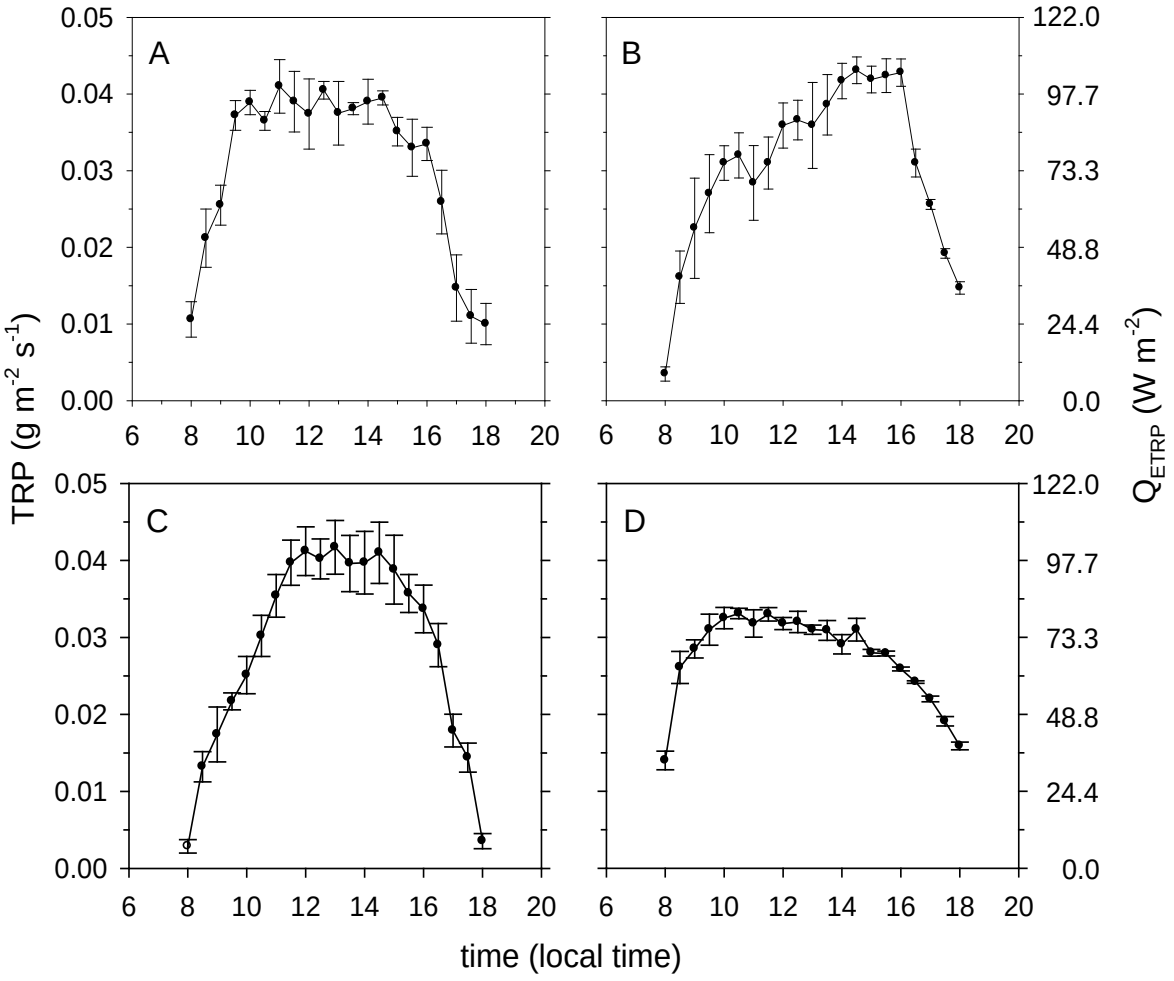

Figure 4.11 Diurnal patterns of transpiration rate (TRP) and latent heat flux (Q_{ETRP}) for *Fraxinus uhdei* (A), *Liquidambar styraciflua* (B), *Eucaliptus camaldulensis* (C), and *Ligustrum lucidum* (D) during doy 84. Data points represent the mean of four measurements on different trees. Bars represent the standard error (S.E.).

The diurnal pattern of canopy conductance (g_C) was similar in the four species showing a maximum value between 12:00 and 15:00 LT. However, *L. styraciflua* and *L. lucidum* showed higher g_C values than *F. uhdei* and *E. camaldulensis*, consistent with transpiration. Average g_C registered values between 12.5 (*E. camaldulensis*) and 20.42 mm s^{-1} (*L. lucidum*), with maxima values of 38.45, 33.34, 23.21 and 21.8 mm s^{-1} for *L.*

styraciflua, *L. lucidum*, *F. uhdei* and *E. camaldulensis*, respectively (Fig. 4.12). These g_C values agree with the measured transpiration.

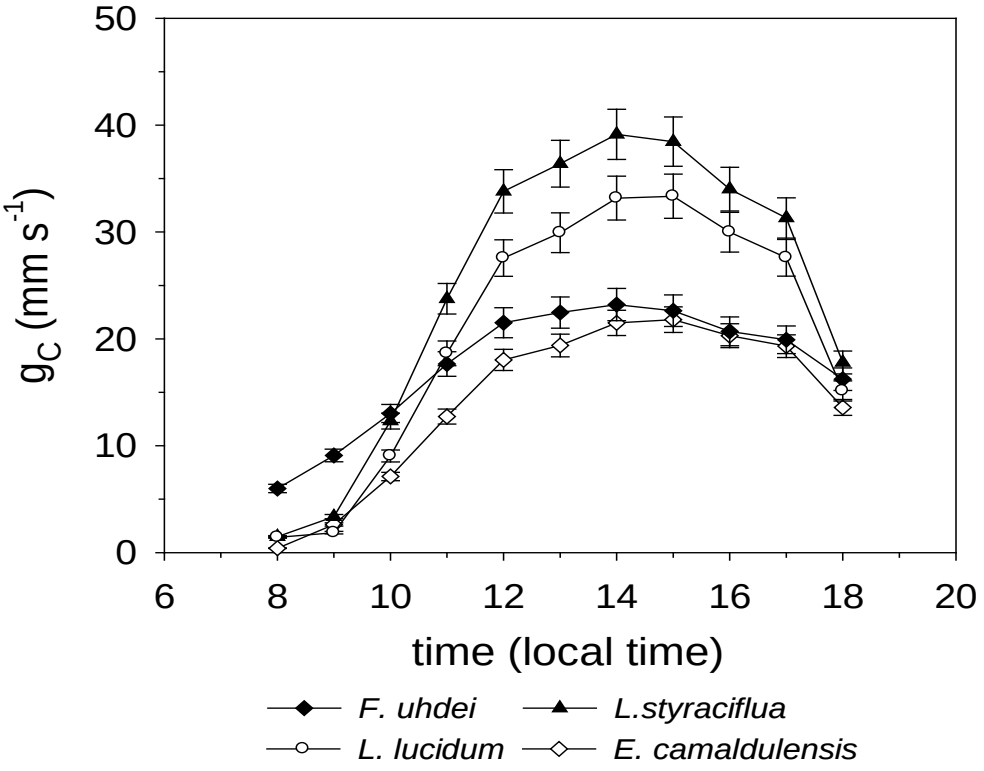

Figure 4.12 Diurnal patterns of canopy conductance (g_C) for a typical day in March for *L. styraciflua* (closed triangles), *L. lucidum* (open circles), *F. uhdei* (closed diamonds), and *E. camaldulensis* (open diamonds). Values are the averaged and bars represent the standard error (S.E.) (n = 20).

4.7 Mitigation of the UHI in Mexico City

Table 4.2 shows the measured and required energy fluxes to decrease air temperature some degrees by reducing sensible heat flux by increasing latent heat flux which is a function of transpiration rates, tree structure parameters like LAI and crown diameter and tree density. The necessary sensible heat flux was calculated by inverting $T_A = 0.03892Q_H + 15.3136$. Values showed on table 4.2 seem to be reasonable taking into account that the measured

value of Q_E is low compared to other energy balance, but higher or similar to the calculated ones, which represent 6% of the vegetated area in the study site.

Table 4.3 shows evidence of the performance of the phenomenological model. Predicted values of the complete model agreed closely with the results from the model for T_A, and each of the different submodels (Q_N, Q_{ETRP}) (Fig. 4.13). In general, values of determination of the model are indicative of a better agreement between observed values of T_A, Q_N and Q_{ETRP}, and values calculated from the model. Although, the model coefficients indicate that the model does explain with some efficiency T_A and Q_N it does not for Q_{ETRP}.

This is most likely due to the fitting of Q_E model for each of the studied species, it is clear to notice that *E. camaldulensis* ($r^2 = 0.5963$) is the species that least fits the model and probably also *F. uhdei*, although this species has a high coefficient of determination ($r^2 = 0.8575$) the root-mean-square error (rmse) is also high, having in the best case, an error of up to 13%, propagating these errors to Q_{ETRP}.

Table 4.2. Measured fluxes (Q_N, Q_S, Q_{HM}, $Q_{EM;}$ Wm^{-2}) and required (Q_{HR}, Q_{ER}) to reduce the air temperature (T_{AM}) 1, 2 and 3 °C (T_{AR}) on day of year (doy) 77 at 14:00 LT and 78 at 15:00 LT, and tree densities (tree ha^{-1}) of two native species, *L. styraciflua* (*Ls*) and *F. uhdei* (*Fu*), and two introduced species *Ligustrum lucidum* (*Ll*) and *E. camaldulensis* (*Ec*), to change the required sensible heat flux to get the required air temperature by increasing the latent heat flux. Numbers in bold indicate the results from the model.

doy/hour	T_{AM}	Q_N	Q_S	Q_{HM}	Q_{EM}	T_{AR}	Q_{HR}	Q_{ER}	*Ls*	*Fu*	*Ll*	*Ec*
77/14:00	28.0	680.0	252.0	329.0	93.9	**27.0**	**300.6**	**33.5**	**17.0**	**8.6**	**16.2**	**42.9**
	28.0	680.0	252.0	329.0	93.9	**26.0**	**274.9**	**59.2**	**30.0**	**15.1**	**28.6**	**75.8**
	28.0	680.0	252.0	329.0	93.9	**25.0**	**249.2**	**84.9**	**43.0**	**21.7**	**41.0**	**108.8**
78/15:00	27.0	703.0	299.0	324.0	79.9	**26.0**	**274.9**	**49.2**	**24.9**	**12.6**	**23.7**	**63.0**
	27.0	703.0	299.0	324.0	79.9	**25.0**	**249.2**	**74.9**	**38.0**	**19.1**	**36.1**	**95.9**
	27.0	703.0	299.0	324.0	79.9	**24.0**	**223.5**	**100.6**	**51.0**	**25.7**	**48.5**	**128.9**

Table 4.3. Statistical performance of the simple phenomenological model at the half-hourly timescale. Fluxes are determined for hours when $Q_N>0$. Intercept and rmse units are in W m^{-2} for the energy fluxes and °C for T_A.

Variable	N	Slope	Intercept	r^2	rmse
Q_N	130	0.9528	11.5225	0.9785	33.37
Q_{ETRP}	168	0.9416	5.2736	0.8499	28.92
Q_E *F. uhdei*	42	0.9825	6.5020	0.8571	11.32
Q_E *L. styraciflua*	42	1.0221	-0.6002	0.8825	9.58
Q_E *L. lucidum*	42	0.8327	8.8061	0.9442	8.48
Q_E *E. camaldulensis*	42	0.9274	5.8852	0.5963	10.29
T_A	130	0.8705	2.7982	0.8891	1.38

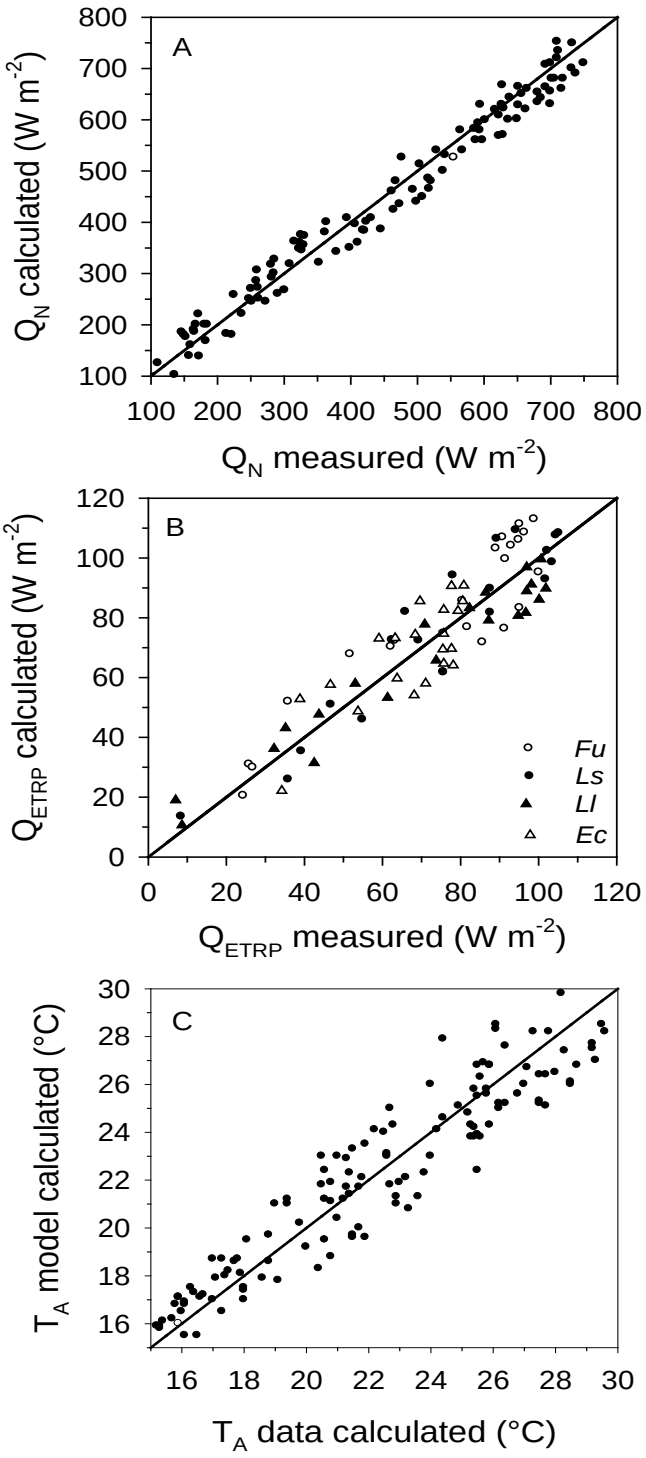

Figure 4.13 Scatterplots of half-hourly measured versus modeled net radiation (A) and tree transpiration (B), and calculated versus modeled air temperature (C). Transpiration (B) is shown for *F. uhdei* (open circles), *L. styraciflua* (closed circles), *L. lucidum* (closed triangles) and *E. camaldulensis* (open triangles). Statistics for fit goodness are reported in Table 4.3.

Because this model is based on the urban energy balance any constraint of their components could change the model results as it is the case in which Q_A and Q_{AD} were neglected; however, when measurements were done, Q_E and Q_H were measured independently, and in the case that Q_A values could be significant, say above 5% of Q_N, its effect is introduced implicitly in the other components (Q_E, Q_H and Q_S) not affecting the UHI mitigation model results. Also, the footprint extension in the study site (1150 m) where there are no important sources or sinks of energy (Fig. 4.1), Q_{AD} effect may be negligible.

The measurements of fluxes and the urban tissue allowed to generate the energy storage parameters (Eq. 3) for this neighborhood. The large value of 0.671 (a_1) indicates the importance of Q_S in the energy balance in this neighborhood of Mexico City, and similar to β, reflects the large proportion of area which is paved and built against green/evaporating area (Velasco et al., 2011). Energy storage is a key component, being the most dissipative constituent of energy balance in the city. According to the measurements, when Q_N registered at noon 693.5 W m^{-2}, Q_S was 290 W m^{-2}, this is the 40%. Averaged Q_N was 449.0 W m^{-2}, whereas Q_S was 224.0 W m^{-2} when $Q_N > 0$, namely 50% of Q_N in average. However, taking into account Eq. 3, Q_S values increase as high as 390 W m^{-2}, being the 53% of Q_N. Similarly to São Paulo, Brazil, where Q_S is the 51% of Q_N (Ferreira, et al., 2013). Although the constitution of studied areas in extratropical cities in North America are different from Mexico City, it is possible to notice that high urbanization affects energy storage, for example, in Vancouver, Canada, this ratio is 48%, but from 17 to 31% in cities with 24 to 49% of vegetation (Grimmond and Oke, 1999b). However, energy storage is not comparable to latent heat flux, although " dissipates" large amounts of energy. This mechanism (Q_S) just redistributes the energy, taking large amounts from early morning until irradiance maximum is reached, and after that it is re-irradiated as heat to their surroundings in the afternoon and night. A major problem with this mechanism is that Q_S may change due to alterations in both, building materials and urban fabric distribution, and therefore probably modify the coefficients of Eq. 3.

Furthermore, Bowen ratio can be used as an urbanization index and also as an indicator of the presence/absence of vegetation in Mexico City, and possibly in other parts

of the world, since its value is high in well urbanized areas with lack of vegetation, as Palacio de Minería (β=8.8, near MER (Fig. 4.1), 1% vegetation) in the historic city center (Oke, et al., 1999), and lower in districts with less urbanization, as E scandon district (β=2.92, near PLA (Fig. 4.1), 6% vegetation) and Pedregal de San Angel (β=1.92, near PED (Fig. 4.1), 50% vegetation), a suburban area (Barradas, et al., 1999) similar to São Paulo, Brazil, university campus (β=1.57, 30% vegetation) (Ferreira, et al., 2013). In general, Bowen ratios in extratropical cities apparently are higher than in Mexico City, from 1.24 to 2.87, taking into account that green areas extension are bigger (24-49 %) (Grimmond and Oke, 1999b). It is interesting to notice that Vancouver showed a similar value to Escandon (β=2.87) with 5.5 fold greener area. This is probably due to the low transpiration rates of urban vegetation in that latitude.

The theoretical results applying the phenomenological model presented here, demonstrate that tree arrangements can efficiently but differentially mitigate the urban heat island in Mexico City, considering their transpiration rates; while there are some slight discrepancies between tree densities, for instance when T_A is reduced from 26 to 25 °C with a tree density of 43.0 and 38.0 trees ha^{-1} for *L. styraciflua* with a similar performance for the other species. This behavior could be due to the difference between observed or measured Q_{EM} on doy 78 which is 15% lower than that observed on doy 77, although Q_N is higher on doy 78 (23 W m^{-2}) than on doy 77. However, and as it was commented above, some of the total Q_{EM} amount in the study site can be due to the practice to spill water to the sidewalks and streets by some shops in the area, a very hard variable to control. A simple strategy to solve this problem would be to discard measured Q_{EM} with the usual increase of tree density as it is possible to get by using tree species with the highest transpiration rates, LAI and crown diameter like *F. uhdei* which is possible to have a no overlapping density with maximum of 105 trees ha^{-1}, corresponding a Q_E value of 411.0 W m^{-2} reducing Q_H to almost null, and T_A could be 15.0 °C. This temperature, Q_E and tree density is just similar to a natural forest. The main problem with this approaching is that Q_S parameters could change releasing energy excess to Q_E and Q_H since a_1 in a mixed forest is 0.11 (McCaughey, 1985) or 0.32 for short grass (Doll et al., 1985). Nevertheless, this approximation shows a reasonable performance of the model (Table 4.3), although *E. camaldulensis* (and *F. uhdei*, but the introduced error is not so large) presented a low

performance on Q_{ETRP} calculation. Maybe this error is due to environmental conditions of plants when making the measurements that were not taken into account when g_S was modeled as air pollution and/or substrate humidity with a differential effect among species, as well as the data number (Barradas et al., 2004), although sufficient to *L. styraciflua* y *L. lucidum*, it was not for the other two species. Therefore, it is necessary to explore further these possibilities in future works.

4.8 Mitigation of the UHI in Mexico: a challenge

In the case of Mexico City, in La Merced (19.412° N, 99.152 W, 2245 m asl) that besides being in the historic center it is also located in the UHI warm center, in January and February, PET is below the upper limit, but most of the day is in the cold stress category except for the period between 12:00 and 14:00 local time (LT) when a value of slightly warm (PET > 23 °C) is registered. From March to August, cold stress is reduced generally from 6:00 to 8:00 and 18:00 to 24:00 LT, while heat stress category predominates from 09:00 until 17:00 lh, even it is distributed until December from 12:00 to 14:00 LT. Thus, in these periods an environment of high thermal pollution occurs mainly in April, May and June which are recorded in 4-6 hours of strong heat stress from 10:00 to 16:00 LT (Fig. 4.14).

Whereas for a city like Veracruz-Boca del Rio (19°11'25"N, 96°09'12"W, 10 m asl) (Fig. 4.15), this index is between 13 and 43 °C with a PET slightly cool to comfortable category from 19:00 to 6:00 LT, from January to March, and November and December, and comfort to slightly warm between 20:00 and 5:00 LT from May to November, dominating the range from warm to very warm range throughout the year from 07:00 to 19:00 LT. As it can be seen in the Veracruz-Boca del Rio urban area, people experience more heat stress than that people may experience in La Merced (Mexico City), however, the cold stress events are less intense and less frequent.

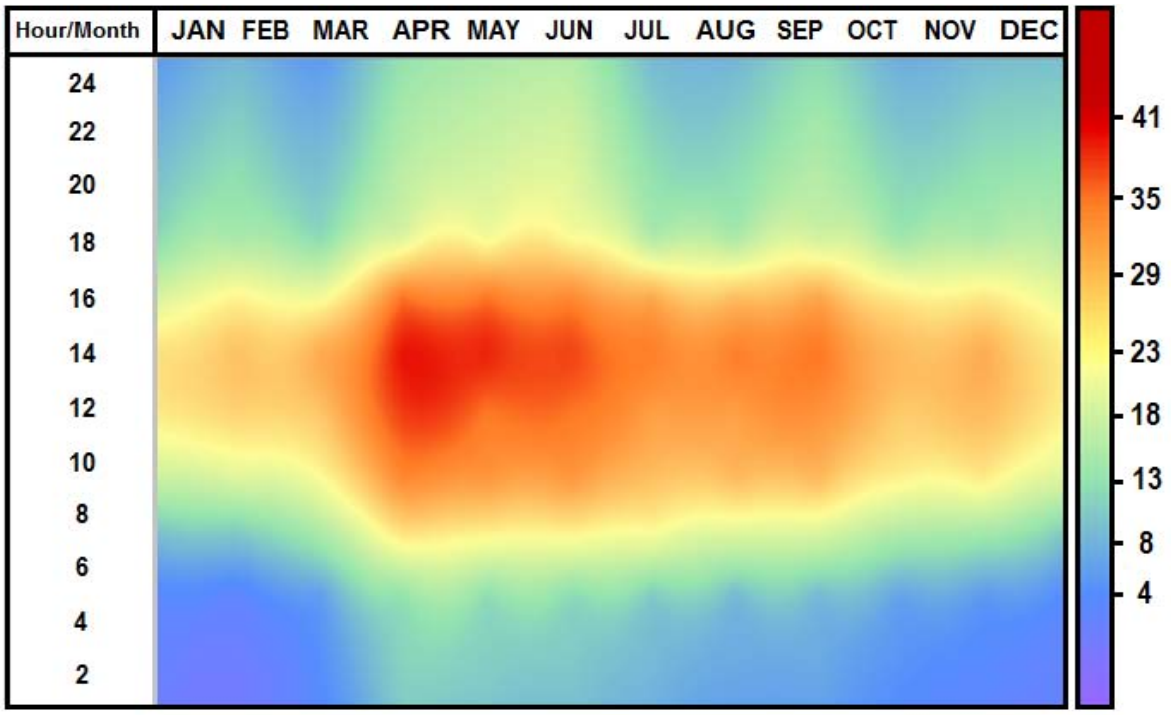

Figure 4.14. Physiological equivalent temperature (PET, °C) distribution throughout the day and year in La Merced, Mexico City, calculated for a typical person in an open urban environment with a physical activity of 80 W m^{-2} (sedentary), normally dressed (0.9 clo) and calm wind (< 0.5 m s^{-1}).

4.9 The challenge

By implementing a UHI mitigation strategy in Mexico, the first factor to consider is climate, since the geographic location and varied topography make the country includes almost all the world climates, i.e. to normalize the cities by the climate type that occur. According to the climate distribution by the CONABIO (1998) there are 60 climate Köppen types in Mexico; however, they could be reduced to nine major climates, depending on the general characteristics of each group. So they stand out as the tropical wet and monsoonal (Af and Am), tropical savana (Aw) and tropical sub wet (A(C)) in group A; tropical and temperate desert (BW) and tropical and temperate steppe (BS) in group B; and temperate wet (Cf and C m), temperate wet and dry (Cw), temperate Mediterranean (Cs) and temperate wet/sub wet (Cb') in group C. Group D climates do not exist in Mexico and those

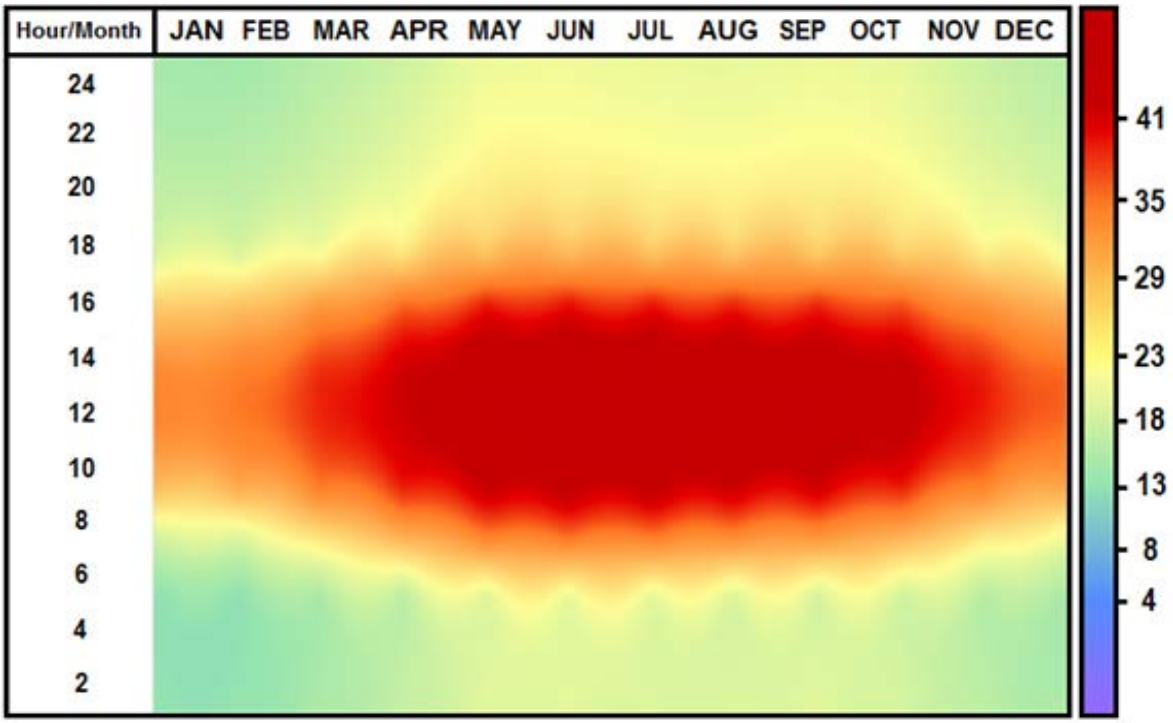

Figure 4.15. Physiological equivalent temperature (PET, °C) distribution throughout the day and year in Veracruz-Boca del Río, calculated for a typical person in an open urban environment with a physical activity of 80 W m^{-2} (sedentary), normally dressed (0.9 clo) and calm wind (< 0.5 m s^{-1}).

in group E can be neglected since the areas in which they occur are very small and undeveloped (Fig. 4.16).

The number of inhabitants is another important factor to consider in mitigating the UHI because it is a component which reflects not only the extent of the city but also the infrastructure, transport and the activity of its inhabitants. While the UHI is manifested from the beginning of the development, this phenomenon can become a problem when the urban population is about 500 thousand or more inhabitants. In Mexico there are ten cities with over one million inhabitants, among which highlights the urban zones of Mexico City and Guadalajara (Table 4.4, Fig. 4.16)

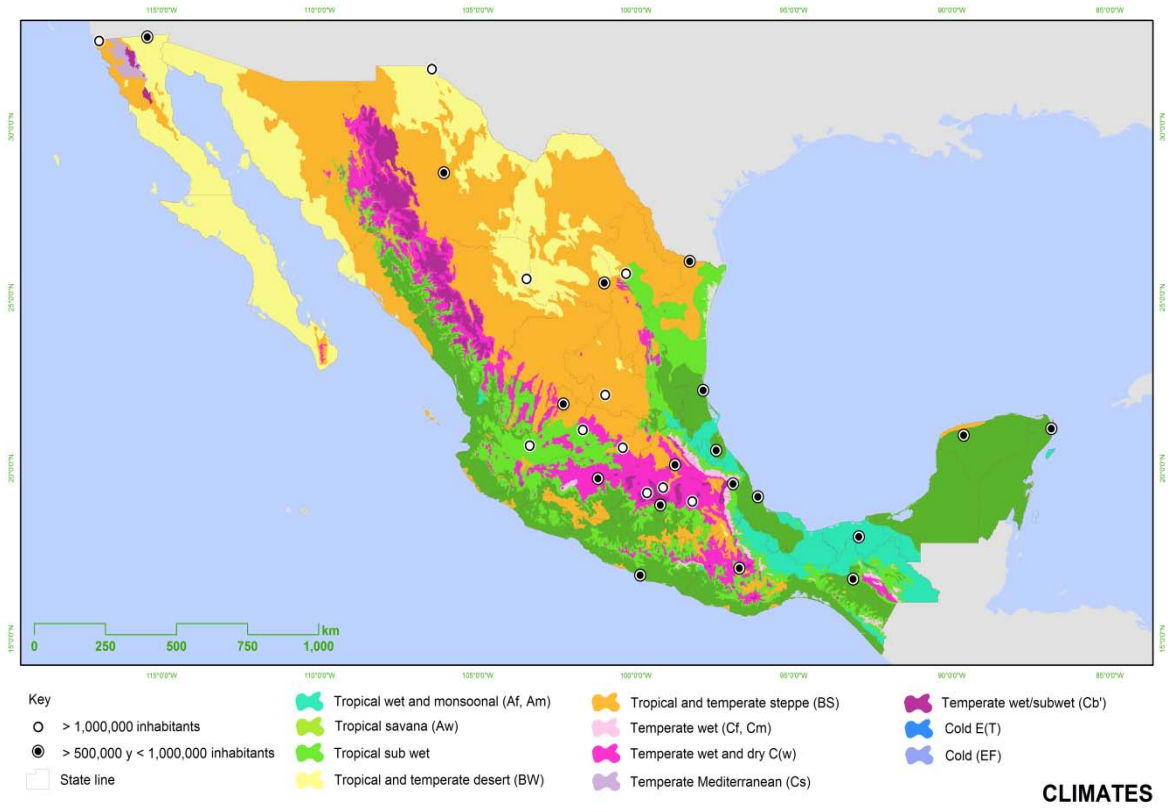

Figure 4.16. Spatial distribution of main climates of Mexico modified from CONABIO (1998), and representative cities with over 500 thousand inhabitants. The distribution of the CONABIO climates is based on Köppen classification.

The Metropolitan Area of Mexico City has a variety of group C climates (México City, Federal District, Csa; Ecatepec, Cfc; and Nezahualcóyotl, Naucalpan and Chimalhuacán, Cwb) as well as the metropolitan area of Guadalajara, Zapopan and Tlaquepaque, Cfb. Therefore, they may be a climate group that requires the same form solution of UHI mitigation, and so on with the other cities and their climate types (Table 4.4).

One alternative and apparently the simplest, is to increase the albedo up to 50% to reduce Q_N through increasing reflection of short wavelength radiation (Eq. 3). If the proportions of the available energy dissipation remain, then it is most likely Q_H decreases and therefore T_A. However, the reflection mechanism is complicated because the reflected solar radiation is also absorbed by the lower layers of the atmosphere, furthermore it has to pass through the air pollutants layer that characterize a city where it is absorbed and thereby

Table 4.4. Climatic urban groups with more than 500,000 inhabitants in Mexico.

City	Inhabitants	Climate type	City	Inhabitants	Climate type
Cities with type C climate					
Mexico C ity (19°25.03'N, 99°09.42"W, 2250 m asl)	8,720,916	Csa	Guadalajara (20°40'N, 103°20'W, 1570 M asl)	1,600,940	Cfb
Ecatepec (19°36.07'N, 99°03.15'W, 2250 m asl)	1,688,258	Cfc	Zapopan (20°43'N, 103°24'W, 1548 m asl)	1,155,790	Cfb
Nezahualcóyotl (19°24.82'N, 99°02'W, 2240 m asl)	1,140,528	Cwb	Tlaquepaque (20°39'N, 103°19'W, 1540 m asl)	542,051	Cfb
Naucalpan (19°28.72'N, 99°14.38' W, 2275 m asl)	833,782	Cwb			
Chimalhuacán (19°25'N, 98°54'W, 2243 m asl)	525,389	Cwb	Puebla (19°03.08'N, 98°13.07'W, 2150 m asl)	1,485,941	Cfc
Aguascalientes (21°53'N, 102°18'W, 2300 m asl)	814,545	Cwb	Morelia (19°42.05'N,101°11 .07'W, 1920 m asl)	684,145	Cwb
Toluca (19°17.53'N, 99°39.23'W, 2667 m asl)	747,512	Cwb	Reynosa (26°01'N, 98°14'W, 33 m asl)	526,888	Cwa
Querétaro (20°35.28N, 100°23.28'W, 1824 m asl)	734,139	Cfc	Durango (24°01.36'N, 104°39.27'W, 1885 m asl)	526,659	Csa
Cities with type B climate					
Tijuana (32°31.85'N, 117°01.2'W, 31 m asl)	1,410,687	Bsk	Mérida (20°58'N, 89°37'W, 10 m asl)	777,615	Bsh
Ciudad Juárez (31°44.37'N,	1,313,338	Bwk	San Lu is Po tosí	730,950	Bsh

106°29.22'W, 1137 m asl)			(22°09'N, 100°58.5'W, 1864 m asl)		
León (21°07.18'N, 101°40.83'W, 1804 m asl)	1,278,087	Bsk	Hermosillo (29°05.73'N, 110°57.05'W, 216 m asl)	701,838	Bwh
Monterrey (25°40.28'N, 100°18.52'W, 540 m asl)	1,133.814	BSh	Guadalupe (25°40.65'N, 100°15.6'W, 480 m asl)	691,931	Bsh
Mexicali (32°39.8'N, 115°39.8'W, 6 m asl)	936,826	Bwh	Saltillo (25°26'N, 101°W, 1560 m asl)	648,929	Bsh
Culiacán (24°48'N, 107°23'W, 68 m asl)	858,826	Bsh	Torreón (25°32.66'N, 103°26.5'W, 1120 m asl)	577,477	Bwk
Chihuahua (28°38.12'N, 106°05.33'W, 1433 m asl)	809,232	Bwk			
Cities with type A climate					
Acapulco (16°51.1'N, 99°54.58'W, 20 m asl)	717,766	Aw	Veracruz (19°11.42'N, 96°09.2'W,10m asl)	552,156	Am
Villahermosa (17°59.22'N, 92°55.17'W, 9 m asl)	640,359	Aw	Tuxtla Gutiérrez (16.75°N, 93.115°W, 522 m asl)	503,320	Aw
Cancún (21°9.63'N, 86°50.85'W, 10 m asl)	628,310	Aw			

I↓ would increase substantially. Also, if the surface temperature decreases, then I↑ could decreases, increasing the proportion of long-wave radiation (Eq. 3) and therefore Q_N. A probably counteract is to make use of "cool" materials which reduce the long-wave

impinging r adiation b y "r eflecting th at k ind of w avelengths" (Synnefa, e t al., 2007); however, all these techniques has been proven as excellent building coolers but not as an effective UHI mitigation factor, and probably this reflection could present a similar albedo mechanism. A dditionally, t he i ncreasing o f al bedo i s a p ermanent p ractice, w hich can reduce significantly T_A in the autumn-winter period, due to the lower angle of the sun, and the l ower s un i nclination t he hi gher a lbedo (Barradas, 2014) . For e xample, t his s un inclination i n the c ity o f M onterrey i s f rom 85.5° t o 40.6°, a nd f rom 8 3.7° t o 47.7° in Mexico C ity, w hereas in T uxtla G utiérrez i s f rom 82.5° t o 49.7°. T he i mmediate consequence is that in spring and summer may have low temperatures, but much lower in fall and winter. For cities with temperate climates it looks like that the albedo increasing is not an appropriate solution.

Another alternative c onsidering th e energy balance to miti gate th e U HI, it is th e implementation o f g reen s paces, b ecause t he v egetation i n g eneral an d t rees i n p articular are capable of absorbing large amounts of energy (2.5 MJ/kg) by the transpiration process increasing Q_E and reducing Q_H and t hen T_A. Nevertheless, t his s olution r equires f rom specific s tudies t o de termine t ranspiration r ates of t he i nvolved pl ants, a nd t he di fferent structure p arameters as l eaf ar ea i ndex, h eight, co verage and t he en ergy b alance components.

However, a r oughly and t heoretical e xercise us ing t ree s ystems w ith hi gh transpiration rates in Mexico City, showed the feasibility of using them as natural cooling systems to mitig ate th e UHI. In a s ystem c omposed ma inly o f n ative tr ee s pecies w ith intermediate tr anspiration r ates Bowen r atio ($\beta = Q_H/Q_E$) w as 0.70, but w hen hi gh transpiration rates trees were chosen, β was 0.28, indicating that this latter system developed a cooling p ower th ree time s g reater th an th e in termediate tr anspiration s ystem (Ballinas, 2011). Nevertheless, β in the Palacio de Minería (city center) was 9.9 (Oke, et al., 1999) s howing a v ery high a ir he ating pot ential w ith no pos sibility t o bui ld g reat t ree arrangements t o i ncrease Q_E. A pos sible s olution f or a f ully ur banized area could be t o replace th e e xisting lo w tr anspiration r ates tr ees b y tr ees o r v egetation w ith high transpiration rates or some evaporative surfaces.

In cities with more than 500,000 inhabitants, the three mainly climate types occur (A, B and C). These all cities can be grouped into their different climate types which could implement similar UHI mitigation solutions for each group regardless of their geographical location. Therefore, it is possible to recommend some UHI mitigation practices solution for cities with different climates.

However, in two climate groups (A, C) there area subgroups classified as humid climates in which the implementation of vegetation to mitigate the UHI is not as effective as in areas with climate type B, since plant transpiration could be reduced by high air humidity, although this reduction could be around a 10%. On the other hand, the increasing of air humidity includes a negative effect on thermal comfort indexes. Probably in cities with this climate type, it would be necessary to apply other methods, as the modification of albedo (cities with climate A) including an appropriate amount of urban vegetation that must be defined. Also the modification of the urban winds (ventilation) can be suitable because it can displace the transpired water vapor taking a positive effect on thermal comfort indexes. However, urban natural ventilation depends on the intensity and persistence of wind and compete more to urban design and architectural layout of the buildings and the design of the same. Certainly, for cities with climates type B and C but not humid, the best possible UHI mitigation strategy is the implementation and/or the increasing of urban vegetation arrangements with high transpiration rates.

CHAPTER 5. CONCLUSIONS

5.1 UHI and Mexico City

The UHI in Mexico City has a distribution in almost all area in the city, with a warm center surrounded by ENEP-Acatlán, Villa de las Flores, San Agustín, Cerro de la Estrella and Plateros meteorological stations, mostly occurred by night; however different to the typical UHI, it establishes also during day, with intensities up to 10 °C (T_{U-R}). This information can be useful according to new areas to expanding with the appropriate planning, in an adequately territorial order. Because of that, it is imperative to identify the UHI phenomenon. There is no doubt that people in cities are the most affected, not only due heat stress but by health problems, therefore it is necessary to implement UHI mitigation strategies since that urban temperatures can affect human health and energy consumption

5.2 Tree transpiration

Even with low irrigation in Mexico City, it is possible to notice that tree transpiration rates can dissipates up to 20% of net radiation. However, in order to understand the transpiration and the water used by trees, it is essential to establish the stomatal conductance response to the environmental variables as vapor pressure deficit, net radiation and air temperature. Because of the different transpiration rates of the studied species, it is possible to select the most suitable species according to the microenvironment where the species are to be planted; however, the most suitable species would be those that showed the highest transpiration rates, as *Liquidambar styraciflua* and *Ligustrum lucidum*, while it would be better to build tree arrangements using the four species making a more biodiversity system since dissipation of net radiation is not large enough to make a difference.

In addition to reduced heat load and probably energy demand, mitigation of Mexico City's heat loads could improve air quality by removing particles from air and public health, as well as reduce the city's contribution to greenhouse gas emissions; however, it is relevant to mention that some tree species could generate volatile organic compounds

(VOC) which can increase air pollution. It is expected that the reduction of urban heat load could reduce the use of energy for air conditioning with a direct decrease on energy costs.

5.3 UHI mitigation

Considering energy balance as a framework to mitigate UHI, the implementation of green spaces is a suitable practice, because vegetation in general and trees in particular are capable of absorbing large amounts of energy by transpiration process, increasing Q_E and reducing Q_H and therefore T_A. The first step is to try to establish the number of trees according to their transpiration rates; then, to determine the possible decrease in air temperature and thereby mitigate more efficiently the UHI, therefore a phenomenological model easy to handle was presented. This model is based on the urban energy balance, however, any constrain of their components could change the model results. Bowen ratio for example, can be used as an urbanization index and also as an indicator of the presence/absence of vegetation in Mexico City, and possibly in other parts of the world, as it was stated before, UHI is not exclusive from a particular city, but it is present in all cities in the world, regardless its size, inhabitants, geographical location.

It is necessary to continue identifying the best tree characteristics and species to design with more precision the spatial distribution of trees to get the sufficient latent heat flux to effectively mitigate the heat island. Unfortunately, the currently urban design could not allow to expand or introduce these tree arrangements in some sites; however, old trees may be changed by others with higher transpiration rates, leaf area index and coverage, or to design other types of vegetation arrangements with high transpiration but no evaporation.

5.4 The Challenge to Mitigate UHI

One of the biggest challenges in Mexico is to mitigate the UHI in its cities since Mexican cities are growing very fast: Cancun, Guadalajara, Mexico City, Monterrey, Queretaro, Tijuana and Tuxtla Gutierrez are the seven cities with the largest real estate growth among the 50 largest cities in the country. The city of Tuxtla Gutierrez grew from 2000 to 2010 by

30% and it is expected this growth remain into 2030. Therefore it is imperative that urgent action in urban planning must be taken, so that this phenomenon would not grow and not become a difficult problem to solve, and with this move towards to a more sustainable city. Mexico City has about 20,116,842 inhabitants in an area of 2,046 km^2 being one of the most populous cities in the world. Its population is estimated to increase to 20.6 million in 2025 and despite that it has one of the largest parks in the Americas (≈6.78 km^{-2}, Chapultepec), the effect of the UHI has been increasing in both size and intensity. These urban increases imply a high demand for goods and services and therefore the effect of the UHI will increase both size and intensity.

5.5 Why mitigate UHI?

Clearly reduction of heat loads in the city is possible even in the dry season with no irrigation, through the evaporative cooling potential from tree-soil-water uptake and transpiration that would probably reduce surface the near-surface air temperatures. Additionally, this reduction in temperatures could be enhanced from the tree shading effect. Furthermore, this currently temperature differences could be enhanced with the global climate change. Also, heat shocks will increased or be enhanced by the UHI effect, and energy consumption for air conditioning also will increase. This is why it is imperative that urgent action in urban planning be taken, so that this phenomenon would not grow and not become a difficult problem to solve, and with this move towards to a more sustainable city.

5.6 Very important...

It is necessary to continue identifying the best tree characteristics and species to design with more precision the spatial distribution of trees to get the sufficient latent heat flux to effectively mitigate the heat island. Unfortunately, the currently urban design could not allow to expand or introduce these tree arrangements in some sites; however, old trees may be changed by others with higher transpiration rates, leaf area index and coverage, or to design other types of vegetation arrangements with high transpiration but no evaporation.

Any tree arrangements to reduce urban heat loads it is essential to establish it in the warmest month as it is the case of this study. It is important to note that this is a multidisciplinary problem which needs of urban developers, ecologists, architects, engineers, climatologists, geographers, sociologists, etc.

The challenge to mitigate UHI is a large and complex task, but necessary.

REFERENCES

Al-Alawi, MM and Mandiwana, KL. 2007. The use of Aleppo pine needles as a biomonitor of heavy metals in the atmosphere. Journal of Hazardous Materials 148, 43–46.

Alberto, JA. 2005. El Crecimiento Urbano y su Incidencia en la Vulnerabilidad Ambiental y Social. E l C aso de l G ran R esistencia. U niversidad N acional del N ordeste, C omunicaciones Científicas y Tecnológicas.

http://www.unne.edu.ar/unnevieja/Web/cyt/com2005/2-Humanidades/H-004.pdf

Alemán, P AM a nd G arcía, E . 1974. T he C limate of M exico. I n: W orld Survey of Climatology, Vol. 11, H. Landsberg, ed.) Elsevier, 419 pp.

Baca-Cruz, A G. 2014. Identificación y c omportamiento de la i sla de c alor e n l a z ona conurbada de V eracruz-Boca del Río en el año 2011. B Sc T hesis. F acultad de I nstrumentación y Ciencias Atmosféricas. UV. Xalapa, Ver.

Ballinas, M . 2011. Mitigación d e l a i sla de calor u rbana: est udio de cas o de la zona metropolitana de la Ciudad de México. Master in Sciences Thesis. Universidad Nacional Autónoma de México, México, D.F., México.

Barradas, VL. 1991. A ir temperature and humidity and human comfort index of some city parks of Mexico City. International Journal of Biometeorology 35, 24-28.

Barradas, V L; Tejeda-Martínez, A ; Jáuregui, E . 1999. Energy b alance m easurements in a suburban vegetated area in Mexico City. Atmos. Environ. 33:4109- 4113.

Barradas, VL. 2000. Energy balance and transpiration in an urban tree hedgerow in Mexico City. Urban Ecosystems 4, 55-67.

Barradas, V L; R amos-Vazquez, A ; Orozco-Segovia, A. 2004. Stomatal co nductance i n a tropical xe rophilous s hrubland a t a lava s ubstratum. International Journal of B iometeorology 48, 119-127.

Barradas, VL. 2 014. E ntre t echos b lancos y az oteas v erdes: cam bio c limático u rbano. Oikos= 11, 8-9.

Basara, J B; Basara, H G; Illston, B G; Crawford, KC. 2010. The impact of the u rban he at island d uring a n intense heat w ave i n O klahoma City. A dv. M eteorol. Vol. 2010, A rticle I D 230365, 10 pp. doi: 1155/2010/230365.

Bauerle, WL ; Post, C J; McLeod, MF ; Dudley, J B; Toler, J E. 2002. M easurement and modeling of the transpiration of a temperate red maple container nursery. A gricultural and F orest Meteorology 114, 45-57.

Bosveld, F C a nd B outen, W. 2001. E valuation of t ranspiration m odels w ith o bservations over a Douglas-fir forest. Agr. Forest. Meteorol. 108:247-264.

Bottino Bernardi, R. 2009. La Ciudad y la urbanización. Estudios Históricos 2, 1- 14.

Borja, J. 2003. La ciudad conquistada. Alianza Editorial, S.A., Madrid.

Brazel, A J and Q uattrochi D A. 2005. Urban c limates. In: E ncyclopedia of W orld Climatology J.E. Oliver, ed.) Springer, Dordrecht, The Netherlands, 766–769.

Cadena, G. 2011. Ingeniería y agro. Revista de Ingeniería 33, 70-87.

Cappelli de Stefens, AM; Campos de Ferreras, AM; Piccolo, MC. 2005. El clima urbano de Bahía Blanca. Editorial Dunken, Argentina.

Čermák, J; Jenik, J; Kucera, J; Zidek, V. 1984. Xylem water flow in a crack willow tree (*Salix fragilis* L.) in relation to diurnal changes of environment. Oecologia 64, 145-151.

Comín del Río, P. 2009. Darwin, una evolución extraordinaria. Pearson Educación, S.A., Madrid.

CONABIO (Comisión Nacional para el Conocimiento y Uso de la Biodiversidad). 1998. Climas.

http://www.conabio.gob.mx/informacion/metadata/gis/clima1mgw.xml?_xsl=/db/metadata/xsl/fgdc_html.xsl&_indent=no

Cruz, MS. 2000. Periferia y suelo urbano en la Zona Metropolitana de la Ciudad de México. *Sociología* 42, 59-90.

Dolman, AJ. 1993. A multiple-source land surface energy balance model for use in general circulation models. Agricultural and Forest Meteorology 65, 21–45.

Doll, D; Ching, JKS; Kaneshiro, J. 1985: Parameterisation of subsurface heating for soil and concrete using net radiation data. Bound.-Layer Meteor. 32, 351–372.

Dye, P J. 1987. Estimating water use by *Eucaliptus grandis* with the Penman-Monteith equation. In: Swanson, R.H., Bernier, P.Y.,Woodward, P.D. (Eds.), Forest hydrology and watershed management. Proceedings of the Vancouver Symposium, International Association of Hydrological Sciences, No. 167, Vancouver.

Ezcurra, E.1991. *De las chinampas a la megalópolis, el medio ambiente de la cuenca de México*. Fondo de Cultura Económica Serie Ciencia vol 91, México, D.F. México. 119 pp.

Ezcurra, E and Mazari-Hiriart, M. 1996. Are megacities viable? A cautionary tale from Mexico City. Environment 38:6—15, 26–35.

Fanjul, L and Barradas, VL. 1985. Stomatal behaviour of two heliophile understorey species of a tropical deciduous forest in Mexico. Journal of Applied Ecology 22: 943-954.

Ferreira, MJ; Pereira de Oliveira, A; Soares, J. 2013. Diurnal variation in stored energy flux in Sao Pãulo city, Brazil. Urban Climate, http://dx.doi.org/10.1016/j.uclim. 2013.06.001

Fuentes-Pérez, CA. 2014. Islas de calor urbano en Tampico, México. Impacto del microclima a la calidad del hábitat. Revista Electrónica Nova Scientia 13, 495-515.

Gao, Q; Zhao, P; Zeng, X; Cai, X; Shen, W. 2002. A model of stomatal conductance to quantify the relationship between leaf transpiration and soil water stress. Plant, Cell and Environment 25, 1373-1381.

García-Cueto, OR; Jauregui-Ostos, E; Toudert, D; Tejeda, A. 2007. Detection of the urban heat island in Mexicali, B.C., Mexico and its relationship with land use. Atmosfera 20, 111-131.

Gartland, L. 2008 Heat islands, understanding and mitigating heat in urban areas. Taylor and Francis. New York.

Grimmond, CSB; Cleugh, HA; Oke, TR. 1991. An objective heat storage modeland its comparison with other schemes. Atmos. Environ. 25B:311-326.

Grimmond, CSB and Oke, TR. 1999a. Aerodynamic properties of urban areas derived from analysis of surface form. J. Appl. Meteorol. 38:1262–1292

Grimmond, CSB and Oke, TR. 1999b. Heat storage in urban areas: local-scale observations and evaluation of a simple model. J. Appl. Meteorol. 38:922-940.

Gu, S; Tang, Y; Cui, X; Kato, T; Du, M; Li, Y; Zhao, X. 2005. Energy exchange between the atmosphere and a meadow ecosystem on the Qinghai-Tibetan plateau. Agricultural and Forest Meteorology 129, 175-185.

Guenther, AC; Geron, T; Pierce, B; Lamb, P; Harley, R. 2000. Natural emissions of non-methane volatile organic compounds, carbon monoxide, and oxides of nitrogen from North America. Atmospheric Environment 34, 2205–2230.

Guzmán-Morales, J; Morton-Bermea, O; Hernández-Alvarez, E; Rodríguez-Salazar, MT; García-Arreola, ME; Tapia-Cruz, V. 2011. Assessment of atmospheric metal pollution in the urban area of Mexico City, using *Ficus benjamina* as biomonitor. Bulletin of Environmental contamination and Toxicology 86, 495-500.

Hinckley, T M and B raatne, JH. 1994. Stomata. In: Wilkinson, R .E. (Ed.), Plant Environment Interactions. Marcel Dekker, Inc, New York, pp. 323–355.

Holtslag, AAM and Van Ulden, AP. 1983. A simple scheme for daytime estimates of the surface fluxes from routine weather data. J. Clim. Appl. Meteorol. 22:517-529.

Höppe, P R. 1999. The physiological equivalent temperature – a universal index for the biometeorological assessment of the thermal environment. Int. J. Biometeorol. 43, 71-75.

INEGI. 2011a. Instituto Nacional de Estadística. Conjunto de datos vectoriales de la serie topográfica y d e r ecursos n aturales. Web l ink: http://mapserver.inegi.org.mx/data/inf_e1m/?s=geo&c =979

INEGI. 2011b. Instituto Nacional de Estadística y Geografía. Censo de Población y Vivienda 2010. Resultados preliminares. Web link: http://www.censo2010.org.mx/doc/cpv10p_pres.pdf

INECC. 2013. Instituto Nacional de Ecología y Cambio Climatico. Web link: http://www2.inecc.gob.mx/publicaciones/libros/517/redes.pdf

Jáuregui, E. 1971. Mesomicroclima de la ciudad de México. Instituto de Geografía, UNAM. Mexico.

Jáuregui, E. 1997. Heat island development in Mexico City. Atmospheric Environment 31, 3821-3831.

Jáuregui, E and Luyando, E. 1998. Long-term association between pan evaporation and the urban heat island in Mexico City. Atmosfera 11, 45-60.

Jarvis, PG. 1976. The interpretation of the variations in leaf water potential and stomatal conductance found in canopies in the field. Philosophical Transactions of the Royal Society, London. B, 273, 593-610.

Jarvis, PG and McNaughton, KG. 1986. Stomatal control of transpiration: scaling up from leaf to region. Advances in Ecology Research 151, 1–49.

Jazcilevich, AD; García, AR; Caetano, E. 2005. Locally induced surface air confluence by complex terrain and its effect on air pollution in the valley of Mexico. Atmos. Environ. 39:5481-5489.

Jones, HG. 1992. Plants and microclimate. Cambridge University Press. Cambridge.

Kelliher, FM; Kostner, BMM; Hollinger, DY; Byers, JN; Hunt, JE; McSeveny, TM; Meserth, R; Weir, PL; Schulze, ED. 1992. Evaporation, xylem sap flow, and tree transpiration in a New Zealand broad-leaved forest. Agricultural and Forest Meteorology 62: 53-73.

Karl, T; Guenther, A; Spirig, C; Hansel, A; Fall, R. 2003. Seasonal variation of biogenic VOC emissions above a mixed hardwood forest in northern Michigan, Geophysical Research Letters 30 (2186), 23. DOI: 10.1029/2003GL018432, 23.

Kornaska, J; Uddling, J; Holmer, B; Lutz, M; Lindberg, F; Pleijel, H; Thorsson, S. 2015. Transpiration of urban trees and its cooling effect in a high latitude city. Int. J. Biomteorol. DOI 10.1007/s00484-015-1014-x.

Kumagai, T; Saitoh, TM; Sato, Y; Morooka, T; Manfroi, OJ; Kuraji, K; Suzuki, M. 2004. Transpiration, canopy conductance and the decoupling coefficient of a lowland mixed dipterocarp forest in Sarawak Borneo: dry spell effects. Journal of Hydrology 287: 237–251.

Landsberg, HE. 1981. The urban climate. International Geophysics Series vol 28. Academic Press, New York.

Laschewski, G and Jendritzky, G. 2002. Effects of the thermal environment on human health: an investigation of 30 years of daily mortality data from SW Germany. Clim. Res. 21, 91-103.

Leuning, R; Kelliher, FM; Murtrie, RE. 1991. Simulation of evapotranspiration by trees. Agricultural Water Management 19, 205–221.

Luber, G and McGeehin, M. 2008. Climate change and extreme heat events. Am. J. Prev. Med. 35:429-435.

Maroco, JP; Pereira, JS; Chaves, M M. 1997. Stomatal responses to leaf-to-air va pour pressure deficit in sahelian species. Australian Journal of Plant Physiology 24, 381–387.

Matzarakis, A and Mayer, H. 1996. Another kind of environmental stress: Thermal stress. NEWSLETTERS No. 18, WHO Collaborating Centre for Air Quality Management and Air Pollution Control. 7-10.

Matzarakis, A; Rutz, F and Mayer, H. 2007. Modelling radiation fluxes in simple and complex environments—application of the RayMan model. Int. J. Biometeorol. 51, 323-334.

McCaughey, J. 1985. Energy balance storage terms in a mature mixed forest at Petawawa Ontario: A case study. Boundary Layer Meteorol. 31:89-101. doi: 10.1007/BF00120036.

Meinzer, FC; Goldstein, G; Holbrook, NM; Jackson, P; Cavelier, J. 1993. Stomatal and environmental control of transpiration in a lowland tropical forest tree. Plant, Cell and Environment 16, 429–436.

Meinzer, FC; Andrade, JL; Goldstein, G; Holbrok, NM; Cavelier, J; Jackson, J. 1997. Control of transpiration from the upper canopy of a tropical forest: the role of stomatal, boundary layer and hydraulic architecture components. Plant, Cell and Environment 20, 1242–1252.

Montenegro, R. 1998. Ecología de sistemas urbanos. Documento del curso: La Gestión Ambiental en el Desarrollo Urbano. Maestría de Gestión Ambiental del Desarrollo Urbano GADU. Facultad de Ingeniería. Universidad Nacional del Comahue. Neuquén.

Nicolas, E; Barradas, V L; Ortuño, MF; Navarro, A; Torrecillas, A; Alarcon, JJ. 2008. Environmental and stomatal control of transpiration, canopy conductance and decoupling coefficient in young lemon trees under shading net. Environmental and Experimental Botany 63, 200-206.

Oke, TR. 1982. The energetic basis of the urban heat island. *Quarterly Journal of the Royal Meteorological Society* 108, 1-24.

Oke, TR. 1988. The urban energy balance. Prog. Phys. Geogr. 12:471–508.

Oke, TR; Spronken-Smith, RA; Jáuregui, E; Grimmond, CSB. 1999. The energy balance of Central Mexico City. Atmos. Environ. 33:3919-3930.

Oliveira, S; Andrade, H; Vaz, T. 2011. The cooling effect of green spaces as a contribution to the mitigation of urban heat: a case study in Lisbon. Building and Environment 46, 2186–2194.

Pitman, JI. 1996. Ecophysiology of tropical dry evergreen forest, Thailand: measured and modelled stomatal conductance of *Hopea ferrea*, a dominant canopy emergent. Journal of Applied Ecology 33, 1366–1378.

Ramos, G. 1998. Simulación de escenarios de ahorro y uso eficiente de energía con medidas de control pasivo. Revista FIDE, Año 7, No. 28, 25 pp.

Reforma Journal. 2014. Calculan calor intenso en ciudades. Interview from Diana Saavedra. 27 de August. Mexico City, Mexico.

http://www.reforma.com/aplicacioneslibre/preacceso/articulo/default.aspx?id=324449&v=4&urlredirect=http://www.reforma.com/aplicaciones/articulo/default.aspx?id=324449&v=4

Rizwan, AM; Dennis, LC; Liu, C. 2008. A review on the generation, determination and mitigation of urban heat island. J. Environ. Sci. 20:120-128.

Roberts, J; Cabral, OMR; de Aguiar, LF. 1990. Stomatal and boundary layer conductances in an Amazonian terra firme rain forest. Journal of Applied Ecology 27, 336–353.

Roberts, JM and Rosier, PTW. 1993. Physiological studies in young Eucaliptus stand in southern India and derived estimates of forest transpiration. Agricultural Water Management 23, 103–118.

Rosenfeld, AH; Akbari, H; Romm, JJ. 1998. Cool communities: Strategies for heat island mitigation and smog reduction. Energ. Build. 28:51–62.

Saltenyte, U. 2016. Top megacities for growth in 2016. http://blog.euromonitor.com/2016/02/top-megacities-for-growth-in-2016.html

Sánchez, G. 1996. El crecimiento urbano del Distrito Federal (Ciudad de México) y su legislación urbanística. *Boletín Mexicano de Derecho Comparado*, Año XXIX, No. 85, 283-302.

SARH (Secretaría de Agricultura y Recursos Hidráulicos). 1982. Normales climatológicas. Dirección General del Servicio Meteorológico Nacional. Mexico.

Shahmohamadi, P; Che-Ani, AI; Maulud, KNA; Tawil, NM; Abdullah, NAG. 2011. The impact of anthropogenic heat on formation of urban heat island and energy consumption balance. Urban Studies Research, 9 pages, http://dx.doi.org/ 10.1155/ 2011/497524.

Schmetz, J and Raschke, E. 1978. A method to parameterize the downward solar radiation at ground. Arch. Meteor. Geophysi. Bioklimatol. Ser B, 26: 143-151.

Schulze, ED and Hall, A E. 1981. Short-term and long-term effects of drought on steady-state and integrated plant processes. Physiological Processes Limiting Plant Productivity (Ed. by C. B. Johnson), pp. 217- 235. Butterworths, London, Boston, Sydney.

Schulze, ED. 1986. Carbon dioxide and water vapour exchange in response to drought in the atmosphere and in the soil. Annual Review of Plant Physiology 37, 247–274.

Schulze, ED; Čermáck, J; Matyssek, R; Penka, M; Zimmermann, R; Gries, W; Kucera, J. 1985. Canopy transpiration and water fluxes in the xylem of the trunk of *Larix* and *Picea* trees –a comparison of xylem flow, porometer and cuvette measurements. Oecologia. 66: 475-483.

Solecki, WD; Rosenzweig, C; Parshall, L; Pope, G; Clark, M; Cox, J; Wiencke, M. 2005. Mitigation of the heat island effect in urban New Jersey. Enviro. Hazards 6:39-49.

Susca, T; G affin, S R; D ell'Osso, G R. 201 1. Positive ef fects of v egetation: U rban h eat island and green roofs. Environmental Pollution 159, 2119-2126.

Stewart, JB. 1988. M odelling s urface conductance of pine f orest. A gricultural a nd Forest Meteorology 43, 19–35.

Synnefa, A; Santamouris, M; Apostolakis, K. 2007. On the development, optical properties and thermal performance of cool colored coatings for the urban environment. Solar Energy 81, 488-497.

Taha, H . 1997. U rban climates a nd he at islands: a lbedo, evapotranspiration, and anthropogenic heat. Energy Build. 25:99-103.

Takebayashi, H a nd M oriyama, M . 2007. S urface heat bu dget on g reen r oof a nd hi gh reflection roof for mitigation of urban heat island. Building and Environment 42:2971 2979.

Tan, CS; Black, TA; Nnyamah, JU. 1978. A simple di ffusion model of evapotranspiration applied to a thinned Douglas-fir stand. Ecology 59, 1221–1229.

Velasco, E ; P ressley, S ; G rivicke, R ; A llwine, E ; C oons, T ; F oster, W ; Jobson, B T; Westberg, H ; R amos, R ; H ernández, F ; M olina, LT; L amb, B . 2009. E ddy c ovariance f lux measurements of pollutant gases in urban Mexico City. Atmos. Chem. Phys. 9:7325 7342.

Velasco, E ; P ressley, S ; G rivicke, R ; A llwine, E ; Molina, L T; L amb, B . 20 11. Energy balance in u rban M exico City: obs ervation and p arameterization du ring t he MILAGRO/MCMA-2006 field campaign. Theor. Appl. Climatol. 103:501–517.

Whitehead, D ; O kali, D JJ; F asehun, F E. 198 1. S tomatal r esponses to e nvironmental variables in two tropical forests species during the dry season in Nigeria. J. Appl. Ecol.18:571-587.

Wong H ien, N a nd C hen, Y. 2009. *Tropical Urban Heat Islands: Climate, buildings and greenery.* Taylor & Francis Editor, United States of America. 259 pp: 58-68.

Wright, IR; Gash, JHC; da Rocha, HR; Roberts, JM. 1996. Modelling stomatal conductance for A mazonian pa sture a nd f orest. I n: G ash JHC, Nobre C A, R oberts JM, Victoria R L (eds) Amazonian deforestation and climate. Institute of Hydrology, Wallingford, pp 437–457.

Zweifel, R; Rigling, A; Dobbertin, M. 2009. Species-specific stomatal response to drought - a link to vegetation dynamics? Journal of Vegetation Science 20, 442-454.

Annexed

Published November 25, 2015

Journal of Environmental Quality SPECIAL SECTION
THE URBAN FOREST AND ECOSYSTEM SERVICES

The Urban Tree as a Tool to Mitigate the Urban Heat Island in Mexico City: A Simple Phenomenological Model

Mónica Ballinas and Víctor L. Barradas*

Abstract

The urban heat island (UHI) is mainly a nocturnal phenomenon, but it also appears during the day in Mexico City. The UHI may affect human thermal comfort, which can influence human productivity and morbidity in the spring/summer period. A simple phenomenological model based on the energy balance was developed to generate theoretical support of UHI mitigation in Mexico City focused on the latent heat flux change by increasing tree coverage to reduce sensible heat flux and air temperature. Half-hourly data of the urban energy balance components were generated in a typical residential/commercial neighborhood of Mexico City and then parameterized using easily measured variables (air temperature, humidity, pressure, and visibility). Canopy conductance was estimated every hour in four tree species, and transpiration was estimated using sap flow technique and parameterized by the envelope function method. Averaged values of net radiation, energy storage, and sensible and latent heat flux were around 449, 224, 153, and 72 W m^{-2}, respectively. Daily tree transpiration ranged from 3.64 to 4.35 Ld^{-1}. To reduce air temperature by 1°C in the studied area, 63 large *Eucalyptus camaldulensis* would be required per hectare, whereas to reduce the air temperature by 2°C only 24 large *Liquidambar styraciflua* trees would be required. This study suggests increasing tree canopy cover in the city cannot mitigate UHI adequately but requires choosing the most appropriate tree species to solve this problem. It is imperative to include these types of studies in tree selection and urban development planning to adequately mitigate UHI.

Core Ideas

- Urban heat island mitigation by vegetation with emphasis on urban trees.
- A phenomenological model of UHI mitigation based on urban energy balance.
- Tree transpiration as a mechanism to urban heat island mitigation.

J. Environ. Qual.
doi:10.2134/jeq2015.01.0056
Received 30 Jan. 2015.
Accepted 31 Aug. 2015.
*Corresponding author (vlbarradas@ecologia.unam.mx).

URBANIZATION, as a drastic transformation of the environment, presents many effects in the settlement area. One of these effects is the urban heat island (UHI). The UHI phenomenon has led to increased air temperatures in urban areas compared with their rural surrounds (e.g., Lee, 1991; Oke, 1995; Kuttler, 1998; Unger, 1999). Temperature rise in a city or urban area is due to the redistribution and storage (heat) of solar radiation energy because of changes in land use. This can be partly explained by the drastic reduction of latent heat flux (Q_E) caused by the impervious layer of concrete and asphalt, the limited contribution of evaporative and green areas, and the sensible heat flux (Q_H) increase, all of which contribute to increased air temperature (T_A).

The UHI in Mexico City can be as high as 6 to 7°C on average but can also be established during the day with intensities of up to 10°C (Ballinas, 2011). Rising temperatures can negatively affect human thermal comfort, which can affect productivity and lead to health issues, mainly in the spring/summer seasons (Seppanen et al., 2004; Tse and So, 2007).

Due to these problems, there are many studies and research examining mitigation of UHI (Rosenfeld et al., 1998; Solecki et al., 2005; Takebayashi and Moriyama, 2007; Rizwan et al., 2008; Shahmohamadi et al., 2011). There are several alternatives to mitigate the UHI by manipulating the urban energy balance and changing some terms and/or factors: (i) changing the albedo to reduce net radiation, (ii) improving ventilation affecting human heat load, and (iii) augmenting evaporative potential areas. The first two alternatives are permanent and can potentially lead to negative effects during the autumn/winter period when albedo increases due to solar inclination, reducing net radiation, and when cool winds could increase wind chill. However, the third alternative may not lead to negative effects in winter, especially when it comes from vegetation, particularly trees. Accordingly, with the proper implementation of urban vegetation, it is possible to mitigate the UHI due to the cooling potential given by transpiration (Barradas, 1991, 2000; Susca et al., 2011; Kornaska et al., 2015).

The release of water vapor to the surrounding air by transpiring plants increases air humidity and decreases air temperature.

M. Ballinas, Centro de Ciencias de la Atmósfera, Universidad Nacional Autónoma de México, Circuito Científico s/n, Ciudad Universitaria, 04510, México, D.F., México; M. Ballinas and V.L. Barradas, Instituto de Ecología, Universidad Nacional Autónoma de México, Circuito Exterior s/n, Ciudad Universitaria, Coyoacán, 04510, México, D.F., México. Assigned to Associate Editor Stephen Livesley.

Abbreviations: CD, crown diameter; DBH, diameter at breast height; doy, day of year; LAI, leaf area index; UHI, urban heat island.

Typical rates of heat loss by evaporation in arid environments with good irrigation range from 24.5 to 29.5 MJ m^{-2} d^{-1}; in temperate climates, rates range from <0.7 (winter) to 7.4 MJ m^{-2} d^{-1} (summer) (Jones, 1992). The release of water vapor corresponding to these heat loss values ranges from 0.28 to 12 L m^{-2} d^{-1}. Transpiration is mainly controlled by stomatal resistance and is dominated by environmental conditions (e.g., Jones, 1992; Meinzer et al., 1993), whereas stomatal resistance depends on the physiological behavior of the plant and is controlled by environmental conditions (e.g., Whitehead et al., 1981; Jones, 1992; Barradas et al., 2004). Therefore, transpiration rates are different among plant species, and individuals of the same species may present transpiration rate variations depending on the prevailing environmental conditions.

Developing an appropriate urban vegetation structure to mitigate UHI requires (i) determining the transpiration behavior of each involved plant species and their structural characteristics and (ii) developing a theoretical model to articulate mitigation scenarios choosing different plant species and modifying environmental conditions. The well-known Penman–Monteith equation (Jones, 1992) is an appropriate model to establish the transpiration behavior of each concerned species and involves physiological and environmental conditions. It is also well known that T_A depends on sensible heat flux (Q_H), giving the base to a theoretical model based on the urban energy balance [$T_A = f(Q_H)$].

The objective of the work described here was to build a simple phenomenological model based on the energy balance to explore the effect of dominant urban trees [*Fraxinus uhdei* (Wenzig) Lingelsh., *Ligustrum lucidum* W.T. Aiton, *Eucalyptus camaldulensis* Dehnh. (Myrtaceae), and *Liquidambar styraciflua* L.] on the mitigation of the UHI in a typical neighborhood of Mexico City in the dry season.

Materials and Methods

The Urban Energy Balance

A simple model of the energy balance (W m^{-2}) in a city is given by the following expression (Oke, 1988):

$$Q_N + Q_A = Q_E + Q_H + Q_S + Q_{AD} \quad [1]$$

where Q_N is the net radiation (available energy), Q_A is the energy given to the system by human activity (industry, internal combustion machines, heating, air conditioning, etc.), Q_E is the latent heat flux (evaporation/transpiration), Q_H is the sensible heat flux (air warming), Q_S is the energy storage in the urban fabric, and Q_{AD} is the horizontal transport of energy (advection).

In many cases the Q_A term can be neglected because the energy consumption is frequently very low compared with solar radiation. This term becomes significant in cold-climate urban centers such as New York, where human activities and energy use are high (20–160 W m^{-2}) as compared with energy provided through solar radiation (700–1000 W m^{-2}) (Taha, 1997). Considering the low energy consumption in Mexico City, this term can be neglected. Also, the Q_{AD} term is commonly neglected in urban areas because the urban fabric is uniform and there are no significant energy sources or sinks in the representative area. According to these assumptions ($Q_A = Q_{AD} = 0$), the urban energy balance is reduced to: $Q_N = Q_E + Q_H + Q_S$.

The Urban Heat Island Mitigation Phenomenological Model

The phenomenological model is based on the reduced urban energy balance, first by estimating Q_N and Q_S. Net radiation can be calculated by:

$$Q_N = [(1-\alpha)R_{SI} + \varepsilon_A \sigma T_A^4 - \varepsilon_c \sigma T_C^4] \quad [2]$$

where R_{SI} is the incident solar radiation (W m^{-2}); α is the surface albedo (urban canopy); ε_A and ε_C are the atmospheric and surface emissivities, respectively; T_A and T_C are air and surface temperature (K), respectively; and σ is the Stefan–Boltzmann constant (4.903×10^{-9} MJ K^{-4} m^{-2} d^{-1}). The R_{SI} value can be estimated as follows (Schmetz and Raschke, 1978):

$$R_{SI} = (\bar{R}/r)^2 (S_0 \cos\Theta)(\mathbf{a}.\mathbf{b}^m) \quad [3]$$

where S_0 is the solar constant (1360 $Wm^{-2} \approx 2750$ μmol m^{-2} s^{-1}); Θ is the zenith distance of the sun ($\cos\Theta$ calculation is given in Appendix A SE1); **a** and **b** are the effective transmission factors; m is the optical air mass; r and $\bar{R}$ are, respectively, the actual and the mean distance of the Earth from the Sun in astronomical units (ua) ($\bar{R}$ = 149,600,000 km = 1 ua); and $r = 1 + 0.033\cos[(t_d 2\pi/365)]$, where t_d is day of the year or the Julian day, and

$$m = [\cos\Theta + 0.15(93.885 - \Theta)^{-1.253}]^{-1} [P_M/P_{NM}] \quad [4]$$

where P_M is the average atmospheric pressure on the site; P_{NM} is the atmospheric pressure at sea level; and **a** and **b** depend on the visibility (km), which is a function of the urban aerosols given by: **a** = 0.0096 ln(visibility) + 0.7947 and **b** = 0.144 ln(visibility) + 0.2397. The atmosphere emissivity, ε_A, estimation is given in Appendix A SE2.

Energy storage (Q_S) is one of the factors that can make the UHI more intense (Grimmond et al., 1991):

$$Q_S = a_1 Q_N + a_2 \left(\frac{\Delta Q_N}{\Delta t} \right) + a_3 \quad [5]$$

where t is the time (30 or 60 min), and a_1, a_2, and a_3 are constants depending on the distribution and the characteristics of the urban fabric. These parameters are 0.671, 0.450 s, and −52 W m^{-2}, respectively (Velasco et al., 2011). Energy storage in this paper is taken to be constant in each time step; then the residual of Q_N is distributed only in Q_H and Q_E in every time step ($Q_N = Q_H + Q_E$). Sensible heat flux is responsible for the air warming; thus, it is possible to parameterize Q_H as a function of T_A [$Q_H = f(T_A)$]. Therefore, $T_A = f(Q_H)$ and $Q_H = Q_N - Q_E$. Finally, $T_A = f(Q_N - Q_E)$, and Q_H and Q_E could be parameterized using the simplified Penman–Monteith approach as follows (Holtslag and Van Ulden, 1983):

$$Q_H = \frac{(1-\alpha_{PM}) + (\frac{\gamma}{S})}{1 + \frac{\gamma}{S}} (Q_N - Q_S) - \beta \quad [6]$$

$$Q_E = \frac{\alpha_{PM}}{1 + \frac{\gamma}{S}} (Q_N - Q_S) + \beta \quad [7]$$

where S is the slope of the saturation vapor pressure versus temperature, γ is the psychrometric constant, and α_{PM} and β are empirical parameters. These parameters are 0.029 and 7.33, respectively, for the study site (Velasco et al., 2011). In this case, Q_E is the measured flux, and Q_{ETRP} is the added flux due to tree transpiration. Finally, air temperature mitigation is calculated as $T_A = f(Q_N - [Q_E + Q_{ETRP}])$. The Bowen ratio was estimated from the relation Q_H/Q_E.

Latent heat flux produced by trees (i.e., Q_{ETRP}) was calculated using the Penman–Monteith model (Bosveld and Bouten, 2001):

$$Q_{ETRP} = \lambda_E = \frac{\Delta Q_N + \rho C_P \left[\frac{VPD}{r_A}\right]}{\Delta + \gamma\left[1 + \frac{r_C}{r_A}\right]} \quad [8]$$

where $Q_{ETRP} = \lambda_E$ is the latent heat flux (W m^{-2}) due to tree transpiration, Δ is the slope of the saturation vapor pressure (kPa °C^{-1}), ρ is the density of air at constant pressure (kg m^{-3}), C_p is the specific heat of air at constant pressure (J kg^{-1} K^{-1}), VPD is the vapor pressure deficit (kPa), γ is the psychrometric constant (kPa K^{-1}), r_C is the resistance of the canopy (s m^{-1}), and r_A is the aerodynamic resistance of the canopy (s m^{-1}). Vapor pressure deficit was calculated with the equation: VPD = e_S(1 − RH), where e_S is the saturation vapor pressure and RH is relative humidity. Aerodynamic resistance (r_A) (s m^{-1}) was estimated with the following relation:

$$r_A = \left[\frac{1}{(K^2)(u)}\right] \ln\left[\frac{Z_W - d}{Z_0}\right] \ln\left[\frac{Z_0 - d}{(0.2)(Z_0)}\right] \quad [9]$$

where Z_W is the height at which the wind was measured (m), d (m) is the level of displacement of zero, K is the constant of von Karmann, u is the wind speed (m s^{-1}), and Z_0 is a measure of the aerodynamic surface heterogeneity, in our case, vegetation (m). Resistance of the canopy (r_C) (m s^{-1}) was calculated as follows:

$$r_C = \frac{r_S}{LAI} = \frac{1}{g_C} \quad [10]$$

where LAI is the leaf area index (m^2 m^{-2}); r_S is the stomatal resistance, which is the inverse of stomatal conductance (g_S); and g_C is the aerodynamic conductance.

Stomatal conductance was parameterized as a function of microclimate variables using the envelope function method (Fanjul and Barradas, 1985; Barradas et al., 2004) by:

$$g_S = g_{SMAX}[g(Q_N)\, g(\text{VPD})\, g(T_A)] \quad [11]$$

where $g(Q_N)$, g(VPD), and $g(T_A)$ are the envelope curve functions of normalized g_S ($g_{SMAX} = 1$) that depend on Q_N, VPD, and T_A and are as follows: $g(Q_N) = (a + Q_N)/(b + Q_N)$, g(VPD) = c + dVPD, and $g(T_A) = e + f T_A + g T_A^2$, where a, b, c, d, e, f, and g are parameters of the model.

Study Site and Observation Period

Measurements were performed in the Escandon district, which is near to the center of the metropolitan area of Mexico City (19°24′12.63″ N, 99°10′34.18″ W, 2245 m asl). The city has a highland subtropical climate. Mean annual precipitation (mean of 40 yr) is 748 mm, and almost 94% occurs during the rainy season (June–November). Winds are light and predominantly from the northeast. Extreme maximum and minimum temperatures are registered in April (26°C) and January (5.3°C), respectively (SARH, 1982), with a marked UHI effect in the urban area (Jauregui, 1997). The UHI effect was established during the daytime, with intensities of up to 10°C ($T_{U\text{-}R}$) (Ballinas, 2011). The studied district is delimited by streets with intensive vehicular traffic, and the land use in the study area is mainly commercial and residential, with 57% occupied by buildings of three to four stories, 37% as roads and paved areas, and 6% covered by vegetation (Fig. 1). The mean height (Z_h) of the surrounding buildings is 12 m, and it was estimated that the aerodynamic surface roughness (Z_0) was 1 m. The zero displacement plane d was calculated to be 8.4 m height according to the rule-of-thumb estimate (d =

Fig. 1. Aerial view around the study site (marked with a white disk). The white circle indicates the 1000-m distance around the measuring tower.

$0.7Z_h$) (Grimmond and Oke, 1999a). During the measurement period, the footprint calculation averaged 1150 m (Velasco et al., 2009). The sensible and latent heat fluxes and Q_N were measured continuously for 13 d from 17 to 30 Mar. 2006. March is one of the warmest months of the year in Mexico City, with mean minimum and maximum temperatures of 7.7 and 24°C, respectively, and average monthly precipitation rate of 9.3 mm.

Measurements

Instruments for measuring heat fluxes were installed on a 25-m tower mounted on a 17-m-tall building giving a total height of 42 m, almost three times the average height of the surrounding buildings. Net radiation was measured with a Kipp and Zonen net radiometer CNR1. Wind speed, virtual temperature, and humidity fluctuations were sampled at 10 Hz with a 3D sonic anemometer (model SATI-3K, Applied Technologies, Inc.) and an open-path infrared gas analyzer (OP-2 IRGA, ADC BioScientific). Fluxes were calculated every 30 min using the eddy covariance method and corrected for the effects of air density using the Webb corrections. A detailed description of the instrumentation and methodology used in the eddy covariance system is provided by Velasco et al. (2009).

Canopy conductance was calculated by measuring g_S and LAI. These measurements were made on four dominant tree species to Mexico City: *Fraxinus uhdei* (Wenz.) Lingelsh. (Oleaceae), *Ligustrum lucidum* W.T. Aiton (Oleaceae), *E. camaldulensis* Dehnh. (Myrtaceae), and *Liquidambar styraciflua* L. (Hamamelidaceae), 13 to 15 m high. *Fraxinus uhdei* and *L. styraciflua* are deciduous trees and are native to Mexico, whereas *L. lucidum* and *E. camaldulensis* are evergreen and introduced species.

Leaf area indices ($n = 4$) were 4.5 (diameter at breast height [DBH], 21.0 cm; crown diameter [CD], 11.0 m) for *F. uhdei*, 4.0 (DBH, 14.8 cm; CD, 8.10 m) for *L. lucidum*, 4.10 (DBH, 15.1 cm; CD, 7.2 m) for *E. camaldulensis*, and 4.5 (DBH, 26.5 cm; CD, 14.5 m) for *L. styraciflua*, as estimated with a canopy analyzer (LAI-2000, LI-COR Ltd.).

Stomatal conductance (g_S) was measured in the same individuals of each species at four sites on at least five fully expanded leaves per plant with a steady-state diffusion porometer (LI-1600, LI-COR); air and leaf temperature (T_A, T_L), RH, and photosynthetically active radiation were also measured with the mounted sensors in the porometer. These measurements were made every half hour from 08:00 to 18:00 local time (LT). Concomitantly, irradiance, air temperature and humidity, and wind speed and direction were measured with a pyranometer (Eppley PSP, Campbell-Scientific), a temperature-humidity probe (HMP35C, Campbell-Scientific), and an anemometer and vane set (03001, RM Young), respectively. The pyranometer, wind sensors, and temperature-humidity probe were installed 3 m above the tree canopy. Transpiration was calculated with the Penman–Monteith model.

Transpiration was estimated from sap flow measurements made in the trunk using steady-state xylem water mass-flow metering systems similar to those described by Čermák et al. (1984) and Schulze et al. (1985) with one instrumental set per tree. Xylem water mass flowmeters were connected to a data logger (21XL, Campbell Scientific); voltage and gauge signals were scanned every 20 s and averages were logged every 30 min.

Results

The Urban Heat Island in Mexico City

Figure 2 shows the spatial distribution of the average temperature at 06:00 and 14:00 LT in January and May 2010 in Mexico City. At 06:00 LT, a warm center is developed and located in the area surrounding by Cerro de la Estrella, San Agustín, Villa de las Flores, ENEP-Acatlán, and Pedregal (PED) stations, oriented to the center-north of the city, with temperature differences ($T_{U\text{-}R}$) near 3.5°C and with a highest T_A of 8.5°C (Fig. 2A). By 14:00 LT (Fig. 2B), the warm area has shifted to the west of the city and is smaller than that observed at 06:00 LT, with a $T_{U\text{-}R}$ of approximately 2.5°C and the highest T_A around 21°C. However, a large area was established in much of the city where temperatures were lower than their surroundings, forming a new island; this effect may have been due to the ventilation of the city because wind speed increases from 13:00 to 15:00 LT up to 4.4 m s^{-1} in combination with the topography of the area (Jazcilevich et al., 2005).

In May 2010, the distribution and the location of the warm center was similar to that presented in January but with higher temperatures. At 06:00 LT, the $T_{U\text{-}R}$ was 0.5°C higher than that observed in January (Fig. 2C); however, $T_{U\text{-}R}$ was higher by about 2°C in May than in January at 14:00 LT (Fig. 2D), with the highest temperature around 26°C. These results are very similar to those observed in 2011.

The temperature difference in the area of La Merced (MER) may be up to 7.1°C, as occurred at 04:00 LT on 21 January. However, there are periods of low $T_{U\text{-}R}$ that are between 0.09 and 1°C at around 01:00 and 14:00 LT, respectively.

Energy Balance

Figure 3 shows the performance of the components of energy balance for a typical day (day of year [doy] 78) during the measurement period. Net radiation increased rapidly from dawn (−106.6 Wm^{-2}) to around midday, reaching a maximum of 693.5 W m^{-2}. In the afternoon, Q_N tended toward zero to reach its minimum in the sunset. On average, Q_N was 449.0 W m^{-2} for $Q_N > 0$.

Sensible and latent heat fluxes increased with the rise in Q_N in the morning to reach their maxima around midday. However, during the day, Q_E, Q_H, and Q_S were not as regular as Q_N. Most of the available energy (53%) was dissipated by Q_S, with values up to 428.0 W m^{-2} early in the afternoon (average daytime value was 224.0 W m^{-2}), followed by Q_H, with a maximum value of 210.0 W m^{-2} late in the morning and an average of 153.0 W m^{-2}; Q_E registered the lowest values, with 204.0 W m^{-2} around midday and an average of 72 W m^{-2}, which is just 16% of Q_N (Fig. 3). The average Bowen ratio was 2.92. During the whole experiment, averaged values were 373.3, 190.0, 121.43, and 41.52 W m^{-2} for Q_N, Q_S, Q_H, and Q_E, respectively.

Relationship between Air Temperature and Sensible Heat Flux

Energy balance and micrometeorological data measured in the Escandon district were used to relate air temperature with the sensible heat flux, taking into account the delay between the emission of sensible heat and T_A for $Q_N > 0$. Air temperature that is not directly proportional to Q_H in time while having a

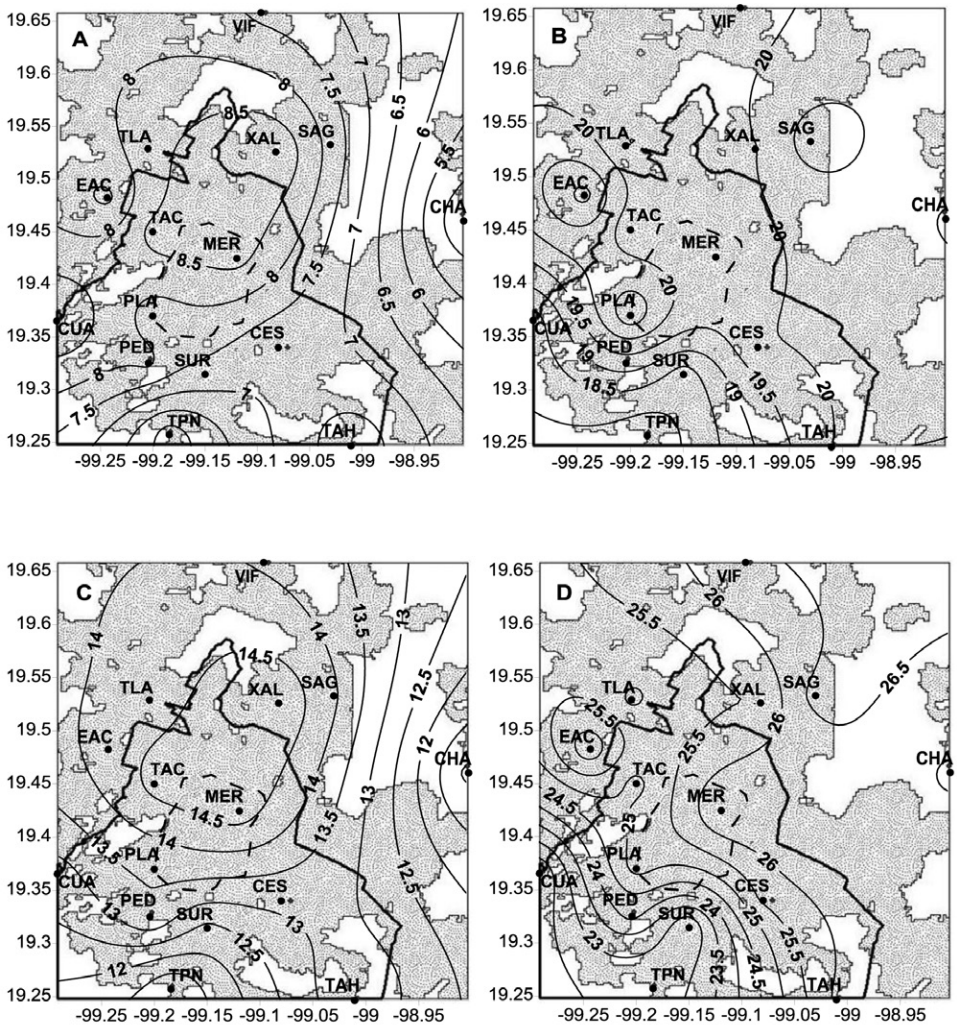

Fig. 2. Average air temperature (°C) distribution in January (A, B) and May 2010 (C, D) at 06:00 (A, C) and 14:00 local time (B, D) in Mexico City. Meteorological network: CES, Cerro de la Estrella; CHA, Chapingo; CUA, Cuajimalpa; EAC, Enep-Acatlan; MER, La Merced; PED, Pedregal; PLA, Plateros; SAG, San Agustín; SUR, Santa Ursula; TAC, Tacubaya; TAH, Tlahuac; TLA, Tlalnepantla; TPN, Tlalpan; VIF, Villa de las Flores; XAL, Xalostoc.

measured flux (i.e., the heating of the air and therefore its temperature) is shown after a certain time. Table 1 shows the relationship between T_A and Q_H at different time steps. Among the changes from 1 to 2 h, the regression coefficient increases; however, this value decreases during the third time lag (after 3 h). This means that air temperature at a given time is given around 2 h after the actual sensible heat flux. As a result, it is possible to consider that there is a time delay of 2 h that produces it (i.e., air temperature has a delay time of 2 h vs. Q_H). Therefore, the effect of air temperature on the sensible heat flux is given as $T_A = 0.03892Q_H + 15.3136$, and finally the diagnosis equation is:

$$T_A = 0.03892[Q_N - (Q_E + Q_{ETRP})] + 15.3 \quad [12]$$

where it can be seen that there is a basal temperature around 15°C during the day when $Q_N > 0$. Q_E is the latent heat flux measured in the study site as a result of the remains of the 6% of vegetation and can be calculated with Eq. [6]; Q_{ETRP} is the necessary latent heat flux provided by vegetation to reduce T_A and can be identified as Eq. [8]. Consequently, this relationship is key in the estimation of air temperature after increasing the latent heat flux by augmenting vegetation.

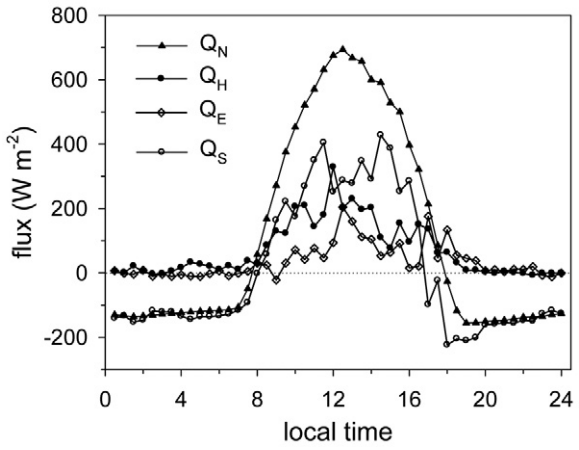

Fig. 3. Energy balance components (W m^{-2}) in the Escandon district in Mexico City in a typical day of the dry season on day of year 78. Q_E, latent heat flux; Q_H, sensible heat flux; Q_N, net radiation; Q_S, energy storage in the urban fabric.

Transpiration and Canopy Conductance

The environmental conditions during the experimental period are shown in Fig. 4. Net radiation increased rapidly from early in the morning to around midday, reaching the maximal values between 640 and 790 W m^{-2}, with an average value for the entire measurement period of 356.4 W m^{-2} when $Q_N > 0$. Average VPD was 9.0 hPa, fluctuating between 23.58 (maximum, registered around midday) and 1.23 hPa (minimum, registered at night). Transpiration differed among species during the experiment. In general, *L. styraciflua* showed the highest values, and *L.*

Table 1. Simple regression parameters of air temperature (T_A) versus sensible heat flux (Q_H) ($T_A = aQ_H + b$) for all data with net radiation >0 measured at Escandon district for actual time and delayed for 1, 2, and 3 h.

a	b	r^2	Hour	n
°C m² W⁻¹	°C			
0.02863 (0.00161)†	15.8831 (0.177)	0.2503	0	1152
0.03544 (0.00147)	15.4896 (0.162)	0.3807	1	1056
0.03892 (0.00137)‡	**15.3136 (0.152)**	**0.4582**	**2**	**960**
0.03865 (0.00139)	15.3698 (0.153)	0.4505	3	864

† Parameter values (SE) are shown ($p < 0.05$).

‡ Numbers in bold indicate the best fit of air temperature versus sensible heat flux.

ligustrum showed the lowest. Changes in the total transpiration per day were observed during the experiment for the four species, ranging between 3.64 and 4.35 L d^{-1}. Averaged TRP values were 4.22, 3.82, 3.64, and 3.59 L d^{-1} for *L. styraciflua*, *F. uhdei*, *L. lucidum*, and *E. camaldulensis*, respectively. These transpiration rates represent a gross energy consumption of 10.30, 9.33, 8.89, and 8.77 MJ d^{-1}, respectively, per species.

Figure 5 shows transpiration rates of the four species on doy 84. Transpiration throughout the day showed generally a unimodal pattern with some slight changes and increasing as irradiance reaches its maximum value around midday. The highest daily transpiration was registered for *L. styraciflua* (1098 g m^{-2} d^{-1}) and the lowest for *E. camaldulensis* (993 g m^{-2} d^{-1}), with maximum rates of 0.043 and 0.032 g m^{-2} s^{-1}, respectively, registered between 13:00 and 15:00 LT. Maximum diurnal transpiration rates represent an energy consumption of 98.9, 105.25, 101.83, and 78.14 W m^{-2} for *F. uhdei*, *L. styraciflua*, *L. lucidum*, and *E. camaldulensis*, respectively.

The diurnal pattern of canopy conductance (g_C) was similar in the four species, showing a maximum value between 12:00 and 15:00 LT. However, *L. styraciflua* and *L. lucidum* showed higher g_C values than *F. uhdei* and *E. camaldulensis*, consistent with transpiration. Average g_C values were between 12.5 mm s^{-1} (*E. camaldulensis*) and 20.42 mm s^{-1} (*L. lucidum*), with maximum values of 38.45, 33.34, 23.21, and 21.8 mm s^{-1} for *L styraciflua*, *L. lucidum*, *F. uhdei*, and *E. camaldulensis*, respectively (Fig. 6). These g_C values agree with the measured transpiration.

Mitigation of the Urban Heat Island in Mexico City

Table 2 shows the measured and required energy fluxes to decrease air temperature by reducing sensible heat flux by increasing latent heat flux, which is a function of transpiration rates, tree structure parameters like LAI and crown diameter, and tree density. The necessary sensible heat flux was calculated by inverting Eq. [7]. The values in Table 2 seem to be reasonable because the measured value of Q_E is low compared with other energy balance but higher or similar to the calculated ones, which represent 6% of the vegetated area in the study site.

Table 3 shows evidence of the performance of the phenomenological model. Predicted values of the complete model agreed closely with the results from the model for T_A and each of the different submodels (Q_N, Q_{ETRP}) (Fig. 7). In general, values of coefficients of determination of the model are indicative of a

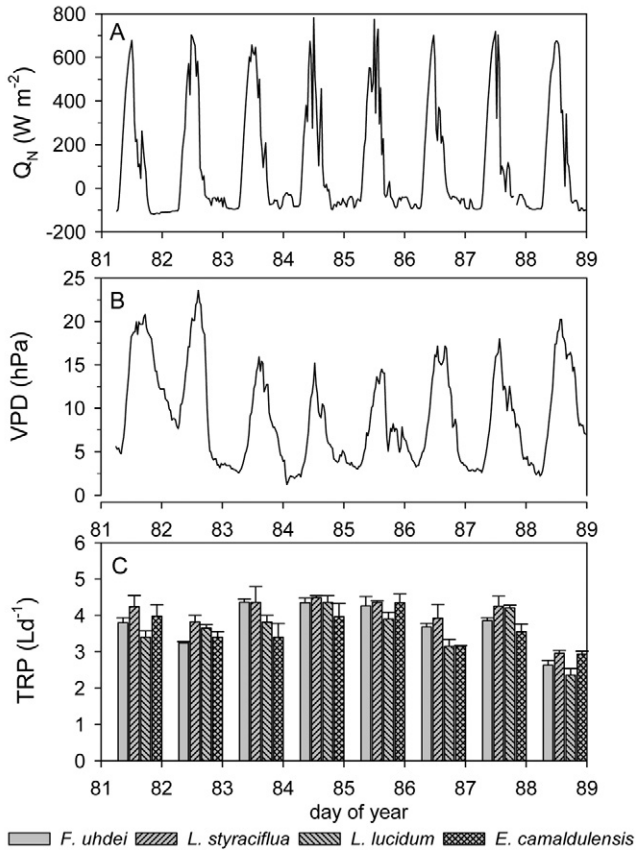

Fig. 4. (A) Net radiation (Q_N; W m^{-2}), (B) vapor pressure deficit (VPD; hPa), and (C) daily transpiration rate (TRP) during the experiment in four tree species in Mexico City. Each histogram is the mean of four trees. Vertical bars on histograms are SEM.

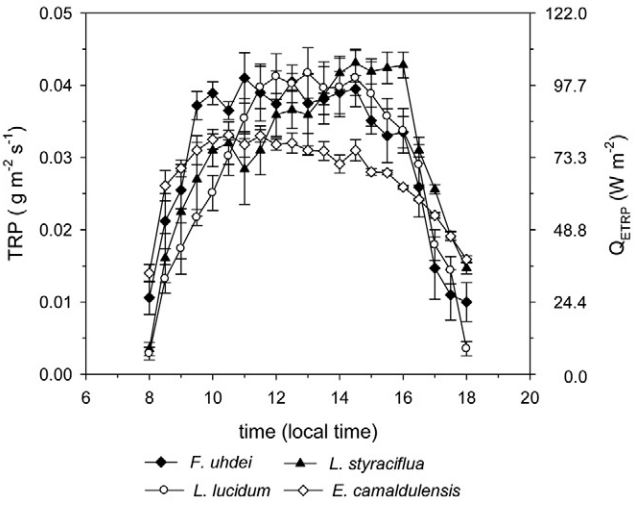

Fig. 5. Diurnal patterns of transpiration rate (TRP) and added flux due to tree transpiration (Q_{ETRP}) for *Fraxinus uhdei*, *Liquidambar styraciflua*, *Eucalyptus camaldulensis*, and *Ligustrum lucidum* during day of year 84. Data points represent the mean of four measurements on different trees. Bars represent SE.

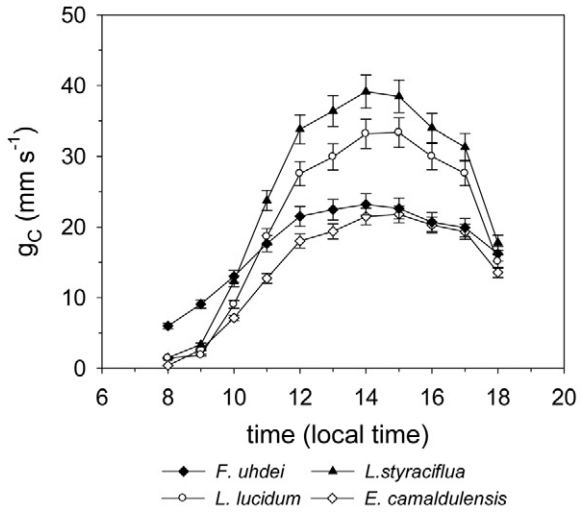

Fig. 6. Diurnal patterns of canopy conductance (g_c) for a typical day in March for *Liquidambar styraciflua* (closed triangles), *Ligustrum lucidum* (open circles), *Fraxinus uhdei* (closed diamonds), and *Eucalyptus camaldulensis* (open diamonds). Values are the average, and bars represent the SE (n = 20).

better agreement between observed values of T_A, Q_N, and Q_{ETRP} and values calculated from the model. Although the model coefficients indicate that the model does explain T_A and Q_N with some efficiency, it does not for Q_{ETRP}. This is most likely due to the fitting of the Q_E model for each of the studied species. *Eucalyptus camaldulensis* (r^2 = 0.5963), probably *F. uhdei*, are the species that least fit the model. Although this species has a high coefficient of determination (r^2 = 0.8575), the RMSE is also high, having, in the best case, an error of up to 13%, propagating these errors to Q_{ETRP}.

Discussion

This work, to our knowledge, is the first attempt to establish the number of trees according to their transpiration rates, to determine the possible decrease in air temperature and thereby the ability to mitigate more efficiently the UHI, and to introduce a phenomenological model that is easy to handle. Because this model is based on the urban energy balance, any constraint of the components could change the model results, as is the case in which Q_A and Q_{AD} were neglected; however, Q_E and Q_H were measured independently, and in the case that Q_A values could be significant, say above 5% of Q_N, its effect is introduced implicitly because the other components (Q_E, Q_H, and Q_S) did not affect the UHI mitigation model results. Also, within the footprint extension in the study site (1150 m) where there are no important sources or sinks of energy (Fig. 1), the Q_{AD} effect may be negligible.

The measurements of fluxes and the urban tissue were allowed to generate the energy storage parameters (Eq. [3]) for this neighborhood. The large value of 0.671 (a_1) indicates the importance of Q_S in the energy balance in this neighborhood of Mexico City and, similar to β, reflects the large proportion of area that is paved and built against the green/evaporating area (Velasco et al., 2011). Energy storage is a key component, being the most dissipative constituent of energy balance in the city.

Table 2. Measured fluxes and required fluxes needed to reduce the air temperature 1, 2, and 3°C on day of year 77 at 14:00 local time and day of year 78 at 15:00 local time and tree densities of two native species and two introduced species needed to change the required sensible heat flux to get the required air temperature by increasing the latent heat flux.

Day of year/hour	T_A†	Measured fluxes‡				T_{AR}§	Required fluxes¶		Tree densities#			
		Q_N	Q_S	Q_H	Q_E		Q_{HR}	Q_{ER}	*Ls*	*Fu*	*Ll*	*Ec*
		W m^{-2}							trees ha^{-1}			
77/14:00	28.0	680.0	252.0	329.0	93.9	**27.0††**	**300.6**	**33.5**	**17.0**	**8.6**	**16.2**	**42.9**
	28.0	680.0	252.0	329.0	93.9	**26.0**	**274.9**	**59.2**	**30.0**	**15.1**	**28.6**	**75.8**
	28.0	680.0	252.0	329.0	93.9	**25.0**	**249.2**	**84.9**	**43.0**	**21.7**	**41.0**	**108.8**
78/15:00	27.0	703.0	299.0	324.0	79.9	**26.0**	**274.9**	**49.2**	**24.9**	**12.6**	**23.7**	**63.0**
	27.0	703.0	299.0	324.0	79.9	**25.0**	**249.2**	**74.9**	**38.0**	**19.1**	**36.1**	**95.9**
	27.0	703.0	299.0	324.0	79.9	**24.0**	**223.5**	**100.6**	**51.0**	**25.7**	**48.5**	**128.9**

† Air temperature.

‡ Q_E, latent heat flux; Q_H, sensible heat flux; Q_N, net radiation; Q_S, energy storage in the urban fabric.

§ Required air temperature.

¶ Q_{ER}, required latent heat flux; Q_{HR}, required sensible heat flux.

Native species: *Ls*, *Liquidambar styraciflua*; *Fu*, *Fraxinus uhdei*. Introduced species: *Ll*, *Ligustrum lucidum*; *Ec*, *Eucalyptus camaldulensis*.

†† Numbers in bold indicate the results from the model.

Table 3. Statistical performance of the simple phenomenological model at the half-hourly timescale. Fluxes are determined for hours at net radiation >0.

Variable†	*n*	Slope	Intercept‡	r^2	RMSE
Q_N	130	0.9528	11.5225	0.9785	33.37
Q_{ETRP}	168	0.9416	5.2736	0.8499	28.92
Q_E, *Fraxinus uhdei*	42	0.9825	6.5020	0.8571	11.32
Q_E, *Liquidambar styraciflua*	42	1.0221	−0.6002	0.8825	9.58
Q_E, *Ligustrum lucidum*	42	0.8327	8.8061	0.9442	8.48
Q_E, *Eucalyptus camaldulensis*	42	0.9274	5.8852	0.5963	10.29
T_A	130	0.8705	2.7982	0.8891	1.38

† Q_E, latent heat flux; Q_{ETRP}, added flux due to tree transpiration; Q_N, net radiation; T_A, air temperature.

‡ Intercept and RMSE units are in W m^{-2} for the energy fluxes and °C for T_A.

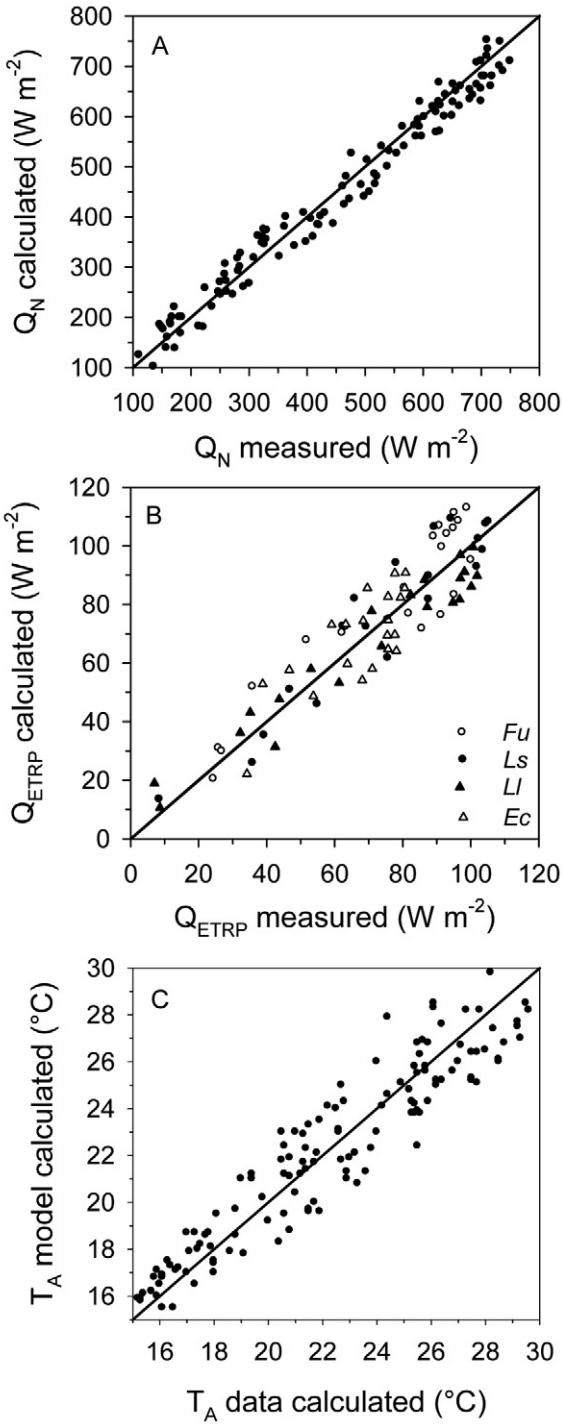

Fig. 7. (A) Scatterplots of half-hourly measured versus modeled net radiation (W m^{-2}) and (B) tree transpiration (W m^{-2}) and (C) calculated versus modeled air temperature (°C). Transpiration (W m^{-2}) is shown for *Fraxinus uhdei* (open circles), *Liquidambar styraciflua* (closed circles), *Ligustrum lucidum* (closed triangles), and *Eucalyptus camaldulensis* (open triangles). Statistics for goodness of fit are reported in Table 3.

According to the measurements, Q_N registered 693.5 W m^{-2} at noon, and Q_S was 290 W m^{-2} (40%). Averaged Q_N was 449.0 W m^{-2}, whereas Q_S was 224.0 W m^{-2} when $Q_N > 0$ (50% of Q_N on average). However, taking into account Eq. [3], Q_S values increase to as high as 390 W m^{-2} (53% of Q_N); these findings are similar to São Paulo, Brazil, where Q_S is 51% of Q_N (Ferreira et al., 2013). Although the constitution of studied areas in extratropical cities in North America are different from Mexico City, it is possible that high urbanization affects energy storage. For example, in Vancouver, Canada, this ratio is 48% but ranges from 17 to 31% in cities with 24 to 49% of vegetation (Grimmond and Oke, 1999b). However, energy storage is not comparable to latent heat flux, although heat flux "dissipates" large amounts of energy. This mechanism (Q_S) just redistributes the energy, taking large amounts from early morning until the irradiance maximum is reached, and after that it is reirradiated as heat to the surroundings in the afternoon and night. A major problem with this mechanism is that Q_S may change due to alterations in building materials and urban fabric distribution and therefore could modify the coefficients of Eq. [3].

The Bowen ratio can be used as an urbanization index and as an indicator of the presence or absence of vegetation in Mexico City, and possibly in other parts of the world, because its value is high in well-urbanized areas with a lack of vegetation, such as Palacio de Minería (β = 8.8, near MER [Fig. 2]; 1% vegetation) in the historic city center (Oke et al., 1999), and lower in districts with less urbanization, such as the Escandon district (β = 2.92, near PLA [Fig. 2]; 6% vegetation) and Pedregal de San Angel (β = 1.92, near PED [Fig. 2]; 50% vegetation), a suburban area (Barradas et al., 1999) similar to the university campus in São Paulo, Brazil (β = 1.57; 30% vegetation) (Ferreira et al., 2013). In general, Bowen ratios in extratropical cities are higher than in Mexico City, ranging from 1.24 to 2.87, taking into account that green areas extensions are bigger (24–49%) (Grimmond and Oke, 1999b). Vancouver showed a similar value to Escandon (β = 2.87), with a 5.5-fold greener area. This is probably due to the low transpiration rates of urban vegetation in that latitude.

The theoretical results applying the phenomenological model presented here demonstrate that tree arrangements can efficiently but differentially mitigate the UHI in Mexico City, considering their transpiration rates, although there are some slight discrepancies between tree densities, for instance when T_A is reduced from 26 to 25°C with a tree density of 43.0 and 38.0 trees ha^{-1} for *L. styraciflua*. This behavior could be due to the difference between observed or measured Q_E on doy 78, which is 15% lower than that observed on doy 77, although Q_N is higher on doy 78 (23 W m^{-2}) than on doy 77. However, some of the total Q_E in the study site can be due water spilled on the sidewalks and streets by shops in the area, a very hard variable to control. A simple strategy to solve this problem would be to discard measured Q_E with the usual increase of tree density because it is possible to get by using tree species with the highest transpiration rates, LAI, and crown diameter (e.g., *F. uhdei*). It is possible to have no overlapping density with as many as 105 trees ha^{-1}, corresponding a Q_E value of 411.0 W m^{-2} and reducing Q_H to almost null, and T_A could be 15.0°C. These temperature, Q_E, and tree density values are similar to a natural forest. The main problem with this approach is that Q_S parameters could change, releasing energy in excess of Q_E and Q_H because a_1 in a mixed forest is 0.11 (McCaughey, 1985) or 0.32 for short grass (Doll et al., 1985). Nevertheless, this approximation shows a reasonable performance of the model (Table 3), although *E. camaldulensis* (and *F. uhdei*, but the introduced error is not so large) presented a low performance on Q_{ETRP} calculation. This error may be due to the environmental conditions that were not taken into account when g_S was modeled because air pollution and/or substrate

humidity showed different effects among species (Barradas et al., 2004). Although these data were sufficient for *L. styraciflua* and *L. lucidum*, they were not for the other two species. Therefore, it is necessary to explore further these possibilities in future works.

It is necessary to continue identifying the best tree characteristics and species to design with more precision the spatial distribution of trees to get sufficient latent heat flux to effectively mitigate the heat island. Unfortunately, the currently urban design could not allow the expansion of the tree arrangements in some sites; however, old trees may be replaced by trees with higher transpiration rates, leaf area index, and coverage, or other types of vegetation arrangements may be designed with high transpiration but no evaporation.

Although this paper reports just four tree transpiration rates, it is possible to establish more than four species in tree arrangements to support biodiversity. Also, a simple reforestation of the city cannot mitigate UHI adequately; it requires choosing the most appropriate tree species to solve this problem. Finally, because the simple phenomenological model presented here is easy to handle, it can be very useful to urban planners, architects, ecologists, and decision-makers to move toward a more sustainable city.

Conclusions

The challenge to mitigate the UHI is huge and complex and is a multidisciplinary problem that requires contributions from urban developers, ecologists, architects, engineers, climatologists, geographers, sociologists, etc. The lack of information in many parts of the world may exacerbate this problem. For example, there may be information about transpiration rates and other vegetation characteristics for some trees and plants but none for key native species. Furthermore, some studies, procedures, techniques, and recommendations made for other cities may not be appropriate for a particular city.

Mexico City has about 20,116,842 inhabitants in an area of 2046 km^2 and is one of the most populous cities in the world. Its population is estimated to increase to 20.6 million in 2025. Although it has one of the largest parks in the Americas (Chapultepec; ~6.78 km^2), the effects of the UHI have been increasing. Furthermore, this current temperature differences could be enhanced by global climate change (Brazel and Quattrochi, 2005). Also, heat shocks will increase or be enhanced by the UHI effect (Luber and McGeehin, 2008; Basara et al., 2010), and energy consumption for air conditioning also will increase. That is why it is imperative to take action in urban planning so this phenomenon would not grow and not become a difficult problem to solve; with these improvements we can move toward a more sustainable city.

Appendix A

SE1

$$\cos\Theta = [(\text{sen}\varphi\cdot\cos\eta)(-\cos\alpha\cdot\text{sen}\chi) - \text{sen}\eta\cdot(\text{sen}\alpha\cdot\text{sen}\chi)$$
$$+ (\cos\varphi\cdot\cos\eta)\cdot\cos\chi]\cdot\cos\delta + [\cos\varphi\lambda\cdot(\cos\alpha\cdot\text{sen}\chi)$$
$$+ (\text{sen}\varphi\cdot\cos\chi]\cdot\text{sen}\delta$$

where φ, η, δ, α, and χ are the latitude, angular time of the day, day of year (solar declination), azimuthal orientation, and the slope of the surface, respectively; δ is given by: $\delta = -23.4 \cos[360(t_d + 10)/365]$; and t_d is day of year or the Julian day (Jones, 1992).

SE2

The atmosphere emissivity can be estimated by:

$$\varepsilon_A = 0.179e^{1/7} \exp(350/T_A)$$

where e is the actual vapor pressure (kPa) = e_SRH and e_S = $0.6108\exp[(17.27T_A)/(T_A + 237.3)]$, where T_A is in °C and RH is 0 to 1.

Acknowledgments

The authors thank Martín Bonifacio for technical assistance, the National Science Foundation and the Metropolitan Environmental Commission of Mexico for providing energy flux data, and the three anonymous reviewers for their critical observations for the improving of this work. This study was supported partially by Grants IN213209-3 and IT201514 from DGAPA-PAPIIT, UNAM, and 127001 from CONACyT-CONAVI. The first author thanks the Postgraduate Program of Earth Sciences of the Universidad Nacional Autónoma de México and CONACyT-México (No. 348420).

References

Ballinas, M. 2011. Mitigación de la isla de calor urbana a partir de la vegetación arbórea. Master's thesis. Centro de Ciencias de la Atmósfera-Instituto de Ecología, UNAM, Mexico, D.F.

Barradas, V.L. 1991. Air temperature and humidity and human comfort index of some city parks of Mexico City. Int. J. Biometeorol. 35:24–28. doi:10.1007/BF01040959

Barradas, V.L., A. Tejeda-Martínez, and E. Jauregui. 1999. Energy balance measurements in a suburban vegetated area in Mexico City. Atmos. Environ. 33:4109–4113. doi:10.1016/S1352-2310(99)00152-1

Barradas, V.L. 2000. Energy balance and transpiration in an urban tree hedgerow in Mexico City. Urban Ecosyst. 4:55–67. doi:10.1023/A:1009591803532

Barradas, V.L., A. Ramos-Vázquez, and A. Orozco-Segovia. 2004. Stomatal conductance in a tropical xerophilous shrubland at a lava substratum. Int. J. Biometeorol. 48:119–127. doi:10.1007/s00484-003-0195-x

Basara, J.B., H.G. Basara, B.G. Illston, and K.C. Crawford. 2010. The impact of the urban heat island during an intense heat wave in Oklahoma City. Adv. Meteorol. 2010:230365.

Bosveld, F.C., and W. Bouten. 2001. Evaluation of transpiration models with observations over a Douglas-fir forest. Agric. For. Meteorol. 108:247–264. doi:10.1016/S0168-1923(01)00251-9

Brazel, A.J., and D.A. Quattrochi. 2005. Urban climates. In: J.E. Oliver, editor, Encyclopedia of world climatology. Springer, Dordrecht, the Netherlands. p. 766–769.

Čermák, J., J. Jenik, J. Kucera, and V. Zidek. 1984. Xylem water flow in a crack willow tree (*Salix fragilis* L.) in relation to diurnal changes of environment. Oecologia 64:145–151. doi:10.1007/BF00376862

Doll, D., J.K.S. Ching, and J. Kaneshiro. 1985. Parameterisation of subsurface heating for soil and concrete using net radiation data. Boundary Layer Meteor. 32:351–372. doi:10.1007/BF00122000

Fanjul, L., and V.L. Barradas. 1985. Stomatal behaviour of two heliophile understorey species of a tropical deciduous forest in Mexico. J. Appl. Ecol. 22:943–954. doi:10.2307/2403242

Ferreira, M.J., A. Pereira de Oliveira, and J. Soares. 2013. Diurnal variation in stored energy flux in Sao Pãulo city, Brazil. Urban Climate 5:36–51. doi:10.1016/j.uclim.2013.06.001

Grimmond, C.S.B., H.A. Cleugh, and T.R. Oke. 1991. An objective heat storage model and its comparison with other schemes. Atmos. Environ. 25:311–326. doi:10.1016/0957-1272(91)90003-W

Grimmond, C.S.B., and T.R. Oke. 1999a. Aerodynamic properties of urban areas derived from analysis of surface form. J. Appl. Meteorol. 38:1262–1292. doi:10.1175/1520-0450(1999)038<1262:APOUAD>2.0.CO;2

Grimmond, C.S.B., and T.R. Oke. 1999b. Heat storage in urban areas: Local-scale observations and evaluation of a simple model. J. Appl. Meteorol. 38:922–940. doi:10.1175/1520-0450(1999)038<0922:HSIUAL>2.0.CO;2

Holtslag, A.A.M., and A.P. Van Ulden. 1983. A simple scheme for daytime estimates of the surface fluxes from routine weather data. J. Clim. Appl. Meteorol. 22:517–529. doi:10.1175/1520-0450(1983)022<0517:ASSFDE>2.0.CO;2

Jauregui, E. 1997. Heat island development in Mexico City. Atmos. Environ. 31:3821–3831. doi:10.1016/S1352-2310(97)00136-2

Jazcilevich, A.D., A.R. García, and E. Caetano. 2005. Locally induced surface air confluence by complex terrain and its effect on air pollution in the valley of Mexico. Atmos. Environ. 39:5481–5489. doi:10.1016/j.atmosenv.2005.05.046

Jones, H.G. 1992. Plants and microclimate. Cambridge Univ. Press, Cambridge, UK.

Kornaska, J., J. Uddling, B. Holmer, M. Lutz, F. Lindberg, H. Pleijel, and S. Thorsson. 2015. Transpiration of urban trees and its cooling effect in a high latitude city. Int. J. Biomteorol. (in press). doi:10.1007/s00484-015-1014-x

Kuttler, W. 1998. Stadtklima. In: E. Heyer, editor, Witterung und Klima. Teubner, Stuttgart, Leipzig. p. 328–364.

Lee, D.O. 1991. Urban-rural humidity differences in London. Int. J. Climatol. 11:577–582. doi:10.1002/joc.3370110509

Luber, G., and M. McGeehin. 2008. Climate change and extreme heat events. Am. J. Prev. Med. 35:429–435. doi:10.1016/j.amepre.2008.08.021

McCaughey, J. 1985. Energy balance storage terms in a mature mixed forest at Petawawa Ontario: A case study. Boundary Layer Meteorol. 31:89–101. doi:10.1007/BF00120036

Meinzer, F.C., G. Goldstein, N.M. Holbrook, P. Jackson, and J. Cavelier. 1993. Stomatal and environmental control of transpiration in a lowland tropical forest tree. Plant Cell Environ. 16:429–436. doi:10.1111/j.1365-3040.1993.tb00889.x

Oke, T.R. 1988. The urban energy balance. Prog. Phys. Geogr. 12:471–508. doi:10.1177/030913338801200401

Oke, T.R. 1995. The heat island of the urban boundary layer: Characteristics, causes and effects. In: J.E. Cermack, editor, Wind climate in cities. Kluwer Academic, Boston, MA. p. 81–107.

Oke, T.R., R.A. Spronken-Smith, E. Jáuregui, and C.S.B. Grimmond. 1999. The energy balance of Central Mexico City. Atmos. Environ. 33:3919–3930. doi:10.1016/S1352-2310(99)00134-X

Rizwan, A.M., L.Y.C. Dennis, and C. Liu. 2008. A review on the generation, determination and mitigation of urban heat island. J. Environ. Sci. (China) 20:120–128. doi:10.1016/S1001-0742(08)60019-4

Rosenfeld, A.H., H. Akbari, and J.J. Romm. 1998. Cool communities: Strategies for heat island mitigation and smog reduction. Energy Build. 28:51–62. doi:10.1016/S0378-7788(97)00063-7

SARH (Secretaría de Agricultura y Recursos Hidráulicos). 1982. Normales climatológicas. Dirección General del Servicio Meteorológico Nacional, Mexico, D.F.

Seppanen, O., W.J. Fisk, and D. Faulkner. 2004. Control of temperature for health and productivity in offices. LBNL-55448. http://escholarship.org/uc/item/39s1m92c (accessed 10 Apr. 2015).

Shahmohamadi, P., A.I. Che-Ani, K.N.A. Maulud, N.M. Tawil, and N.A.G. Abdullah. 2011. The impact of anthropogenic heat on formation of urban heat island and energy consumption balance. Urban Studies Research. 2011:497524. doi:10.1155/2011/497524

Schmetz, J., and E. Raschke. 1978. A method to parameterize the downward solar radiation at ground. Arch. Meteor. Geophys. Bioklimatol. Ser. B 26:143–151. doi:10.1007/BF02242668

Schulze, E.-D., J. Čermák, R. Matyssek, M. Penka, R. Zimmermann, W. Gries, and J. Kucera. 1985. Canopy transpiration and water fluxes in the xylem of the trunk of *Larix* and *Picea* trees: A comparison of xylem flow, porometer and cuvette measurements. Oecologia 66:475–483. doi:10.1007/BF00379337

Solecki, W.D., C. Rosenzweig, L. Parshall, G. Pope, M. Clark, J. Cox, and M. Wiencke. 2005. Mitigation of the heat island effect in urban New Jersey. Environ. Hazards 6:39–49. doi:10.1016/j.hazards.2004.12.002

Susca, T., S.R. Gaffin, and G.R. Dell'Osso. 2011. Positive effects of vegetation: Urban heat island and green roofs. Environ. Pollut. 159:2119–2126. doi:10.1016/j.envpol.2011.03.007

Taha, H. 1997. Urban climates and heat islands: Albedo, evapotranspiration, and anthropogenic heat. Energy Build. 25:99–103. doi:10.1016/S0378-7788(96)00999-1

Takebayashi, H., and M. Moriyama. 2007. Surface heat budget on green roof and high reflection roof for mitigation of urban heat island. Build. Environ. 42:2971–2979. doi:10.1016/j.buildenv.2006.06.017

Tse, W.L., and A.T.P. So. 2007. The importance of human productivity to air-conditioning control in office environments. HVAC&R Research 13:3–21.

Unger, J. 1999. Urban-rural air humidity differences in Szeged, Hungary. Int. J. Climatol. 19:1509–1515. doi:10.1002/(SICI)1097-0088(19991115)19:13<1509::AID-JOC453>3.0.CO;2-P

Velasco, E., S. Pressley, R. Grivicke, E. Allwine, T. Coons, W. Foster, B.T. Jobson, H. Westberg, R. Ramos, F. Hernández, L.T. Molina, and B. Lamb. 2009. Eddy covariance flux measurements of pollutant gases in urban Mexico City. Atmos. Chem. Phys. 9:7325–7342. doi:10.5194/acp-9-7325-2009

Velasco, E., S. Pressley, R. Grivicke, E. Allwine, L.T. Molina, and B. Lamb. 2011. Energy balance in urban Mexico City: Observation and parameterization during the MILAGRO/MCMA-2006 field campaign. Theor. Appl. Climatol. 103:501–517. doi:10.1007/s00704-010-0314-7

Whitehead, D., D.J.J. Okali, and F.E. Fasehun. 1981. Stomatal responses to environmental variables in two tropical forests species during the dry season in Nigeria. J. Appl. Ecol. 18:571–587. doi:10.2307/2402418

Contents lists available at ScienceDirect

Urban Forestry & Urban Greening

journal homepage: www.elsevier.com

Transpiration and stomatal conductance as potential mechanisms to mitigate the heat load in Mexico City

Mónica Ballinas [a, b], Víctor L. Barradas [a, *]

[a] *Instituto de Ecología, Universidad Nacional Autónoma de México, Circuito Exterior s/n, Ciudad Universitaria, Apdo. Postal 70-275, 04510 México, D.F., Mexico*
[b] *Centro de Ciencias de la Atmósfera, Universidad Nacional Autónoma de México, Circuito de la Investigación, 04510 Mexico, D.F. Mexico*

ARTICLE INFO

Article history:
Received 25 March 2014
Received in revised form 29 July 2016
Accepted 16 August 2016
Available online xxx

Keywords:
Energy balance
Green areas
Latent heat flux
Urban landscape
Urban vegetation

ABSTRACT

Transpiration rates and stomatal and canopy conductances were monitored in *Eucalyptus camaldulensis*, *Fraxinus uhdei*, *Liquidambar styraciflua* and *Ligustrum lucidum* in México City, to explore the potential of trees to reduce the urban heat load. The experiment was carried out over a 2-week period between 11 and 27 April 2013. Four trees of each species were used. Total conductance was obtained from daily measurements of transpiration and vapor pressure deficit between 22 and 27 April, and canopy conductance from stomatal conductance and leaf area index measurements. *L. styraciflua* registered the highest average (4.35 L d^{-1}) transpiration rate, whereas *F. uhdei* registered the minima (3.64 L d^{-1}). Averaged canopy conductance registered values between 40 mm s^{-1} (*E. camaldulensis*) and 50 mm s^{-1} (*L. lucidum*). These results show that transpiration was strongly dominated by vapor pressure deficit (VPD) and controlled by stomatal conductance. According to the envelope function model, stomata was more sensitive to VPD than irradiance or air temperature. Finally, the presented transpiration rates are capable to reduce up to 20% of net radiation in Mexico City. With these results, it is possible to build tree arrangements to dissipate the greatest possible amount of heat produced in the city.

1. Introduction

The urban heat island (UHI) is one of the most common forms of thermal pollution, since air temperature increases in urban area compared to surrounding rural, vegetated areas (e.g. Lee, 1991; Oke, 1995; Kuttler, 1998; Unger, 1999). Because the urban surface is impervious, evapotranspiration (latent heat flux) is reduced drastically and sensible heat flux increases UHI intensity. This contamination increases the human heat load, and people experience thermal discomfort (heat stress) which can affect human productivity mainly in the spring-summer period in temperate and subtropical regions. At present, air conditioning systems are used to mitigate this heat load, increasing energy consumption (mainly electricity). However, these air conditioner systems have a very low efficiency and "take" the heat from the inside and "put" it in the outside of the buildings, producing a probable feedback that could enhance UHI and therefore thermal pollution with a possible increase in energy consumption.

This urban heat island phenomenon is very noticeable in Mexico City (Jauregui, 1997). Average minimum temperature differences between the historical center and the rural area (T_{U-R}) can reach up to 6 °C (Jauregui and Luyando, 1998), and has remained relatively constant. However, to date UHI is also established during the daytime, with maximum temperature differences up to 10 °C (T_{U-R}) (Ballinas, 2011).

Mitigating UHI is important not only because increased urban temperatures differences can affect human health and productivity and increase energy consumption. The total sale of electricity in Mexico City in 1996 was 121.579 GW h^{-1} of which 28.4 GW h^{-1} (23.4%) was consumed by the domestic sector, 5.69 GW h^{-1} was required to refresh the space inside buildings (air conditioning, evaporative cooling, fans) (Ramos, 1998), and 8.52 GW h^{-1} in commercial buildings and services in the metropolitan area.

Nevertheless, with proper implementation of urban vegetation, it is possible to mitigate the UHI due to the cooling potential from shading and transpiration (Barradas, 1991, 2000; Susca et al., 2011).

Release of water vapor to the atmosphere by transpiring plants increases air humidity and decreases air temperature by converting sensible to latent heat. Typical rates of heat loss by evaporation in arid environments with good irrigation range from 24.5 to 29.5 MJ m^{-2} d^{-1} whereas in humid temperate climates, rates range from <0.7 (winter) to 7.4 MJ m^{-2} d^{-1} (summer) (Jones, 1983). The volume of water vapor corresponding to these heat loss values ranges from 0.28 to 12 L m^{-2} d^{-1}.

However, in proposing the release of water vapor as a mechanism to mitigate the UHI, it is necessary to understand that water vapor exchange rate between the vegetated surface and the atmosphere is a key component of the energy exchange process at the air–land interface (Kumagai et al., 2004). Understanding how urban transpiration is affected by radiation and controlled by stomatal opening and closing is vital to selecting vegetation to mitigate the UHI. In particularly, microclimate and tree structural characteristics may affect tree conductance to water vapor that regulates transpiration

Conductance has two components, canopy conductances that depends on physiological behaviors, in series with aerodynamic conductance that defines coupling of stomata to the atmosphere (Herbst, 1995; Magnani et al., 1998). A decoupling coefficient represents the

* Corresponding author.
Email address: vbarrada@ecologia.unam.mx (V.L. Barradas)

http://dx.doi.org/10.1016/j.ufug.2016.08.004
1618-8667/

relative contribution of canopy and aerodynamic conductance in controlling rates of canopy transpiration (Jarvis and McNaughton, 1986). Meanwhile, canopy conductance strongly depends on variable stomatal responses to environment factors as vapor pressure deficit, air temperature (Schulze and Hall 1981; Schulze 1986; Maroco et al., 1997; Meinzer et al., 1997; Barradas et al., 2004) and irradiance (Pitman 1996; Gao et al., 2002; Zweifel et al., 2009). All these factors are responsible for canopy transpiration as a whole (Jones, 1992), and their effects must be studied before establishing tree systems to mitigate UHI.

The objective of the work described here was to examine whole tree transpiration, and canopy conductance for four tree predominant urban tree species (*Fraxinus uhdei, Ligustrum lucidum*, *Eucaliptus camaldulensis* and *Liquidambar styraciflua*) in the urban environment in the dry season in Mexico City to examine the cooling potential of the UHI of each species.

2. Materials and methods

2.1. Study site

Measurements were made in Mexico City (19°19′N, 99°11′W, 2230 m asl). The mean annual rainfall (mean of 40 years) is 748 mm, and nearly 94% occurs during the rainy season (June–November). Winds are light and predominantly from the Northeast. Extreme temperatures occur in April (26 °C) and January (5.3 °C) (SARH, 1982), with a marked heat island effect in the urban areas (Jauregui, 1971), not only at night but also during daytime, with differences of up to 10 °C (T_{U-R}) compared to surrounding areas (Ballinas, 2011). Measurements were made in the dry season in the month of April, the warmest and one of the driest months of the year. During measurements, maximum average temperature was 28 °C and precipitation was registered only the last six days of March with 10.2 mm.

2.1.1. Plant material

Measurements were made on four individuals of four dominant species to Mexico City: *Fraxinus uhdei* (Wenz.) Lingelsh. (Oleaceae), *Ligustrum lucidum* W.T. Aiton (Oleaceae), *Eucaliptus camaldulensis* Dehnh. (Myrtaceae) and *Liquidambar styraciflua* L. (Hamamelidaceae). *F. uhdei* and *L. styraciflua* are deciduous trees and native to Mexico, whereas *L. lucidum* and *E. camaldulensis* are evergreen and introduced species. Trees were located in a suburban area in the south of the city in the National University campus around the football stadium. The trees were located along a street sidewalk forming a single row of planted trees completely surrounded (around a radius of 300 m) by paved areas of asphalt and cement, in an area with no buildings around, and a water collection area (bare soil) around the trunks of the trees of 0.25 m^2 (square of 0.5 m). Trees were planted intermixed in north-south rows spaced 6 m apart with no overlapping of their crowns and they were randomly selected. Tree species structural parameters are shown in Table 1. Urban vegetation in public areas is administered by the municipality.

2.1.2. Measurements

Transpiration was estimated from sap flow measurements made in the trunk using steady-state xylem water mass-flow metering systems similar to those described by Čermák et al. (1984) and Schulze et al. (1985) with one instrumental set per tree. Sap flow (F) was calculated from $F = (P_S - P_l)k/(C_W \Delta T)$, where Ps is input power to the heater, C_W is the heat capacity of water, k is the dimensionless relation of measured segment length to total tree circumference, ΔT is the temperature difference across the heater which is maintained constant and P_1 reflects heat loss due to conduction and convection which is determined during nights when sap flow is absent. During steady-state the applied power does not normally exceed 2 W (with a potential maximum of 20 W). During the measuring period, 5 electrodes per system of the size 60 × 15 × 1 mm were inserted up to 50 mm into the trunk while depth of insertion of thermocouples was 25 mm according to the measured sapwood depth (3–4.5 cm) obtained by taking samples with a Pressler drill. The measuring point was insulated with a polyurethane and aluminized mylar jacket from outside by protecting against weathering and to minimize external effects on ΔT. Water mass-flowmeters were connected to a data logger (21XL, Campbell Scientific, Logan, Utah, USA); voltage and gauge signals were scanned every 20 s and averages were logged every 30 min. Heat storage in the stem segment during each 30 min interval was estimated by measuring the changes in stem temperature during the first and the last minutes of each interval.

Table 1
Leaf area indices (LAI, m^2 m^{-2}), diameter at breast height (DBH, cm), crown diameter (CD, m) and leaf size (LS, long (l, cm), wide (w, cm)) for the studied species. LAI was estimated with a canopy analyzer (LAI-2000, LI-COR Ltd., Lincoln, Nebraska, USA) (n = 4 for LAI) and (n = 40 for LS).

Species	LAI	DBH	H	CD	Leaf Size (l,w)
F. uhdei	4.5	21.0	15.0	11.0	8.02 (1.57), 3.50 (1.16)
L. lucidum	4.0	14.8	13.0	8.10	6.13 (1.14), 3.02 (0.86)
E. camaldulensis	4.1	15.1	14.0	7.2	11.63 (2.42), 3.15 (0.81)
L. styraciflua	4.5	26.5	14.0	14.5	6.25 (1.17), 5.95 (1.38)

Stomatal conductance (g_S) was measured in the same individuals as used for sap flow measurements of each species on at least five total including sunlit and shaded expanded leaves per plant in the mid level of the tree, with a steady-state diffusion porometer (LI-1600, LI-COR, Lincoln, Nebraska, USA); air temperature (T_A), relative humidity (RH) and photosynthetically active radiation (PAR) were also measured with the mounted sensors in the porometer. Concomitantly, irradiance, air temperature and humidity, wind speed and direction were measured with a pyranometer (Eppley PSP, Campbell-Scientific, USA), a temperature-humidity probe (HMP35C, Campbell-Scientific, USA), and an anemometer and vane set (03001, RM Young, USA), respectively. Irradiance, wind sensors and temperature-humidity probe were installed 3 m above the highest tree canopy in a telescopic tube, that is to say these sensors were installed 18 m above the floor surface. The outputs from all sensors were connected to a data logger (21×, Campbell Scientific, USA) and scanned every 30 s and 30 min averages logged. Sensors above the canopy were calibrated before the study and cleaned every week during the study period. Measurements were made during 16 days in April in Mexico City from 07:00 to 20:00 LST, and stomatal conductance and related measurements were made at 0.5–1 h intervals during four days (104, 106, 110 and 114). It did not rain either before, during or after measurements.

2.1.3. Total conductance and decoupling coefficient

Total tree conductance (g_T, m s^{-1}) was estimated from every 30 min averaged transpiration (TRP, kg m^{-2} s^{-1}) and mean vapor pressure deficit (*VPD*, Pa) as:

$$g_T = \frac{\lambda\gamma}{\rho\varepsilon C_p}\frac{TRP}{VPD} \quad (1)$$

where γ (Pa $°C^{-1}$) is the psychrometric constant, λ (J kg^{-1}) is the latent heat of evaporation of water, ρ (kg m^{-3}) is the air density, ε is

the mole fraction of water in air (0.622 kg water per kg air) and Cp is the specific heat of dry air at constant pressure (J kg^{-1} °C^{-1}). Although leaf-air VPD is the actual driver, air VPD is a reasonable proxy because it was independent of the g_S measurements. Air VPD was calculated every 30 min.

Total conductance is the sum of canopy (g_C) in series with aerodynamic (g_A) conductance ($g_T = g_C + g_A$). Canopy conductance (m s^{-1}) was approximated as the product of mean stomatal conductance (m s^{-1}) and leaf area index (*LAI*, m^2 m^{-2}; $g_C = g_S LAI$) (Jones, 1992). Aerodynamic conductance (m s^{-1}), calculated as the inverse of aerodynamic resistance ($g_A = 1/r_A$), was estimated from the difference of total resistance ($r_T = 1/g_T$) and canopy resistance ($r_C = 1/g_C$) as:

$$\frac{1}{g_A} = r_A = \frac{1}{g_T} - \frac{1}{g_C} \tag{2}$$

A dimensionless decoupling coefficient (Ω_C) was calculated to analyze the dependence of canopy transpiration on physical or physiological factors. A formula to express the relative sensitivity of canopy transpiration to a marginal change in stomatal conductance was introduced by Jarvis and McNaughton (1986):

$$\Omega_C = \frac{1}{\left(1 + \left[\frac{\gamma}{s+\gamma}\right]\right)(g_A/g_C)} \tag{3}$$

where S (Pa °C^{-1}) is the rate of change of saturation water vapor pressure with temperature (°C).

2.1.4. Stomatal conductance model

The model used for analyzing and predicting stomatal conductance ($g_S = 1/r_S$) from the driving variables has been previously described by Jarvis (1976) and modified by Dolman (1993) and Wright et al. (1996). The model is based on the hypothesis that steady-state stomatal conductance depends on environmental variables (Stewart 1988; Roberts et al., 1990; Barradas et al., 2004). This method consists in selecting the data of the likely upper limit of the function (envelope function) represented by a cloud of points in each of the diagrams produced by plotting stomatal conductance versus any environmental variable. The envelope function method has three assumptions: (1) the envelope function represents the optimal stomatal response to a selected climate variable (*e.g.* irradiance); (2) the points below the selected function are the result of a change in any of the other variables (*e.g.* vapor pressure deficit, air temperature), and (3) there are no synergistic interactions (Jarvis, 1976; Fanjul and Barradas, 1985; Barradas et al., 2004). The model takes the form:

$$\frac{1}{r_S} = g_S = g_{SMAX}\, g(I)\, g(T_A)\, g(VPD) \tag{4}$$

where g_{SMAX} is the maximum value of the measured stomatal conductance, and g(I), g(T_A), g(VPD), are the normalized boundary-line functions (0–1 values) that incorporate the effects of irradiance I, air temperature T_A, air vapor pressure deficit (VPD).

3. Results

3.1. Transpiration and canopy conductance

The environmental conditions during the experimental period are shown in Fig. 1. VPD average was 1.28 kPa fluctuating between 3.27 (maximum) and 0.087 kPa (minimum). of 0.0871 (night time) (Fig. 1A). Irradiance increased rapidly from early in the morning to around midday, reaching the maxima values between 850 and 1050 J m^{-2} s^{-1} with an average value for all the measurement period of 445.7 J m^{-2} s^{-1} (Fig. 1B). Changes in the total amount of transpiration per day (TRP) were observed during the experiment for the four species (Fig. 1C). TRP differed among species during the experiment. In general *Liquidambar styraciflua* reached the highest values as high of 5.43 L on day 116 whereas *Eucaliptus camaldulensis* registered as low as 2.69 L on day 102. Over the measuring period (days 101–116), average TRP values for species were 4.35, 4.09, 3.90 and 3.64 L d^{-1} (0.028, 0.023, 0.025, 0.027 mm d^{-1}) for *Liquidambar styraciflua*, *Fraxinus uhdei*, *Eucaliptus camaldulensis* and *Ligustrum lucidum*, respectively. These transpiration rates represent a gross energy consumption of 10.6, 10.0, 9.5 and 8.9 MJ d^{-1} per species, equivalent to 37, 35, 33 and 31% of the average incoming short-wave radiation, respectively.

Fig. 2 shows transpiration rates of the four species on day 114, one of the days when stomatal conductance measurements were carried out. Transpiration throughout the day showed generally a uni-modal pattern with some slight changes, increasing with irradiance to reach its maximum value around midday. The day pattern of TRP showed that transpiration before 8:00 and after 17:00 LST was negligible. The highest daily transpiration was registered by *L. styraciflua* (936 g m^{-2} d^{-1}) and the lowest by *L. lucidum* (755 g m^{-2} d^{-1}) with maxima hourly rates of 0.043 and 0.034 g m^{-2} s^{-1}, respectively, between 12 and 14:00 LST. Maximum diurnal transpiration rates represent an energy consumption of 77, 80, 105 and 92 J m^{-2} s^{-1} for *E. camaldulensis*, *F. uhdei*, *L. styraciflua* and *L. lucidum*, respectively.

The diurnal course of total conductance (g_T) was similar to transpiration in the four species showing a maximum value between 12 and 16:00 LST. However, g_T was lower than those values corresponding to g_C after midday for *L. styraciflua* and *L. lucidum*, and around 16:00 LST for *E. camaldulensis* and *F. uhdei* (Fig. 3). Aerodynamic conductance (g_A) patterns were similar in the four species with two peaks, one from midnight to early morning (24:00–06:00 local time) and the other from late in the morning until the evening (10:00–20:00 L h) with values as high as 111.41 mm s^{-1} at noon (*L. lucidum*). During daytime, g_C in average registered values between 39.8 (*E. camaldulensis*) and 49.7 mm s^{-1} (*L. lucidum*) and 21.8 (15:00 LST) and 33.7 (13:30 LST) mm s^{-1}, respectively. Aerodynamic conductance was from three to five times higher than canopy conductance (Fig. 3).

In general, Ω_C values were low, averaging from 0.086 (*L. lucidum*) to 0.125 (*F. udhei*) with maximum values between 0.67 (*F. uhdei*) and 0.56 (*L. lucidum*) and minimum from 0.0003 (*L. lucidum*) and 0.0007 (*L. styraciflua*) (Data not shown). The highest Ω_C values were recorded around sunrise and/or sunset and the lowest from 12:00 to 18:00 local time, showing a similar pattern for *L. styraciflua*, *L. lucidum* and *F. uhdei*. High values are consistent with low g_A values in the four species.

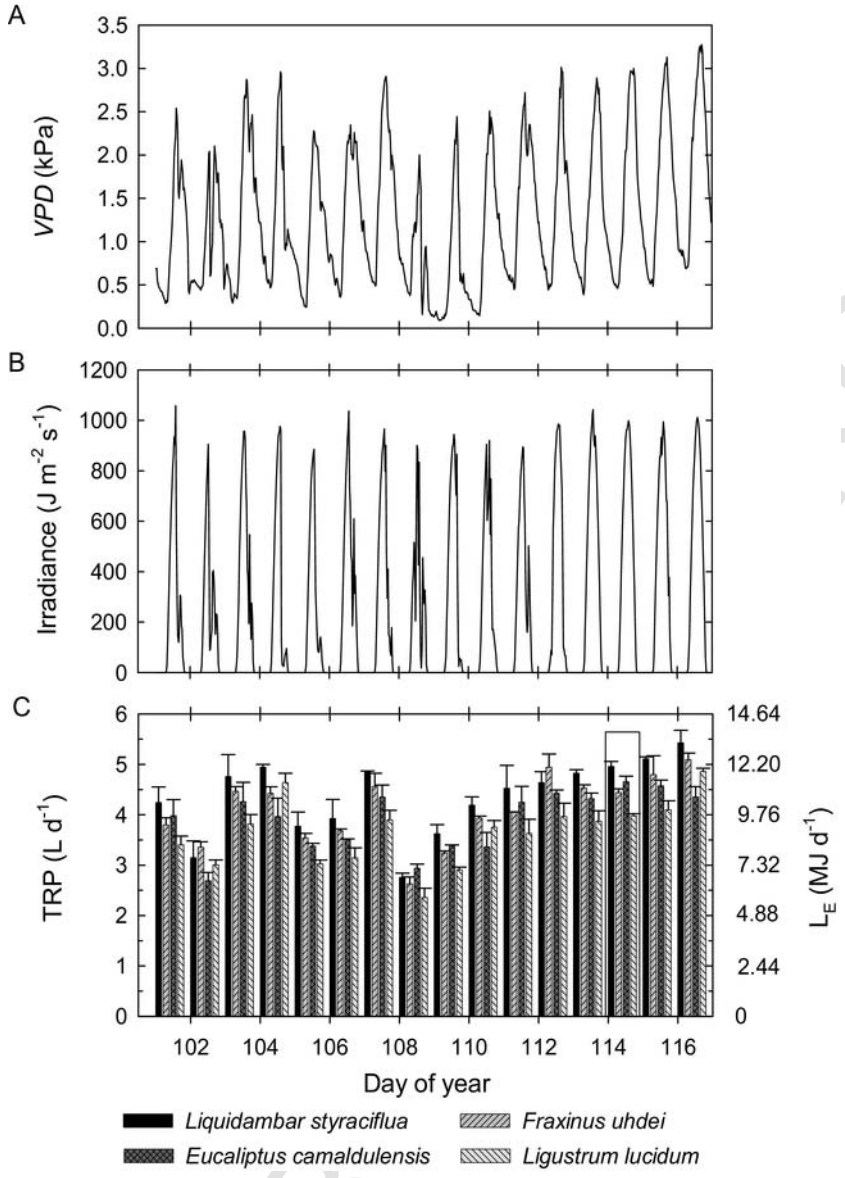

Fig. 1. Vapor pressure deficit (VPD, kPa) (A), irradiance (B) and daily transpiration (TRP) in volumetric units and latent heat flux (L_E) in energy units (C) during the experiment in four tree species in Mexico City. Each histogram is the mean of four trees. Vertical bars on histograms are S.E. of the mean.

3.2. The stomatal conductance model

The plotted data of individual measurements of normalized g_S plotted against irradiance (Fig. 4) during the experiment, showed a significant scatter, but the probable envelope function of the data was described by a hyperbolic relationship of the form: $g(I) = AI/(B + I)$, where A is the maximum value of the g_S or g_{SMAX} and B is the stomata sensitivity to I, with coefficients of determination between 0.90 and 0.98. The relationships and parameter values for the four species are given in Fig. 4. The values of B for *L. Lucidum* and *F. udhei* were consistently lower this is that *L. styraciflua* and *E. camaldulensis* have higher light saturation points and so less shade tolerant.

The effect of T_A on g_S was described by a second degree polynomial of the form: $g_S = a + bT_A + cT_A^2$ where a, b and c are constants. These constants and relationships are shown in Fig. 4 with coefficients of determination (r^2) between 0.91 and 0.98. The optimal (T_O) and extreme temperatures (T_{min} and T_{MAX}) of stomatal function were calculated from this polynomial relationship by computing the roots and the first derivative for each species and season. Maximum stomatal conductance occurred around 28.3 ± 2.0 °C for the four studied species, whereas extreme temperatures of g_S were similar for *E. camaldulensis*, *F. uhde*i and *L. lucidum* with higher temperature value than *L. styraciflua*.

Stomatal conductance in the four species tended to decrease linearly as VPD increased. Stomatal sensitivity to VPD differed among the four species. *E. camaldulensis* and *L. styraciflua* showed higher sensitivity to VPD than *L. lucidum* and *F. uhdei*. Stomatal conductance of *E. camaldulensis* was approximately 25, 49, and 59% more sensitive to VPD, than *L. styraciflua*, *F. uhdei* and *L. lucidum*, respectively (Fig. 4).

Liquidambar styraciflua showed the maximum stomatal conductance (10.00 mm s^{-1}), whereas *Ligustrum lucidum* was intermediate

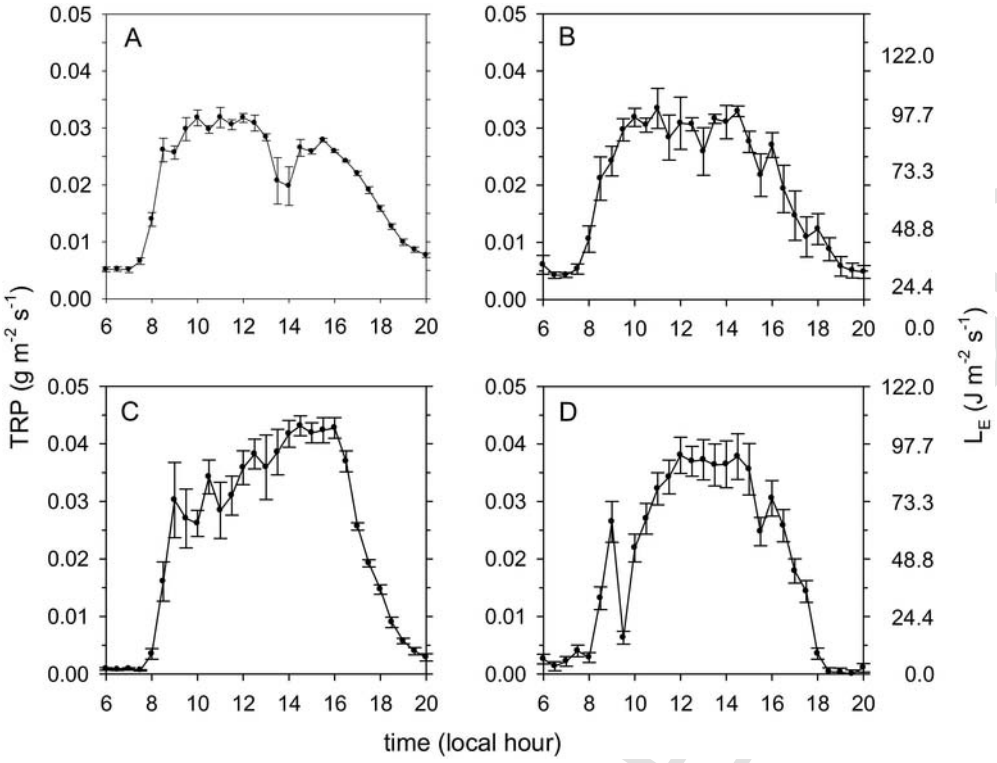

Fig. 2. Diurnal patterns of transpiration rate (TRP) and latent heat flux (L_E) for *Eucaliptus camaldulensis* (A), *Fraxinus uhdei* (B), *Liquidambar styraciflua* (C) and *Ligustrum lucidum* (D) during day of year 114. Data points represent the mean of four measurements on different trees. Bars represent the standard error.

(8.42 mm s^{-1}), to *F. uhdei*, and *E. camaldulensis* with the lowest values (6.00 and 5.41 mm s^{-1}, respectively).

4. Discussion

Tree transpiration is a reliable mechanism to mitigate high heat loads in Mexico City, and therefore to mitigate the urban heat island effect, even with the relatively low transpiration rate registered by *E. camaldulensis* on day 102. However, it looks like that *L. styraciflua* and *L. lucidum* have the greatest cooling potential to mitigate UHI, because they registered the highest transpiration rate values, as much as 105 J m^{-2} s^{-1} early in the afternoon (14:00–16:00 LST, on day 114). It also appears, in the scope of this study, that *L. styraciflua* and *L. lucidum* are better options to reduce the heat loads through evaporative cooling, mainly in the early afternoon, when the maximum temperature is recorded. Although it is difficult to compare transpiration rates in different places in the world because of the particular micrometeorological and soil conditions, transpiration rates of the studied species were in reasonable agreement with other results in the world. Transpiration rates here appear to be low compared with other TRP values found in other species and much lower than those observed in non-stressed Douglas fir in Vancouver (Tan et al., 1978) or beech forest in Maruia, New Zealand (Kelliher et al., 1992) or non stressed red maple in South Carolina, but higher than stressed red maple (Bauerle et al., 2002). It is necessary to point out that in Mexico City trees are not commonly irrigated and transpiration may be lower during the dry season due to water stress. Nevertheless, actual transpiration rates can potentially dissipate up to 20% of net radiation at noon when it is around 560–600 J m^{-2} s^{-1}.

According to Leuning et al. (1991) and Roberts and Rosier (1993), the response of stomatal conductance to vapor pressure deficit is an important factor in estimating the amount of water used by trees. Several authors have indicated the role of leaf conductance in the control of water use and its relationship with the coupling between canopy and atmosphere (Dye, 1987; Hinckley and Braatne, 1994). In this sense, Jarvis and McNaughton (1986) introduced a dimensionless decoupling coefficient (Ω_C), which approaches one as stomatal control decreases. Conversely when Ω_C approaches 0 stomatal control of transpiration is high, such that fractional change in stomatal conductance (proportional to canopy conductance) would lead to an equal change in transpiration (Gu et al., 2005; Nicolas et al., 2008).

The low values of the decoupling coefficient (Ω_C) found in this study suggest that all the studied species were well coupled to the atmosphere, particularly around midday from 10:00 to 18:00 local time. It is interesting to note that *E. camaldulensis* presents a different decoupling coefficient pattern through than that showed for the other species. This could be due to the size of its crown (1.3–1.5 fold) and the length of its leaves (2 fold) which are larger than the ones of the others species. *L. lucidum* was slightly more coupled to the atmosphere than the other species as indicated by its relatively higher Ω_C values. Nevertheless, the other three species also showed low Ω_C values. These results demonstrate that water vapor exchange was strongly dominated by VPD and controlled by stomatal conductance, mainly in between sunrise and sunset.

The results here indicated that the higher VPD, the smaller g_S. The fit of g_S versus VPD (r^2 = 0.91–0.97) showed a higher sensitivity of g_S to this driving variable in the four studied species. *E. camaldulensis* was most sensitive compared to the other three species (Fig. 5).

On the other hand, the variation in stomatal conductance has been attributed to VPD and T_A (Schulze and Hall 1981; Schulze 1986; Maroco et al., 1997; Meinzer et al., 1997), or to a combination of these factors. The curve lines of g_S versus T_A show that the responses of g_S to T_A are very similar between species, but *L. styraciflua*

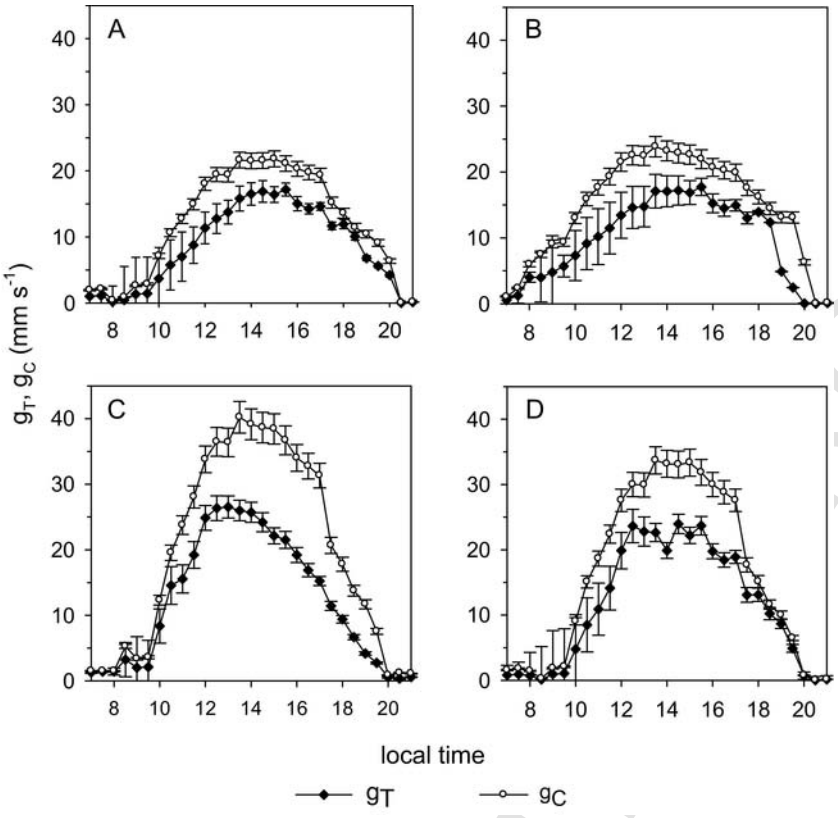

Fig. 3. Diurnal patterns of total conductance (g_T, black squares), canopy conductance (g_C, white circles) and aerodynamic conductance (g_A, black diamonds) for *Eucalyptus camaldulensis* (A), *Fraxinus uhdei* (B), *Liquidambar styraciflua* (C) and *Ligustrum lucidum* (D) during day of year 114, when intensive measurements were made. Values are the averaged and bars represent the standard error (n = 4), for canopy conductance (N = 20, 5 measures per tree per 4 trees).

showed a slightly lower range between T_{MAX} and Tmin than the others species.

Furthermore, previous studies also have demonstrated the effect of *I* on g_S (Pitman 1996; Meinzer et al., 1997; Gao et al., 2002; Zweifel et al., 2009). Although the four studied species reach the maximum conductance at an irradiance of 300 J m^{-2} s^{-1}, *L. lucidum* reached 80% of the change of g_S at 9 J m^{-2} s^{-1} (the more sensitive species to *I*) and *L. styraciflua* at 100 J m^{-2} s^{-1}. These differences indicate that *L. lucidum* is more shade tolerant than *L. styraciflua*.

Because of the different transpiration rates of the studied species, it is possible to select the most suitable species according to the microenvironment where the species are to be planted. However, the most suitable species for reducing urban heat island would be those that showed the highest transpiration rates such as *Liquidambar styraciflua* and *Ligustrum lucidum*. Nevertheless, it would be better to build tree arrangements using the four species making a more biodiverse system. In this regard, it should be stressed that two of the studied species are not native, and therefore they may be objectionable because of the current preference of native species. However, the city as a completely artificial system could benefit from introduced species with higher transpiration rates. Most likely, the studied species may have a higher transpiration rate if they were irrigated, so could further reduce the urban heat load. Therefore, a recommendation could be a controlled irrigation of the studied species during the dry season in order to increase transpiration, and thereby reduce the heat load. Irrigation must be carefully addressed since water supplies are scarce in the dry season and trees would be competing with human consumption.

Results of this study show clearly that reduction of heat loads is possible even in the dry season with no irrigation through evaporative cooling from tree transpiration that utilizes soil water uptake and transpiration, that would probably reduce surface and near-surface air temperatures. Additionally, this reduction in temperatures could be enhanced from tree shading (Oliveira et al., 2011).

However, special care has to be taken when extrapolate these results to an annual variation since the measurement period was very short and water stress can change over the year because limiting transpiration (Domec and Garner, 2003) or changes in the stomatal responses and/or leaf function or a combination of both mechanisms (Sperry et al., 1993). Even so, a good approximation could be done using the g_S and TRP models (reverse Eq. (1) and (4), respectively). Although, it is necessary to take into account that measurements were made in the driest and warmest month and this modeling was performed when the xylem conductivity and stomatal conductance were at their lowest with a wide ranges of the environmental variables (T_A, DPV, *I*) to have a better appreciation of their effects on g_S and TRP.

Nevertheless, to build tree arrangements to reduce urban heat loads it is essential to essential to do it during the warmest month as it is the case of this study since the UHI mitigation is more important in the dry season.

In addition to reduced heat load and energy demand using trees, mitigation of Mexico City's heat loads could improve air quality by removing particles from air (Al-Alawi and Mandiwana, 2007; Guzmán-Morales et al., 2011) and public health, as well as reduce the city's contribution to greenhouse gas emissions. However, it is relevant to mention that some tree species could generate volatile organic

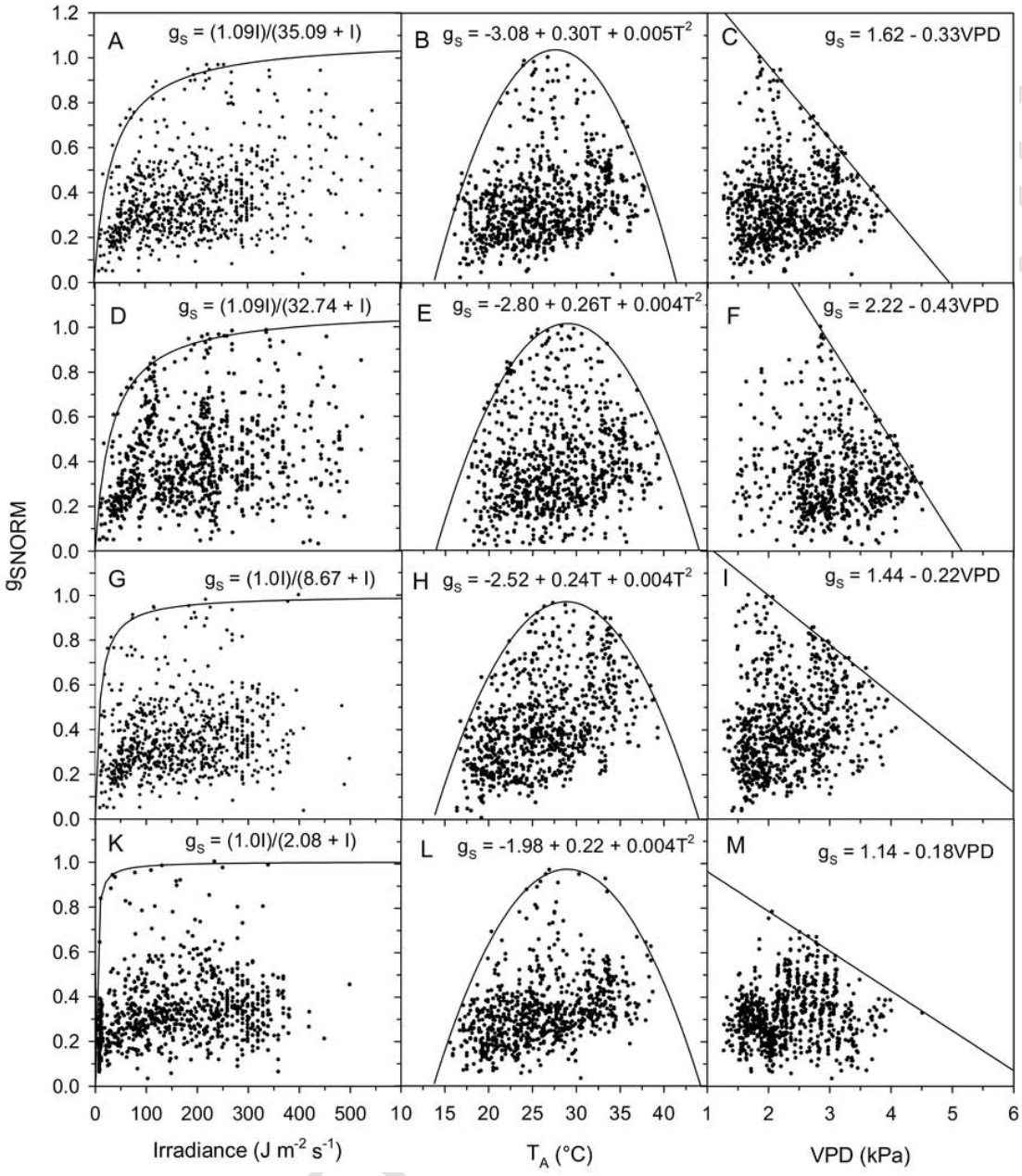

Fig. 4. Scatter diagram and probable boundary line of normalized stomatal conductance (g_S) plotted against irradiance (I), air temperature (T_A) and vapor pressure deficit (VPD) for *Liquidambar styraciflua* (A–C), *Eucaliptus camaldulensis* (D–F), *Fraxinus uhdei* (G–I) and *Ligustrum lucidum* (K–M) when intensive measurements were made during the experiment.

compounds (VOC) which can increase air pollution (Guenther et al., 2000; Karl et al., 2003; Yang et al., 2009).

The information presented in this study can be useful to those specialists who are involved in planning and development of the city to estimate heat loads reduction using trees studied here to mitigate UHI. Mitigate UHI with trees is a multidisciplinary problem which the combined efforts of urban developers, ecologists, architects, engineers, climatologists, geographers, sociologists, etc.

Acknowledgements

We thank to two anonymous reviewers for their critical observations and in thoughtful contributions for the improving of this work. This study was supported partially by grant IN213209 from DGAPA-PAPIIT, UNAM. The first author thanks the Postgraduate Program of Earth Sciences of the UNAM and CONACyT-México (No. 348420). The second author thanks the DGAPA-UNAM, for financial support during his stay in Portugal.

References

Čermák, J., Jenik, J., Kucera, J., Zidek, V., 1984. Xylem water flow in a crack willow tree (Salix fragilis L.) in relation to diurnal changes of environment. Oecologia 64, 145–151.

Al-Alawi, M.M., Mandiwana, K.L., 2007. The use of Aleppo pine needles as a bio-monitor of heavy metals in the atmosphere. J. Hazard. Mater. 148, 43–46.

Ballinas, M., 2011. Mitigación de la isla de calor urbana: estudio de caso de la zona metropolitana de la Ciudad de México. Master in Sciences Thesis. Universidad Nacional Autónoma de México, México, D.F., México.

Barradas, V.L., Ramos-Vazquez, A., Orozco-Segovia, A., 2004. Stomatal conductance in a tropical xerophilous shrubland at a lava substratum. Int. J. Biometeorol. 48, 119–127.

Barradas, V.L., 1991. Air temperature and humidity and human comfort index of some city parks of Mexico City. Int. J. Biometeorol. 35, 24–28.

Barradas, V.L., 2000. Energy balance and transpiration in an urban tree hedgerow in Mexico City. Urban Ecosys. 4, 55–67.

Bauerle, W.L., Post, C.J., McLeod, M.F., Dudley, J.B., Toler, J.E., 2002. Measurement and modeling of the transpiration of a temperate red maple container nursery. Agric. Forest Meteorol. 114, 45–57.

Dolman, A.J., 1993. A multiple-source land surface energy balance model for use in general circulation models. Agric. Forest Meteorol. 65, 21–45.

Domec, J.-C., Garner, B.L., 2003. Relationship between growth rates and xylem hydraulic characteristics in young mature and old-growth ponderosa pine trees. Plant Cell Enviorn. 26, 471–483.

Dye, P.J., 1987. Estimating water use by Eucaliptus grandis with the Penman-Monteith equation. In: Swanson, R.H., Bernier, P.Y., Woodward, P.D. (Eds.), Forest Hydrology and Watershed Management. Proceedings of the Vancouver Symposium. International Association of Hydrological Sciences, Vancouver. No. 167.

Fanjul, L., Barradas, V.L., 1985. Diurnal and seasonal variation in the water relations of some deciduous and evergreen trees of a deciduous dry forest of the western coast of Mexico. J. Appl. Ecol. 24, 289–303.

Gao, Q., Zhao, P., Zeng, X., Cai, X., Shen, W., 2002. A model of stomatal conductance to quantify the relationship between leaf transpiration and soil water stress. Plant Cell Environ. 25, 1373–1381.

Gu, S., Tang, Y., Cui, X., Kato, T., Du, M., Li, Y., Zhao, X., 2005. Energy exchange between the atmosphere and a meadow ecosystem on the Qinghai-Tibetan plateau. Agric. Forest Meteorol. 129, 175–185.

Guenther, A.C., Geron, T., Pierce, B., Lamb, P., Harley, R., 2000. Fall. Natural emissions of non-methane volatile organic compounds, carbon monoxide, and oxides of nitrogen from North America. Atmos. Environ. 34, 2205–2230.

Guzmán-Morales, J., Morton-Bermea, O., Hernández-Alvarez, E., Rodríguez-Salazar, M.T., García-Arreola, M.E., Tapia-Cruz, V., 2011. Assessment of atmospheric metal pollution in the urban area of Mexico City, using Ficus benjamina as biomonitor. Bull. Environ. Contam. Toxicol. 86, 495–500.

Herbst, M., 1995. Stomatal behaviour in a beech canopy: an analysis of Bowen ratio measurements compared with porometer data. Plant Cell Environ. 18, 1010–1018.

Hinckley, T.M., Braatne, J.H., 1994. Stomata. In: Wilkinson, R.E. (Ed.), Plant Environment Interactions. Marcel Dekker Inc., New York, pp. 323–355.

Jarvis, P.G., McNaughton, K.G., 1986. Stomatal control of transpiration: scaling up from leaf to region. Adv. Ecol. Res. 151, 1–49.

Jarvis, P.G., 1976. The interpretation of the variations in leaf water potential and stomatal conductance found in canopies in the field. Philos. Trans. R. Soc. London: B 273, 593–610.

Jauregui, E., Luyando, E., 1998. Long-term association between pan evaporation and the urban heat island in Mexico City. Atmosfera 11, 45–60.

Jauregui, E., 1971. Mesomicroclima de la ciudad de México. Instituto de Geografía, UNAM, Mexico.

Jauregui, E., 1997. Heat island development in Mexico city. Atmos. Environ. 31, 3821–3831.

Jones, H.G., 1983. Plants and the Aerial Environment. Cambridge University Press, Cambridge.

Jones, H.G., 1992. Plants and Microclimate. Cambridge University Press, Cambridge.

Karl, T., Guenther, A., Spirig, C., Hansel, A., Fall, R., 2003. Seasonal variation of biogenic VOC emissions above a mixed hardwood forest in northern Michigan. Geophys. Res. Lett. 30 (2186), 23. http://dx.doi.org/10.1029/2003GL018432.

Kelliher, F.M., Kostner, B.M.M., Hollinger, D.Y., Byers, J.N., Hunt, J.E., McSeveny, T.M., Meserth, R., Weir, P.L., Schulze, E.-D., 1992. Evaporation, xylem sap flow, and tree transpiration in a New Zealand broad-leaved forest. Agric. Forest Meteorol. 62, 53–73.

Kumagai, T., Saitoh, T.M., Sato, Y., Morooka, T., Manfroi, O.J., Kuraji, K., Suzuki, M., 2004. Transpiration, canopy conductance and the decoupling coefficient of a lowland mixed dipterocarp forest in Sarawak Borneo: dry spell effects. J. Hydrol. 287, 237–251.

Kuttler, W., 1998. In: Heyer, E. (Ed.), Stadtklima. Witterung und Klima, Teubner, Stuttgart-Leipzig, pp. 328–364 (1998).

Lee, D.O., 1991. Urban-rural humidity differences in London. Int. J. Climatol. 11, 577–582.

Leuning, R., Kelliher, F.M., Murtrie, R.E., 1991. Simulation of evapotranspiration by trees. Agric. Water Manage. 19, 205–221.

Magnani, F., Leonardi, S., Tognetti, R., Grace, J., Borghetti, M., 1998. Modeling the surface conductance of a broad-leaf canopy: effects of partial decoupling from the atmosphere. Plant Cell Environ. 21, 867–879.

Maroco, J.P., Pereira, J.S., Chaves, M.M., 1997. Stomatal responses to leaf-to-air vapour pressure deficit in sahelian species. Aus. J. Plant Physiol. 24, 381–387.

Meinzer, F.C., Andrade, J.L., Goldstein, G., Holbrok, N.M., Cavelier, J., Jackson, J., 1997. Control of transpiration from the upper canopy of a tropical forest: the role of stomatal, boundary layer and hydraulic architecture components. Plant Cell Environ. 20, 1242–1252.

Nicolas, E., Barradas, V.L., Ortuño, M.F., Navarro, A., Torrecillas, A., Alarcon, J.J., 2008. Environmental and stomatal control of transpiration, canopy conductance and decoupling coefficient in young lemon trees under shading net. Environ. Exp. Bot. 63, 200–206.

Oke, T.R., 1995. The heat island of the urban boundary layer: characteristics, causes and effects. In: Cermack, J.E. (Ed.), Wind Climate in Cities. Kluwer Academic Publishers, Boston, pp. 81–107.

Oliveira, S., Andrade, H., Vaz, T., 2011. The cooling effect of green spaces as a contribution to the mitigation of urban heat: a case study in Lisbon. Build. Environ. 46, 2186–2194.

Pitman, J.I., 1996. Ecophysiology of tropical dry evergreen forest, Thailand: measured and modelled stomatal conductance of Hopea ferrea, a dominant canopy emergent. J. Appl. Ecol. 33, 1366–1378.

Ramos, G.,1998. Simulación de escenarios de ahorro y uso eficiente de energía con medidas de control pasivo, Revista FIDE, Año 7, No. 28, 25 pp.

Roberts, J.M., Rosier, P.T.W., 1993. Physiological studies in young Eucaliptus stand in southern India and derived estimates of forest transpiration. Agric. Water Manage. 23, 103–118.

Roberts, J., Cabral, O.M.R., de Aguiar, L.F., 1990. Stomatal and boundary layer conductances in an Amazonian terra firme rain forest. J. Appl. Ecol. 27, 336–353.

SARH (Secretaría de Agricultura y Recursos Hidráulicos, 1982. Normales Climatológicas. Dirección General del Servicio Meteorológico Nacional, Mexico.

Schulze, E.-D., Hall, A.E., 1981. Short-term and long-term effects of drought on steady-state and integrated plant processes. In: Johnson, C.B. (Ed.), Physiological Processes Limiting Plant Productivity. Butterworths London, Boston Sydney, pp. 217–235.

Schulze, E.-D., Čermáck, J., Matyssek, R., Penka, M., Zimmermann, R., Gries, W., Kucera, J., 1985. Canopy transpiration and water fluxes in the xylem of the trunk of Larix and Picea trees—a comparison of xylem flow, porometer and cuvette measurements. Oecologia 66, 475–483.

Schulze, E.-D., 1986. Carbon dioxide and water vapour exchange in response to drought in the atmosphere and in the soil. Annu. Rev. Plant Physiol. 37, 247–274.

Sperry, J.S., Alder, N.N., Eastlack, S.E., 1993. The effect of reduced hydraulic conductance on stomatal conductance and xylem cavitation. J. Exp. Bot. 44, 1075–1082.

Stewart, J.B., 1988. Modelling surface conductance of pine forest. Agric. Forest Meteorol. 43, 19–35.

Susca, T., Gaffin, S.R., Dell'Osso, G.R., 2011. Positive effects of vegetation: urban heat island and green roofs. Environ. Pollut. 159, 2119–2126.

Tan, C.S., Black, T.A., Nnyamah, J.U., 1978. A simple diffusion model of evapotranspiration applied to a thinned douglas-fir stand. Ecology 59, 1221–1229.

Unger, J., 1999. Urban-rural air humidity differences in Szeged, Hungary. Int. J. Climatol. 19, 1509–1515.

Wright, I.R., Gash, J.H.C., da Rocha, H.R., Roberts, J.M., 1996. Amazonian deforestation and climate. In: Gash, J.H.C., Nobre, C.A., Roberts, J.M., Victoria, R.L. (Eds.), Modelling Stomatal Conductance for Amazonian Asture and Forest. Institute of Hydrology, Wallingford, pp. 437–457.

Yang, D.S., Son, K.C., Kays, S.J., 2009. Volatile organic compounds emanating from indoor ornamental plants. Hort. Sci. 44, 396–400.

Zweifel, R., Rigling, A., Dobbertin, M., 2009. Species-specific stomatal response to drought—a link to vegetation dynamics?. J. Veg. Sci. 20, 442–454.